UNIVERSITY
OF TASMANIA

The biosynthesis of two naturally-occurring auxins in *Pisum sativum* L.

by

Nathan Tivendale, BBiotech (Hons)

School of Plant Science

School of Chemistry

Submitted in fulfilment of the requirements of the degree Doctor of Philosophy

University of Tasmania, Hobart, Australia

August 2012

Declaration of Originality

I hereby declare that, to the best of my knowledge, this thesis contains no material which has been accepted for a degree or diploma by the University or any other institution, except by way of background information and duly acknowledged in the thesis, and no material previously published or written by another person except where due acknowledgement is made in the text of the thesis, nor does the thesis contain any material that infringes copyright.

Authority of Access

This thesis may be made available for loan and limited copying and communication in accordance with the Copyright Act 1968.

Statement regarding published work contained in the thesis

The publishers of the papers comprising parts of Chapters 3, 4, 6 and 7 hold the copyright for that content, and access to the material should be sought from the respective journals. The remaining non-published content of the thesis may be made available for loan and limited copying and communication in accordance with the Copyright Act 1968

Nathan Tivendale
School of Plant Science/School of Chemistry
University of Tasmania
October 2012

List of published works

Paper 1: Quittenden LJ[1], Davies NW[2], Smith JA[3], Molesworth PP[3], Tivendale ND[1,3], Ross JJ[1] (2009) Auxin biosynthesis in pea: characterization of the tryptamine pathway. Plant Physiology **151:** 1130-1138

Located in Chapter 3

Paper 2: Tivendale ND[1,3], Davies NW[2], Molesworth PP[3], Davidson SE[1], Smith JA[3], Lowe EK[2], Reid JB[1], Ross JJ[1] (2010) Reassessing the role of *N*-hydroxytryptamine in auxin biosynthesis. Plant Physiology **154:** 1957-1965

Located in Chapters 4 and 7

Paper 3: Ross JJ[1], Tivendale ND[1,3], Reid JB[1], Davies NW[2], Molesworth PP[3], Lowe EK[2], Smith JA[3], Davidson SE[1] (2011) Reassessing the role of YUCCAs in auxin biosynthesis. Plant Signaling and Behavior **6:** 437-439

Located in Chapters 4 and 7

Paper 4: Tivendale ND[1,3], Davidson SE[1], Davies NW[2], Smith JA[3], Dalmais M, Bendahmane A[4], Quittenden LJ[1], Sutton L[1], Bala RK[1], Le Signor C[5], Thompson R[5], Horne J[2], Reid JB[1], Ross JJ[1] (2012) Biosynthesis of the halogenated auxin, 4-chloroindole-3-acetic acid. Plant Physiology **159:** 1055-1063

Located in Chapters 6 and 7

[1]School of Plant Science, University of Tasmania, Hobart, Australia
[2]Central Science laboratory, University of Tasmania, Hobart, Australia
[3]School of Chemistry, University of Tasmania, Hobart, Australia
[4]Unité de Recherche en Génomique Végétale, Evry, France
[5]Unité Mixte de Recherche 1347 Agroécologie, Institut National de la Recherche Agronomique, Dijon, France

Abstract

Auxins are a group of phytohormones, including indole-3-acetic acid (IAA) and 4-chloroindole-3-acetic acid (4-Cl-IAA), that are involved in many aspects of plant growth, including phototropism, gravitropism, shoot elongation, root initiation and flowering. The structure of the primary auxin—IAA—was determined over 70 years ago, but the biosynthesis of this molecule, and the other naturally-occurring auxins, has remained unclear. Five pathways have been proposed for IAA biosynthesis, one tryptophan (Trp)-independent pathway and four Trp-dependent pathways. Each of the Trp-dependent pathways is named after its primary intermediate, giving rise to the indole-3-acetaldoxime, tryptamine, indole-3-acetamide and indole-3-pyruvic acid pathways. At the outset of this research, the evidence for each of these pathways was incomplete, even in the model organism *Arabidopsis thaliana*. This thesis reports the determination of the primary auxin biosynthesis route in the seeds of *Pisum sativum* (pea). The indole-3-acetaldoxime pathway was not investigated, as it has been shown previously that pea lacks the necessary enzymes for this pathway and is devoid of endogenous indole-3-acetaldoxime. First, the tryptamine pathway was examined. The mass spectral characterisation of authentic *N*-hydroxytryptamine (synthesised in our laboratory), a reported intermediate in the tryptamine pathway and the alleged *in vitro* product of the YUCCA enzymes, cast serious doubts over the role of this compound in auxin biosynthesis. It was also shown, through injection of labelled [D_4]Trp and [D_5]tryptamine, that tryptamine is not converted to IAA in pea seeds, indicating that this pathway does not function in these organs. This left three possible pathways to auxin. Through *in vivo* feeding experiments, the Trp-independent and the indole-3-acetamide pathways were eliminated as possibilities in pea seeds. The remaining pathway, the indole-3-pyruvic acid pathway, was investigated using a number of lines of enquiry. First, the functional activity of two Trp aminotransferase genes from pea (*PsTAR1* and *PsTAR2*) was investigated using purified recombinant PsTAR1 and PsTAR2. This showed that these proteins convert Trp to indole-3-pyruvic acid and 4-chlorotryptophan to 4-chloroindole-3-pyruvic acid. A standard of the latter compound was synthesised in our laboratory, for comparison with the enzyme product. Secondly, feeding studies using [$^{13}C_6$]IAA and [D_5]Trp indicated that Trp is converted to 4-Cl-Trp, which is then converted to 4-Cl-IAA. Taken together, the evidence presented in this thesis supports parallel biosynthesis of IAA and 4-Cl-IAA by the IPyA pathway and its chlorinated version.

Acknowledgements

First of all I would like to thank my Lord and Saviour, Jesus Christ, through whom all things were made. It is a privilege and a pleasure to study God's creation.

Next, a gargantuan thankyou to my supervisory team—John Ross, Jason Smith and Jim Reid—for countless hours spent directing, guiding, encouraging and helping me over the past 3.5 years and making me the scientist I am today. John, your love for data and your enthusiasm for science is quite inspiring.

A big thanks to Noel Davies for explaining to me the secrets of GC-, LC- and UPLC-MS and analysing countless samples for me. Thanks to Heather Nonhebel for supplying [D_5]IAAld, Yunde Zhao for supplying *AtYUC1*, Volker Magnus for supplying 4-Cl-IAA and Jerry Cohen for supplying [D_4]4-Cl-IAA. Thanks to Sandra for doing qPCR analyses and revealing to me the magic of molecular biology. Thanks to Peter Molesworth for much-appreciated help in the organic synthesis lab. Thanks to Laura Quittenden for guiding me through several techniques for hormone analysis. Thanks to Sam Cook, Vincent Walter, James Horne, Richard Wilson and Edwin Lowe for technical assistance in several analyses. Thanks to the Glasshouse staff—Ian Cummings, Tracy Winterbottom and Michelle Lang—for looking after my plants and keeping them healthy.

To my fellow PhD candidates, who shared this journey with me—Scott McAdam, Erin Howard and Frances Sussmilch—a massive thanks for your friendship, advice, encouragement and countless hours of 500, 3-Up, Gin, Wizard, Viewpoint and many other enjoyable games.

Thanks to the University Fellowship of Christians for all the great teaching, encouragement and fellowship I have received over the years.

Thanks to the Australian Federal Government for providing financial support while I undertook this degree.

Thankyou to my parents for having me; I really appreciate it. Thanks to my siblings for the long phone conversations and all the good times we had. Thankyou to all my friends who helped me get through my PhD without even realising they were doing so: Brad Stewart, Chris Butler, Connor Sweeney, Lucy Murfet, Sam Green, Mike Lynch, Aaron Johnstone, Jono Haines, Dan Shepheard, Sam Hesketh and Mark Moncur. To my son Micah: thankyou for sleeping through

the night and being cute. Finally a huge thankyou to my wife, Amy, for so many things: for your loving, supportive, respectful, and helpful attitude towards me, for your superb cooking skills, for your gentle and quiet spirit, and for putting up with my mood swings and other ‘quirky’ traits; I love you.

Abbreviations

^{1}H NMR	proton nuclear magnetic resonance spectroscopy
1-HT	1-hydroxytryptamine
^{13}C NMR	carbon-13 nuclear magnetic resonance spectroscopy
2-OT	2-oxytryptamine
4-Cl-IAA	4-chloroindole-3-acetic acid
4-Cl-indole	4-chloroindole
4-Cl-IPyA	4-chloroindole-3-pyruvic acid
4-Cl-Trp	4-chlorotryptophan
4-HT	4-hydroxytryptamine
6-HT	6-hydroxytryptamine
α-HT	α-hydroxytryptamine
ABA	abscisic acid
AO	aldehyde oxidase
CE	collision energy
AMP	ampicillin
ACN	acetonitrile
APCI	atmospheric pressure chemical ionisation
BSTFA	*N*,*O*-bis(trimethylsilyl)-trifluoroacetamide
CaMV	Cauliflower mosaic virus
d	doublet
dd	doublet of doublets
δ	chemical shift
dNTP	deoxynucleotide triphosphate

DCM	dichloromethane
DPA	days post-anthesis
DPM	decays per minute
DTT	dithiothreitol
EDTA	ethylenediaminetetraacetic acid
ESI	eletrospray ionisation
EtOH	ethanol
FMO	flavin monooxygenase
FW	fresh weight
FW_T	total fresh weight
GC-MS	gas chromatography-mass spectrometry
h	hours
HO-TAM	hydroxytryptamine
HPLC	high-performance liquid chromatography
HSQC	^{13}C-^{1}H heteronuclear single quantum coherence
IAA	indole-3-actic acid
iaaH	indole-3-acetamide hydrolase
IAAld	indole-3-acetaldehyde
iaaM	tryptophan-2-monooxygenase
IAAsp	indole-3-acetylaspartate
IAGlu	and indole-3-acetylglutamate
IAM	indole-3-acetamide
IAN	indole-3-acetonitrile
IAOx	indole-3-acetaldoxime

ICA	indole-3-carboxaldehyde
ID	internal diameter
IEt	indole-3-ethanol
ILA	indole-3-lactic acid
IPTG	isopropyl β-D-1-thiogalactopyranoside
IPyA	indole-3-pyruvic acid
IR	infra-red
LB	Luria broth
LC-MS	liquid chromatography-mass spectrometry
m	multiplet
m/z	mass:charge ratio
MBP	maltose-binding protein
MeOH	methanol
MRM	multiple reaction monitoring
MS	Murashige and Skoog OR mass spectrometry
NAcTAM	*N*-acetyltryptamine
$NADP^+$	β-nicotinamide adenine dinucleotide phosphate (oxidised form)
NADPH	β-nicotinamide adenine dinucleotide phosphate (reduced form)
NEB	New England Biolabs
NHT	*N*-hydroxytryptamine
NPC	no-protein control
OD_{600}	optical density at 600 nm
oxIAA	2-oxindole-3-acetic acid
PCR	polymerase chain reaction

PFPA	pentafluoropropanoic anhydride
PLP	pyridoxyl-5-phosphate
PMSF	phenylmethylsulfonyl fluoride
PPh_3	triphenylphosphine
ppm	parts per million
R:FR	red : far red
R_f	retardation factor
rpm	revolutions per minute
RT	retention time
s	singlet
SDS	sodium dodecylsulfate
SDS-PAGE	sodium dodecylsulfate polyacrylamide gel electrophoresis
SIM	selected ion monitoring
SIR	selected ion recording
SOC	super-optimal broth with catabolite repression
t	triplet
TAM	tryptamine
TB	terrific broth
td	triplet of doublets
TEA	triethylamine
THF	tetrahydrofuran
TILLING	Targeting Induced Local Lesions IN Genomes
TLC	thin-layer chromatography
Trp	tryptophan

UPLC	ultra-performance liquid chromatography
V_T	total volume
WT	wild-type

Contents

Chapter 1 An introduction to auxin biosynthesis

A common feature of all living organisms is their ability to carry out a wide variety of chemical reactions, both biosynthetic (anabolic; energy-requiring) and catabolic (energy-releasing; Goodwin and Mercer, 1983). These processes are catalysed and controlled by enzymes and regulate many aspects of growth and development. Biosynthetic reactions give rise to primary metabolites (essential for life) and a host of secondary metabolites (Mann, 2004). Secondary metabolites are distinguished from primary metabolites in that they have restricted distribution, are often genera-, species- or strain-specific and are biosynthesised *via* specialised pathways chiefly from one of the following primary metabolites: α-amino acids, acetyl coenzyme A, mevalonic acid or shikimic acid (Hendrickson, 1965; Herbert, 1989; Mann, 2004). Plant secondary metabolites can be classified according to their biosynthetic origin into three major groups: terpenoids, alkaloids and other nitrogen-containing metabolites, and phenols (Walton and Brown, 1999). There are over 100 000 known plant secondary metabolites, with a panoply of roles in plant growth and development (Walton and Brown, 1999). A particularly important class of plant secondary metabolites is the phytohormones. These include ethylene (fruit ripening), gibberellins (stem elongation), cytokinins (cell division), ABA (stomatal control), brassinosteroids (cell elongation), auxins (growth in response to various stimuli), jasmonates and strigolactones (shoot branching control and underground communication with neighbouring organisms; Gomez-Roldan et al., 2008; Umehara et al., 2008) (Walton and Brown, 1999). To classify and fully understand the function of plant secondary metabolites, it is essential to determine the biosynthetic pathways leading to these compounds.

Biochemical pathway determination may be conducted using two different approaches. The first, and by far the most prevalent in recent times, is the molecular biology-based approach. Typically, in a mutant screen, traits of interest are identified and the gene of interest may be isolated by genotyping mutant individuals (forward genetics; Alonso and Ecker, 2006). Alternatively, a gene may have been previously identified and to determine its function *in vivo* mutants carrying a lesion in that gene are isolated (reverse genetics; Alonso and Ecker, 2006). Through phenotypic analyses of mutants and determining the effects on selected biochemical pathways, the role of the gene products in the biochemistry of the plant may be determined. The second main approach involves chemistry-based methods. A hypothetical biochemical pathway

may be tested using labelled putative intermediates, which are 'fed' to plants of interest; methods of administration include injection (e.g. Ross et al., 1993; Adelstein and Manning, 1995) and absorption from growth media (e.g. Cooney and Nonhebel, 1991; Quittenden et al., 2009). After a suitable time period, the end product or products of interest may be extracted and analysed for the presence of the label. Detection of the label in the final product provides evidence that the applied compound is part of the pathway. Conversely, if the label is not detected in the final product, then the putative intermediate is probably not an intermediate in that pathway. Often both of the main approaches are required to accurately determine a biochemical pathway; use of one approach in isolation can lead to incorrect conclusions, which are later overturned by more thorough analysis.

Auxins, an important group of naturally-occurring hormones found in all land plants and several plant-associated and soil-dwelling microbes (reviewed in Costacurta and Vanderleyden, 1995), are the subject of much study and discussion. There are four known auxins: IAA, indole-3-butyric acid, phenylacetic acid and 4-Cl-IAA (the only known halogenated phytohormone; Thain and Hickman, 2001). Auxin was the first phytohormone identified and the initial hints of it date back as far as 1872, when Theophil Ciesielski postulated the presence of a 'transmitted influence', which was present in the tip of plant shoots and responsible for gravitropism (Ciesielski, 1872). This idea was expanded upon by Charles and Frances Darwin eight years later, who showed that this 'transmitted influence' has a role in phototropism also (Darwin, 1880). In addition, auxins have been shown to play roles in lateral root formation, control of shoot architecture (reviewed in Woodward and Bartel, 2005), organ patterning (reviewed in Davies, 2004; see also Cheng et al., 2006; Cheng et al., 2007), and vascular development (reviewed in Davies, 2004). For many years, the action of auxin was thought to be principally due to the establishment of auxin gradients, through basipetal transport of auxin from its site of biosynthesis, the developing leaves and shoot tip, to the root tip; this transport occurs *via* an auxin-specific transport system (Davies, 2004). However, evidence for the importance of local auxin biosynthesis continues to accumulate (reviewed in Chandler, 2009); however, establishment of auxin gradients is still thought to be important for a number of processes (see, for example, Benková et al., 2003; Pagnussat et al., 2009). There have been many studies devoted to the effects of auxin in plant growth and the mechanism through which these effects

occur (reviewed in Zazimalova and Napier, 2003; Davies, 2004); however, at the outset of the present study, the understanding of auxin biosynthesis was far from satisfactory.

In 1937 the structure of the primary auxin, IAA, was determined (Went and Thimann, 1937; reviewed in Normanly et al., 1995). For a range of plant and microbial species, many IAA biosynthetic intermediates were suggested, including TAM (Winter, 1966), IPyA (Moore and Shaner, 1968), IAOx (Helmlinger et al., 1987), IAAld (Sembdner et al., 1981), IEt (Ernstsen et al., 1987; Monteiro et al., 1987), IAN (Sembdner et al., 1981; Helmlinger et al., 1987) and IAM (Igoshi et al., 1971; Takahashi et al., 1975; Saotome et al., 1993; Rajagopal et al., 1994). By the 1980s the amino acid Trp (a 3-substitiuted indole, like IAA), synthesised from indole (Erdmann and Schiewer, 1971), had been well established as an IAA precursor in a wide variety of plant species (for reviews, see Sembdner et al., 1981; Bartel, 1997; Woodward and Bartel, 2005; Chandler, 2009; Normanly, 2010) and many IAA biosynthetic pathways, most originating from Trp, had been proposed (see Figure 1.1). Yet, since the elucidation of the structure of IAA, over 80 years ago, there has been much confusion and debate over the biosynthesis of IAA. Genetic redundancy within each pathway (for examples, see Cheng et al., 2006, 2007; Stepanova et al., 2008; Tao et al., 2008), has made mutant generation difficult and can lead to other complications. Another possible reason for the confusion, commonly given, is that perhaps no single pathway dominates IAA biosynthesis across all species. Nevertheless, the pathways of auxin biosynthesis are now beginning to be understood (for reviews, see Bartel et al., 2001; Davies, 2004; Ljung et al., 2005; Woodward and Bartel, 2005; Strader and Bartel, 2008; Chandler, 2009).

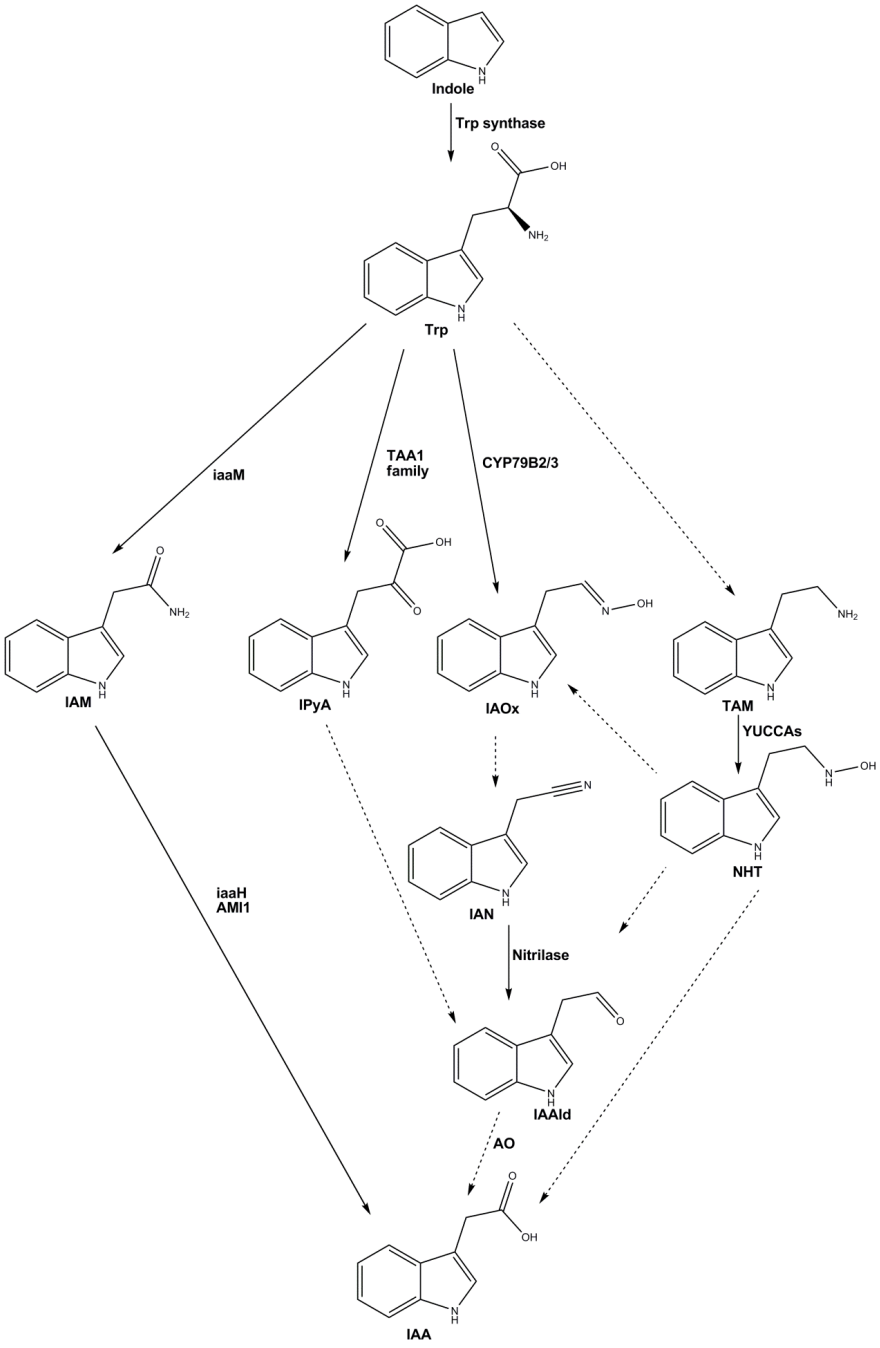

Figure 1.1 – Proposed Trp-dependent auxin biosynthetic pathways, incorporating evidence from a number of species including *Arabidopsis thaliana* (Barlier et al., 2000; Hull et al., 2000; Mikkelsen et al., 2000; Bak et al., 2001; Zhao et al., 2001; Jackson et al., 2002; Ljung et al., 2002; Pollmann et al., 2002; Cohen et al., 2003; Mikkelsen et al., 2004; Cheng et al., 2006, 2007; Jeong et al., 2007; Kim et al., 2007; Ikeda et al., 2009; Sugawara et al., 2009), *Pisum sativum* (Moore and Shaner, 1968; Moore, 1969; Tivendale, 2008; Quittenden et al., 2009; Sutton, 2009), *Solanum lycopersicum* (Cooney and Nonhebel, 1989, 1991; Expósito-Rodríguez et al., 2007), *Zea mays* (Glawischnig et al., 2000; Kriechbaumer et al., 2006; Hendrickson Culler and Cohen, 2007; Gallavotti et al., 2008), *Nicotiana tobacum* (Songstad et al., 1990) petunia (Tobeña-Santamaria et al., 2002) and several species of IAA-synthesising microbes, such as *Agrobacterium tumerfaciens*, *Pseudomonas savastanoi* and *Enterobacter cloacae* (Comai and Kosuge, 1982; Camilleri and Jouanin, 1991; Koga et al., 1991a; Koga et al., 1991b; Koga et al., 1992; Koga et al., 1994).

There are four proposed Trp-dependent IAA biosynthetic pathways, each named after the intermediate immediately after Trp in the pathway—the IAOx, TAM, IPyA and IAM pathways (see reviews mentioned above). A Trp-independent pathway has also been proposed, in light of analysis of the *Arabidopsis* Trp auxotroph mutants, *trp3-1* and *trp2-1*, which reportedly accumulate amide- and ester-linked IAA conjugates (Normanly et al., 1993), despite having low Trp levels (Müller and Weiler, 2000). Of the five proposed IAA biosynthetic pathways, only one has been completely characterised. The iaaM/iaaH pathway, in which Trp is converted to IAM (catalysed by the tryptophan-2-monooxygenase, iaaM) which is subsequently hydrolysed to IAA (catalysed by the IAM hydrolase, iaaH), is known to operate in various plant pathogens such as *Agrobacterium tumerfaciens* and *Pseudomonas savastanoi* (Comai and Kosuge, 1982; Yamada et al., 1985).

The TAM pathway was first proposed by Winter (1966) after auxin-like activity of TAM was observed in *Avena* coleoptile elongation assays. TAM has been reported as an endogenous compound in *Solanum lycopersicum* L. (tomato; Schneider et al., 1972; Cooney and Nonhebel, 1991), *Oryza sativa* L. (rice; Ishihara et al., 2008), *Arabidopsis thaliana* L. (Sugawara et al., 2009) *Hordeum vulgare* L. (barley; Schneider et al., 1972) and *Pisum sativum* L. (pea; Quittenden et al., 2009). However, several groups have cast doubt over the importance of this pathway in IAA biosynthesis. Cooney and Nonhebel (1991) reported on the labelling of IAA and TAM after applying D_2O to tomato shoots. Initially IAA and TAM became labelled at a similar rate, but TAM continued to accumulate label up to 21 h, whereas IAA did not. Cooney and Nonhebel inferred from this result that TAM is synthesised from a separate Trp pool to IAA, and is not a major IAA precursor. Similarly, Songstad et al. (1990) report that, while *Nicotiana tobacum* L. (tobacco) plants over-expressing Trp decarboxylase accumulate high levels of TAM, IAA levels are unaffected (see Chapter 3 for a critique of Songstad et al., 1990 and Cooney and Nonhebel, 1991). Nevertheless, in the last 10 years, interest in this pathway as a major source of IAA has increased, due in large part to the discovery of the *YUCCA* gene family (Zhao et al., 2001), although the role of these enzymes in TAM-dependent IAA biosynthesis is debatable (discussed more in Chapter 4).

The IPyA pathway is important in a number of IAA-synthesising microorganisms (Koga et al., 1992; Koga, 1995) and appears to operate in some plant species as well (Cooney and Nonhebel, 1989; Tam and Normanly, 1998; Stepanova et al., 2008; Tao et al., 2008). Recently, Trp

aminotransferase genes were isolated from *Arabidopsis* (Stepanova et al., 2008; Tao et al., 2008); the proteins encoded by these genes catalyse the formation of IPyA from Trp. The IPyA decarboxylase thought to be required to convert IPyA to IAAld is yet to be identified in plants, although the AO required to convert IAAld to IAA has been identified in *Arabidopsis* (Seo et al., 1998) and pea (Zdunek-Zastocka, 2007). However, this does not confirm the operation of the IPyA pathway, as IAAld may be an intermediate for other pathways (see Figure 1.1; also see Bartel et al., 2001; Woodward and Bartel, 2005).

IAM has been identified as an endogenous compound in *Arabidopsis* (Pollmann et al., 2002) and is thought by some to be widespread in the plant kingdom (reviewed in Lehmann et al., 2010). In *Arabidopsis*, IAM is thought to be generated from IAOx, which is synthesised from Trp by CYP79B2/3, although there is some debate as to whether this pathway normally operates in plants (Ljung et al., 2002). IAM has also been identified in extracts from pea, rice, *Zea mays* L. (maize) and tobacco, but these species lack the CYP79B2/3 homologues and are devoid of endogenous IAOx (Sugawara et al., 2009) and therefore it is proposed that IAM can also be synthesised *via* an IAOx-independent pathway (Figure 1.1). However, this pathway remains uncharacterised.

In this thesis, auxin biosynthesis in pea is examined. Pea is a useful model species for several reasons: it has a reasonably short generation time (six weeks from planting to anthesis), is easily cultivated, and is an agriculturally important crop. Furthermore, due to their size and composition (soft testa, liquid endosperm), pea seeds lend themselves favourably to injection of putative biosynthetic intermediates and are free from auxin-synthesising microbes, which often present a complicating factor in other plant systems (e.g. pea roots, as reported in Quittenden et al., 2009). These attributes make pea and excellent species in which to study auxin biosynthesis in developing seeds. Only a little is known about auxin biosynthesis in pea. The IAOx pathway is unlikely to be in operation in pea seeds, for reasons given above (Tivendale, 2008; Quittenden et al., 2009). It has recently been shown that the TAM pathway can operate in pea roots (Quittenden et al., 2009), but this does not automatically imply the operation of this pathway in seeds (see Chapter 4). The TAM, IAM, IPyA and Trp-independent pathways are yet to be thoroughly investigated in pea seeds, and hence they will be the focus of this thesis.

The study begins with an investigation of the metabolic fate of TAM in pea roots and identification of a new TAM metabolite (Chapter 3); these results lead to a critique of the reports published by Songstad et al. (1990) and Cooney and Nonhebel (1991). Next the role of the YUCCAs is critically re-examined, casting serious doubts over their role in the TAM pathway and over the proposed biosynthetic intermediate NHT. The study of the YUCCAs and their biochemical function continues, through synthesis of alternative oxidation products of TAM (Chapter 5). Attention is then given to the *PsTAR* gene family, and its importance in both IAA and 4-Cl-IAA biosynthesis in developing pea seeds is demonstrated, using several techniques, including *in vitro* functional assays (Chapter 6). Lastly, the findings of an extensive chemical-based study of auxin biosynthesis in developing pea seeds is reported (Chapter 7), and final conclusions are drawn (Chapter 8).

Chapter 2 General Materials and Methods

This chapter details various experimental procedures that are used throughout this study.

Plant material

Unless otherwise stated, the line used was Hobart Line 107, which was derived from cultivar Torsdag and is wild type with respect to internode length genes. All plants were grown, two seeds per pot, in sterilised pasteurised peat moss/sand potting mix. Plants were grown under a mixed light source in an air-conditioned glasshouse and watered regularly, as described in Jager et al. (2007). Experimental seeds typically ranged between 30 and 150 mg (FW) and had not reached contact point.

Water

Water applied to growing plants was obtained from the domestic water supply. Purified water (either deionised or Milli-Q) was used for all other purposes.

Chemicals

[Phenyl-^{14}C (U)]indole (American Radiolabeled Chemicals, Inc.), [D_6]indole (Isotec), L-Trp (Sigma-Aldrich Co.), [3-^{14}C]L-Trp (Perkin Elmer), 4-Cl-Trp (Amatek Chemical Co., Ltd.), IPyA (Sigma-Aldrich Co.), ILA (Aldrich), ICA (Sigma-Aldrich Co.), TAM (Sigma-Aldrich Co.), [α-^{14}C]TAM (ViTrax Radiochemicals), IAAld (Sigma-Aldrich Co.), IAA (Sigma-Aldrich Co.), and [$^{13}C_6$]IAA (Cambridge Isotope Laboratories, Inc.) were obtained commercially. [D_4]4-Cl-IAA was supplied by Prof. Jerry Cohen and unlabelled 4-Cl-IAA was supplied by Dr Volker Magnus (Ruđer Bošković Institute, Zagreb, Croatia). [D_4]L-Trp was synthesised in the same way as [D_5]Trp, as described in Quittenden et al. (2009). All other compounds were synthesised in our laboratory as described previously (Tivendale, 2008; Quittenden et al., 2009) or below. All labelled compounds, except [α-^{14}C]TAM, were labelled on the indole ring, rather than the side chain.

Deuterated 4-Cl-Trp

A suspension of DL-4-Cl-Trp (69 mg) in DCl in D_2O, prepared by the careful addition of thionyl chloride (0.5 mL; Riedel-de Haën) to D_2O (4.5 mL), was stirred at room temperature for four weeks in a sealed vial. The solvent was removed under reduced pressure and a fresh portion of DCl in D_2O was added and the suspension stirred for a further four weeks. This process was repeated a second time, before evaporation under reduced pressure to yield deuterated DL-4-Cl-Trp as the hydrochloride salt. The product was checked for deuterium incorporation by UPLC-MS (D_4: 15 %, D_3: 25 %, D_2: 33 %, D_1: 23 %, unlabeled: 5 %).

IAM

Deuterated IAM was synthesised by Dr Peter Molesworth (UTAS, Hobart) as follows. Thionyl chloride (0.5 mL) was added drop-wise to a solution of IAA methyl ester (97.2 mg) in monodeuterated methanol (CH_3OD; 3 mL) held at 0 °C using an ice bath. The solution was heated in a sealed tube using a Discover 100 microwave reactor for 2 h at 100 °C. The solvent was then removed under reduced pressure. ^1H NMR ($CDCl_3$) showed only partial conversion to the desired product. The crude mixture was again dissolved in CH_3OD (3 mL) and chilled to 0 °C before addition of Thionyl chloride (0.5 mL). The solution was again heated in a sealed tube using a Discover 100 microwave reactor for 1 h at 100 °C. After cooling and removal of the solvent under reduce pressure, the crude purple mixture was purified by filtration through silica gel (32-63 μm mesh) using 20 % v/v ethyl acetate/hexanes mixture; removal of the solvent gave an off white solid (47.7 mg). The entirety of this product was heated in a sealed tube with MeOH (2 mL) and aqueous ammonia (33 % v/v, 3 mL) for 4 h at 70 °C. After cooling the solvent was removed under reduce pressure, yielding deuterated IAM (mixture of D_5, D_6 and D_7) as an orange solid (43.6 mg).

GC-MS analysis of the product revealed that it was contaminated with deuterated IAA. Therefore, 1.00 mL of a 10 $ng.\mu l^{-1}$ solution of deuterated IAM (contaminated with deuterated IAA) was passed through an anion exchange column, preconditioned with potassium phosphate buffer (pH 8.55). The column was washed twice with buffer, and the eluate collected and analysed by UPLC-MS for IAM and IAA. The latter could not be detected. The eluate was then partitioned against ethyl acetate (3 x 1.00 mL). The organic phase was dried under N_2 and the

residue redissolved in Methanol (1.00 mL). 10 µl of this solution was combined with 10 µl of unlabelled IAM (10 ng.µl^{-1}) and the mixture was made up to 100 µl with acetic acid in H_2O (0.4 % v/v) and analysed by UPLC-MS. To ensure no proton/deuterium exchange was occurring during analysis, the solvent was evaporated under reduced pressure and the residue dissolved in acetic acid in H_2O (1 % v/v) and left at room temperature. After 1 h, the solvent was evaporated and replaced with fresh solvent. After 48 h, the solvent was again evaporated and the residue dissolved in Methanol (500 µl). 10 µl of this solution was combined with 5 µl of unlabelled IAM (10 ng.µl^{-1}) and 80 µl of acetic acid (0.4 % v/v in H_2O). This mixture was analysed by UPLC-MS and the concentration was determined to be 560 pg.µl^{-1}. No proton/deuterium exchange was observable.

IAAld

IAAld was commercially obtained as the sodium bisulfite salt (Sigma-Aldrich Co.) and was hydrolysed to obtain the free aldehyde, prior to use. IAAld·$NaHSO_3$ was dissolved in HCl (1 M) to a final concentration of 250 ng.µl^{-1} and left on ice for 1 h, after which the solution was neutralised with and equivalent volume of K_2HPO_4/KH_2PO_4 buffer (pH 8.5). [D_5]IAAld was supplied by Dr Heather Nonhebel (University of New England, Armidale, NSW, Australia).

Substrate administration

Solutions of ^{2}H-, ^{13}C- or ^{14}C-labeled substrates in H_2O were injected into immature pea seeds (30-135 mg), which contained liquid endosperm, using a syringe sterilised with ethanol in H_2O (80 % v/v). Substrates were either injected into *in situ* seeds through the pericarp and testa (method adapted from Ross et al., 1993) or excised seeds placed in a Petri dish on moist filter paper (as shown in Figure 2.1). After *in situ* injections, seeds were typically left overnight (ca. 17 h) before harvesting. Excised seeds were normally left for 3 h under a mixed white light source (fluorescent/ natural daylight) at room temperature before harvesting.

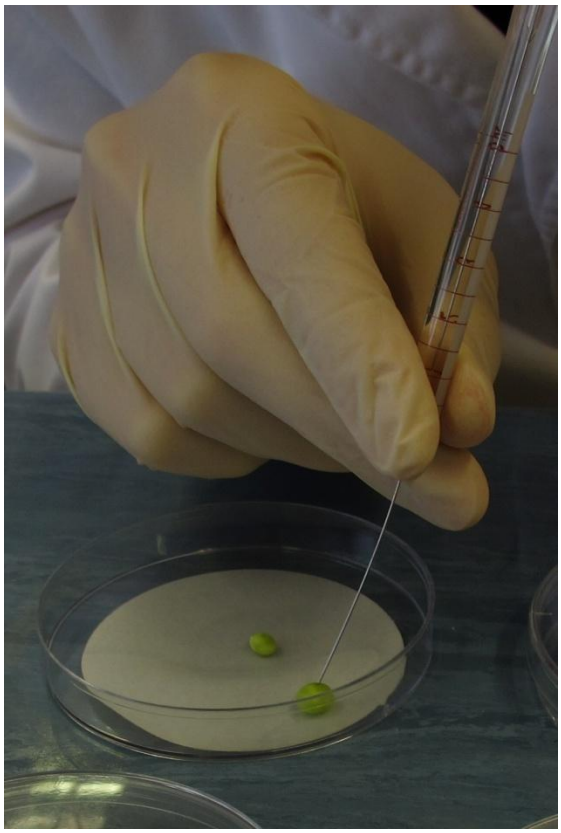

Figure 2.1 – Method for injecting labelled substrates into pea excised pea seeds.

Harvesting of plant material and preparation of extracts

Methanol/BHT method

Required plant portions were harvested into -20 °C methanol/H_2O (80 % v/v) containing 250 mg.L^{-1} butylated-hydroxytoluene (BHT) and left at -20 °C for approximately 4 h, after which the plant material was macerated using a 'Bamix' and left to extract overnight (ca. 17 h) at 4 °C. The extracts were then vacuum-filtered through Whatman No.1 filter paper and stored at -20 °C until needed.

Liquid N_2 method

Pea seeds were quickly frozen in liquid N_2 and ground into a powder, which was immersed in methanol at 4 °C for 1 h. The extract was then decanted.

Liquid endosperm method

The end of the seed containing the embryo was removed with a razor blade. The liquid endosperm was then removed from the seed using a pipette.

Sep-Pak procedure

A Waters Sep-Pak Vac RC C_{18} cartridge was pre-conditioned with methanol (ca. 12 mL) followed by 0.4 % v/v acetic acid in H_2O (ca. 12 mL). The sample solvent was reduced to ca. 1 mL under reduced pressure and loaded onto the Sep-Pak using three 1.00 mL portions of acetic acid in H_2O (0.4 % v/v). After the loading volume had flowed through under reduced pressure, the Sep-Pak was washed with 1.00 mL of acetic acid in H_2O (0.4 % v/v). The desired eluent (typically 50:49.6:0.4 MeOH/H_2O/acetic acid; ca. 12 mL) was then passed through the Sep-Pak under reduced pressure and the eluate collected.

Methylation in preparation for GC-MS

In preparation for GC-MS, some samples were methylated. The sample was placed in a scintillation vial and the solvent evaporated under N_2. MeOH (200 μL) and (trimethylsilyl)diazomethane in diethyl ether (750 μL; 0.2 M) were placed in the vial, which was then capped, shaken and left for 30 min at room temperature, after which the liquid was removed under N_2. The residue was washed from the scintillation vial into a GC-MS vial, using three 100 μL washes of diethyl ether.

Trimethylsilylation in preparation for GC-MS

The sample was placed in a GC-MS vial and the solvent evaporated under N_2. Pyridine (10 μL) and BSTFA (40 μL) were added to the vial which was incubated at 80 °C for 20 min, after which the solvent evaporated under N_2. A further 20 μL of BSTFA was added and the mixture incubated at 80 °C for a further 15 min, after which the solvent was evaporated under N_2 and the residue transferred in chloroform to an auto-sampling vial.

HPLC procedures

Reverse phase HPLC (Waters Associates, Milford, USA) was used to separate the various components of extracts to allow identification and quantification of trace metabolites. Two HPLC systems, each consisting of a Rheodyne Manual Injector fitted with a 2 mL sample loading loop, a Waters Absorbance Detector and a μBondapak C_{18} 10 μm, 100 mm x 8 mm Radial-Pak cartridge (Jager et al., 2005), were used, primarily for separation of radio-labelled metabolites. The two systems differed in pump function. The first utilised two Waters 510 Millipore HPLC pumps and the second utilised a Waters 1525 HPLC pump.

HPLC loading

An aliquot of the extract was purified using a C_{18} Sep-Pak (see procedure above) and the eluate evaporated under reduced pressure. The residue was then dissolved in 2 mL of initial conditions, and injected into the HPLC using a filtered syringe.

HPLC program 1 (2x Waters 510 Millipore Pump)

Eluent A: 1 % v/v acetic acid in H_2O, eluent B: 1 % v/v acetic acid in ACN; flow rate: 1 $mL.min^{-1}$. Gradient: 0-20 min: 10-60 % B, 20-30 min: 60-100 % B, 30-35 min: 100 % B

HPLC program 2 (Waters 1525 Binary Pump)

Eluent A: 1 % v/v acetic acid in water, eluent B: 1 % v/v acetic acid in ACN; flow rate: 1 $mL.min^{-1}$. Gradient: 0-25 min: 5-70 % B, 25-40 min: 70-100 %B, 40-50 min: 100 % B.

Scintillation counting

Ready Safe Liquid Scintillation Cocktail (Beckman Coulter; 4 mL) was added to samples of the appropriate volume (ca. 0.5-2 mL). Vigorous shaking ensured proper mixing. The samples were then analysed using a Beckman LS 6500 Multipurpose Scintillation Counter.

LC-MS

In preparation for LC-MS an aliquot of the sample was taken and the solvent removed under reduced pressure; the residue was then transferred in 3 x 500 μL of MeOH to a scintillation vial.

The solvent was then evaporated under N_2 and the residue transferred to an auto-sampling vial in 100 μL of ACN.

For LC-MS analysis three systems were used. The first was a Waters Alliance 2690 HPLC coupled to a Finnegan LCQ Classic ion trap mass spectrometer was used, with a μBondapak C_{18} 10 μm, 100 mm x 8 mm Radial-Pak cartridge. The mass spectrometer was operated in APCI mode, using a vaporiser temperature of 360 °C, a capillary temperature of 165 °C, with N_2 sheath gas at 240 kPa. This LC-MS system will be referred to as the 'Alliance' for the remainder of this thesis.

The second system was comprised of a Thermo Finnegan Surveyor Plus HPLC coupled to a Thermo Finnegan LTQ Orbitrap MS (which is made up of a high resolution electrostatic trap MS and a standard 2D iontrap MS; however, for most analyses, only the iontrap MS was used). The second system also utilised a μBondapak C_{18} 10 μm, 100 mm x 8 mm Radial-Pak cartridge. This system will be referred to as the 'Finnegan' in this thesis.

The third LC-MS system consisted of a Thermo Fischer Surveyor MS-plus HPLC with a μBondapak C_{18} 10 μm, 100 mm x 8 mm Radial-Pak cartridge coupled to a Thermo Fischer LTQ Orbitrap high resolution MS. The MS was operated in both APCI and ESI modes. In APCI mode a vaporiser temperature of 350 °C and a capillary temperature of 200 °C were used, with a N_2 sheath and auxiliary gas at 40 and 10, respectively, and a tube lens voltage of 50 V. In ESI mode a source voltage of 5 kV was applied at the tip with a capillary temperature of 300 °C, N_2 sheath and auxiliary gases at 50 and 10, respectively and a tube lens voltage of 50 V. The CE for MS/MS experiments was 35 %. The system was run using the following conditions: eluent A: 1 % v/v acetic acid in H_2O; eluent B: 1 % v/v acetic acid in ACN; flow rate: 1 $mL.min^{-1}$; gradient: 0-20 min: 10-60 % B, 20-30 min: 60-100 % B, 30-35 min: 100 % B. This system will be referred to as the 'Orbitrap' in this thesis.

Typically the LC-MS systems were operated in SIM mode. For all three systems, ions to be monitored were selected based on the fragmentation patterns of synthetic standards of the compounds of interest.

GC-MS

Two GC-MS systems were used.

The first GC-MS system was comprised of a Varian 3800 GC coupled to a Varian 1200 triple quadrupole MS; Varian Star analysis software was used. The column was a Varian 'Factor Four' VF-5 ms (30 m x 0.25 mm ID and 0.25 μm film thickness), using a Varian 1177 split/splitless injector, operated at 250 °C in splitless mode, which typically delivered 1 μL to the column. Helium was used as the GC carrier gas, to give a flow of 1.4 $mL.min^{-1}$ (constant flow mode). The transfer line between the GC and MS was maintained at 290 °C. The ion source temperature was 220 °C. Frequently, SIM mode was used. Where full scan analyses were required, the range *m/z* 70 to 470 was scanned at 3 $scans.s^{-1}$. This GC-MS system will be referred to as the 'Varian' in this thesis.

The second GC-MS system consisted of a Hewlett Packard 5890 GC coupled to a Kratos Concept ISQ MS, controlled by a Mach 3 data system. 1 μL splitless injections were made at 250 °C onto a Hewlett Packard HP1 column (25 m x 0.32 mm ID, 0.17 μm film thickness). Helium was used as the carrier gas at a flow rate of 2 $mL.min^{-1}$, under a pressure of 190 kPa. The temperature gradient was as follows: 60-150 °C at 30 $°C.min^{-1}$, 150-290 °C at 10 $°C.min^{-1}$. This GC-MS system will be referred to as the 'Kratos' in this thesis.

UPLC-MS

In preparation for UPLC-MS analysis aqueous samples were diluted with acetic acid in MeOH (5 % v/v) such that the final mixture contained H_2O/MeOH/acetic acid in a ratio of 80:19:1; for methanol based extracts, the solvent was evaporated (either under N_2 or under reduced pressure) and the residue reconstituted in acetic acid in H_2O (1 % v/v).

Samples were analysed using a Waters Acquity H-series UPLC coupled to a Waters Xevo triple quadrupole mass spectrometer. A Waters Acquity UPLC BEH C_{18} column (2.1- x 100-mm x 1.7-μm particles) was used. There were two solvent combinations: (1) 5 mM ammonium acetate (pH 5.4; Solvent A) and acetonitrile (Solvent B) and (2) 1 % v/v acetic acid in H_2O (Solvent A) and acetonitrile (Solvent B).

Acetic acid program

Using solvent combination (1), the UPLC program was 80 % A:20 % B to 50 % A:50 % B at 4.5 minutes, and this was followed by immediate re-equilibration to starting conditions for 3 min.

The flow rate was 0.35 mL min^{-1}, the column was held at 35 °C and the sample compartment was at 6 °C. Approximate RTs using this solvent combination were 0.89 min for Trp, 1.0 min for keto-IPyA, 1.2 min enol-IPyA, 1.3 min for both IAA and [$^{13}C_6$]IAA, 1.1 min for 4-Cl-Trp, 1.3 min for keto-4-Cl-IPyA, 2.0 min for enol-4-Cl-IPyA and 2.2 min for 4-Cl-IAA and [$^{2}H_3$]4-Cl-IAA.

pH 5.4 program

Using solvent combination (2), the UPLC program was 80 % A:20 % B to 50 % A:50 % B at 4.5 minutes, and this was followed by immediate re-equilibration to starting conditions for 3 min. The flow rate was 0.35 mL min^{-1}, the column was held at 35 °C and the sample compartment was at 6 °C. RTs using this solvent combination were approximately 1.7 min for keto-IPyA, 3.5 min for enol-IPyA, 2.7 min for IAA, 2.2 min for keto-4-Cl-IPyA, 3.9 min for enol-4-Cl-IPyA and 3.3 min for 4-Cl-IAA.

'Slow' program

For improved separation of interfering peaks for IAM analyses solvent combination (2) and a slower gradient were employed; this was a linear gradient from 99 % A:1 % B to 80 % A:20 % B at 6 min, followed by a linear gradient to 40 % A:60 % B at 12 min followed by immediate re-equilibration to starting conditions for 3 min.

Mass spectrometer

The mass spectrometer for UPLC-MS was operated in positive ion electrospray mode with a needle voltage of 2.8 kV, and MRM was used to detect all analytes. The ion source temperature was 130 °C, the desolvation gas was N_2 at 950 $L.h^{-1}$, the cone gas flow was 100 $L.h^{-1}$ and the desolvation temperature was 450 °C. Data was processed using MassLynx software.

For Trp, IAA, IPyA and IAM, all MRM transitions were monitored in a single time window with a dwell time of 92 ms per channel. The channels were: IAA: *m/z* 176.15 to 130.1, $^{13}C_6$ IAA: *m/z* 182.15 to 136.1 (cone voltage 18 V, CE 18 V), Trp: *m/z* 205.2 to 146.1 (cone 17 V, CE 17 V) and *m/z* 205.2 to 188.1 (cone 17 V, CE 10 V), IPyA: *m/z* 204.2 to 130.1 (cone 18 V, CE 22 V) and *m/z* 204.2 to 158.1 (cone 18 V, CE 22 V), ILA: *m/z* 206.1 to *m/z* 160.05, cone voltage 18V, CE 12 V, IAM: *m/z* 175.1 to 130.1 and *m/z* 181.1 to 135.1 (cone 24 V, CE 15 V).

The chlorinated analogues were analysed in 3 overlapping time windows. The first window from 0 to 1.6 min was for 4-Cl-Trp (dwell 95 ms per channel), the second window from 0 to 6 min was for 4-Cl-IPyA (dwell 66 ms per channel) and the third from 1.6 to 6 min was for 4-Cl-IAA and [D_4]4-Cl-IAA (dwell 66 ms per channel). MRM channels for the chlorinated species were: 4-^{35}Cl-Trp: *m/z* 239.2 to 222.2, 4-^{37}Cl-Trp: *m/z* 241.2 to 224.2, [D_3]4-Cl-Trp: *m/z* 242.2 to 225.2 and *m/z* 242.2 to 224.2 (cone 19 V, CE 12 V), 4-^{35}Cl-IPyA: *m/z* 238.2 to 164.1 and 238.2 to 192.1, 4-^{37}Cl- IPyA: *m/z* 240.2 to 166.1 (cone 20 V, CE 24 V), 4-^{35}Cl-IAA: *m/z* 210.05 to 164.05, [D_2]4-^{35}Cl- IAA and 4-^{37}Cl- IAA: *m/z* 212.05 to 166.05, [D_3]4-^{35}Cl-IAA: *m/z* 213.05 to 167.05 (cone 20 V, CE 18 V).

When full scan MS/MS was required, the cone voltage and the CE were 20 V.

NMR

The majority of NMR analyses were conducted on a Varian 300 MHz NMR Spectrometer System using VNMR 6.1C software. Water-suppression ^{1}H NMR and multiplicity-edited ^{13}C-^{1}H HSQC NMR analyses were conducted using a Varian Inova wide bore 400 MHz Spectrometer with Mnova 6.1 software (Mestrelab Research, S.L. Spain). Typically, for ^{1}H spectra four scans were acquired and for ^{13}C spectra 4000+ scans were acquired.

Molecular procedures

Luria Broth (LB)

NaCl, Tryptone Peptone (Amresco) and yeast extract (Amresco) were dissolved in H_2O to give final concentrations of 10 g.L^{-1}, 10 g.L^{-1} and 5 g.L^{-1}, respectively and the mixture was stirred at room temperature for ca. 10 min. The pH was then adjusted to ca. 7-7.5 using conc. NaOH. The resulting solution was autoclaved before use and the appropriate antibiotic was added (100 mg.L^{-1}).

Agar gel for plates

Agar powder (Amresco) was added to LB to give a final concentration of 1.5 % w/v. The resulting mixture was autoclaved and stored at 55 °C until required.

Glycerol stocks

0.2 µl of glycerol in H_2O (80 % v/v; Amresco) was placed in a 1.5 mL screw-top vial and autoclaved. After the glycerol had cooled, 0.85 µL of an overnight culture (in LB) was added and the mixture shaken vigorously. The tube was snap frozen in liquid N_2 and stored at -70 °C.

Super-Optimal Broth with Catabolite repression (SOC)

Tryptone Peptone (2 g) and yeast extract (0.5 g) were dissolved in H_2O (97.5 mL) and the solution was autoclaved. Just before use, sterile $MgSO_4$ (1 M; 1 mL), $MgCl_2$ (1 M; 1 mL), NaCl (5 M; 200 µL), KCl (1 M; 250 µL), D-glucose (Amresco; anhydrous; 0.36 g) and the appropriate antibiotic (final concentration: 100 $mg.L^{-1}$) were added.

Terrific Broth (TB)

The broth base was made up by dissolving Tryptone Peptone (12 g), yeast extract (24 g) and glycerol (50 % v/v; 8 mL) in H_2O (900 mL). This mixture was autoclaved and just prior to use K_2HPO_4/KH_2PO_4 buffer (0.89 M; pH 7.8; 100 mL) was added.

Protein expression and purification

The following procedure (adapted from the NEB pMAL Protein Fusion and Purification Instruction Manuel) was used for expression and purification of PsTAR1- PsTAR2- and AtYUC1-maltose-binding protein (MBP) fusion products.

A starter culture was prepared by inoculating SOC (15 mL), containing AMP (Sigma-Aldrich Co.; 100 µg mL^{-1}), with *E. coli* (JM109, Promega) known to contain the gene of interest in-frame in the pMAL vector. A 'vector only' starter culture was also prepared. The starter cultures were incubated at 37 °C for 16 h with shaking, after which the OD_{600} for each sample was determined by UV-Vis spectrophotometry with SOC as a blank. 10 mL of each starter culture was diluted to 1.0 L with sterile TB containing AMP (100 mg L^{-1}). These broths were incubated at 37 °C, with shaking, until the OD_{600} was greater than or equal to 0.5 (TB blank; usually between 3 and 6 h). The mixtures were then cooled to ca. 30 °C and IPTG (Sigma-Aldrich Co.; filter-sterilized) was added to each one to a final concentration of 300 µM. For *PsTAR1* and *PsTAR2*, PLP (Sigma-Aldrich Co.; filter-sterilized) was added to a final concentration of 200 µM; for *AtYUC1*,

riboflavin was added to a final concentration of 8 $mg.L^{-1}$. The resulting broth was incubated for ca. 20 h with shaking at 23-30 °C.

The flasks were then briefly cooled on ice and the OD_{600} of each sample was determined (>0.5). Aliquots (0.5 mL) from each sample were taken for SDS-PAGE. The remainders of each sample were centrifuged at 4.0 x 10^3 g for 20-30 min at 4 °C after which the supernatants were discarded. The pellets were re-suspended in lysis buffer [30 mL; 50 mM K_2HPO_4/KH_2PO_4 buffer (pH 8.5), 1 mM DTT (Aldrich), 1 mM EDTA (Sigma-Aldrich, Co.), 0.2 mM PLP (Sigma-Aldrich, Co.), 0.5 M PMSF (Sigma-Aldrich Co.; added just before use)] and the resulting broth was cooled overnight to -20 °C.

The slurries were thawed in cold water, sonicated (on ice, using a probe sonicator) in 15 sec bursts for a total of 4 min. The resulting slurries were centrifuged at 4 °C and 2.0 x 10^4 g for 20 min to obtain the crude extract (supernatant), which was kept at -20 °C until purification.

MBP (vector only) and MBP-fusion proteins were purified as follows. The agarose bead suspension (part of the NEB pMAL Protein Fusion and Purification kit) was poured into a glass chromatography column (2.5-cm ID), which was then washed with H_2O (120 mL), SDS (45 mL; 0.1 % v/v), cold H_2O (60 mL) and finally column buffer (75 mL; 100 mM K_2HPO_4/KH_2PO_4; pH 8.5) at a flow rate of 5 $mL.min^{-1}$. The crude extract, diluted 1 in 6 with lysis buffer, was loaded onto the column at a flow rate of 3 $mL.min^{-1}$. The column was then washed with cold washing buffer [50 mM K_2HPO_4/KH_2PO_4 buffer (pH 8.5), 0.2 mM PLP, 0.5 mM PMSF (added just before use); 180 mL, flow rate 5 mL min^{-1}]. The protein was eluted with elution buffer (10 mM maltose in washing buffer; 15 mL) followed by column buffer (15 mL). Fractions (2.5 mL) were collected and the total protein concentration determined by spectrophotometry (Thermo Scientific NanoDrop 8000); the fractions were stored at -70 °C until needed.

Chapter 3 Metabolism of tryptamine in pea[1]

Introduction

There are many anabolic and catabolic processes occurring simultaneously in all living organisms. Sometimes biosynthetic pathways are thought of as linear and separate from other processes, but this may not always be the case; rather, many biosynthetic processes are part of a complex matrix of interconnected pathways (Mann, 2004). This fact, along with others, increases the complexity of the study of biosynthesis and can lead to incorrect interpretation of results.

Several proposed IAA biosynthetic pathways include TAM as an intermediate. TAM was proposed as an IAA precursor after its auxin-like activity in *Avena* coleoptile elongation assays was observed (Winter, 1966) and has been identified as an endogenous compound in tomato (Cooney and Nonhebel, 1991) and pea (Quittenden et al., 2009). TAM has been substantiated as an IAA precursor in pea roots (Quittenden et al., 2009) despite previous suggestions that TAM is not a major precursor in tomato (Cooney and Nonhebel, 1991). Songstad et al. (1990) also claimed that TAM was probably not a major IAA precursor in tobacco. Their logic was as follows: a mutant was generated that had high TAM levels, but when the IAA levels of the plant were determined, they were normal; they suggest that TAM is quickly sequestered into a vacuole, and therefore unavailable for IAA synthesis. However, if the TAM pathway is part of a network of pathways, then high amounts of this intermediate may be able to be diverted into other pathways. More recently there has been renewed focus on the TAM pathway due to isolation of the YUC genes from *Arabidopsis* (Zhao et al., 2001; Cheng et al., 2006, 2007), tomato (Expósito-Rodríguez et al., 2007), rice (Yamamoto et al., 2007), petunia (Tobeña-Santamaria et al., 2002) and maize (LeClere et al., 2010).

In this series of experiments, the metabolic fate of TAM in pea roots is examined using [^{14}C]TAM. The aim is to demonstrate whether or not TAM is converted to compounds other than IAA and, if it is, to identify these compounds.

[1] Part of this study has been published in the research article Quittenden LJ, Davies NW, Smith JA, Molesworth PP, Tivendale ND, Ross JJ (2009) Auxin biosynthesis in pea: characterization of the tryptamine pathway. Plant Physiology **151:** 1130-1138

Materials and Methods

This study was comprised of two main experiments: feeding of [^{14}C]TAM to pea roots and creation of an extract from a relatively large amount of root material for analysis of endogenous compounds (Table 3.1). All samples derived by extracting plant material have an ‘e’ after their number and samples which came from the feeding tubes have the letters ‘ft’ after the sample number.

Table 3.1 - Sample abbreviations and related data for pea root extracts.

Sample abbreviation	Description	Substrate	Amount of substrate fed (DPM)	FW (g)	Volume (mL)
3.1e	Pea root extract	[^{14}C]TAM	9.0 x 10^6	0.7090	225
3.1ft	[^{14}C]TAM feeding tube	[^{14}C]TAM		N/A	10.5
3.2e	Pea root extract	[^{14}C]TAM	9.0 x 10^5	0.5277	220
3.2ft	[^{14}C]TAM feeding tube	[^{14}C]TAM		N/A	10.5
3.3e	Pea root extract	No substrate	No substrate	0.5353	325
3.3ft	Feeding tube			N/A	11.5
3.4ft	[^{14}C]TAM feeding tube	[^{14}C]TAM	9.0 x 10^5	0.000	12.0
4.1e	Pea root extract	No substrate	No substrate	28.57	540
12.1e	Pea root extract	[^{14}C]NAcTAM	1.5 x 10^5 DPM		

Preparation [^{14}C]TAM-fed root extracts

MS agar medium was prepared in water (1.0 L), using Murashige and Skoog basal medium (Sigma; 3.08 g) sucrose (20.73 g) and agar powder (1.14 g). The medium was sterilised, along with 500 mL of water, by autoclaving for 1 h. Agar was then poured into each of 60 sterile plastic tubes (10 mL in each) and, after the agar was set, one pea seed was planted in each tube,

as previously described by Quittenden et al. (2009). The testa of each seed was sterilised with ethanol prior to planting. The tubes were loosely capped and left in the dark for 1 week (under conditions previously described in Jager et al., 2007), after which the germinated seeds were removed from the agar, and eight were placed in each of two plastic tubes, full of sterile water, such that the seeds were hanging on the edge of the tube and the roots dangling in the water. To one of these tubes was added 40.5 µL of [^{14}C]TAM (ca. 9.0 x 10^{6} DPM; 8.1 x 10^{-2} µmol) in ethanol (3.1), and to another 4.05 µL of [^{14}C]TAM (ca. 9.0 x 10^{5} DPM; 8.1 x 10^{-3} µmol) in ethanol (3.2). Two control tubes were also prepared, one with no substrate and eight roots (3.3), and another with 4.05 µL of [^{14}C]TAM (ca. 9.0 x 10^{5} DPM; 8.1 x 10^{-3} µmol) but no roots (3.4).

After 24 h, the roots were removed from their respective tubes, washed in sterile water, weighed and extracted using the MeOH/BHT method (extracts 3.1e, 3.2e and 3.3e). The water from the feeding tubes formed samples 3.1ft and 3.2ft and the water from the two control treatment tubes formed samples 3.3ft and 3.4ft.

Preparation of untreated root extract

To determine if NAcTAM (Figure 3.1) is an endogenous component of pea roots, 180 pea seeds were planted in regular pots (six per pot) in 100 % potting mix and grown as normal. After six days, the germinated seeds were removed from the pots and the roots separated from the rest of the plant and harvested into MeOH/BHT (4.1e).

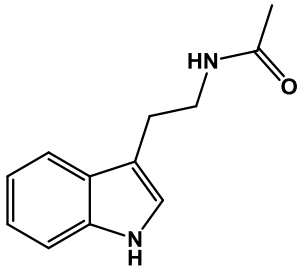

Figure 3.1 – Structural formula for NAcTAM.

Preparation of [^{14}C]*N*-acetyltryptamine-fed root extracts

To determine if NAcTAM could be metabolised by the roots, an extract from roots that had been fed [^{14}C]NAcTAM (obtained by HPLC separation of a pea root extract after feeding [^{14}C]TAM, as in 3.1e) were prepared in the same manner as described in the previous section (12.1e).

Analysis of extracts

To determine the extent of uptake of the applied [^{14}C]TAM, an aliquot (1 mL) was taken from each of three extracts (3.1e, 3.2e and 3.3e) and analysed by scintillation counting. Aliquots (1 mL) from each of the four feeding tubes were also analysed by scintillation counting.

To obtain a 'global picture' of TAM metabolism in these organs, aliquots of 3.1e (1 mL) and 3.2e (1 mL) were separated on HPLC (Program 1; see Chapter 2) and the fractions subjected to scintillation counting. To identify the metabolites, aliquots of 3.1e (20 mL), 3.2e (20 mL) and 3.4 (3 mL) were prepared for LC-MS as described in Chapter 2 and analysed by LC-MS on the Alliance.

To determine if NAcTAM was an endogenous compound in pea roots, an aliquot of 3.1e (3 mL) was separated on HPLC (Program e1; see Chapter 2) and 100 μl from each fraction was taken for scintillation counting. An aliquot (300 μL; 323 DPM; 2.9 pmol) of fraction 21 was taken as an internal standard and added to 4.1e (75 mL), which was then put through a Sep-Pak, eluting with ACN in H_2O (80 % v/v). The eluate was evaporated under reduced pressure and the residue separated on HPLC (Program 2; see Chapter 2). Aliquots (100 μL) from each fraction were taken and subjected to scintillation counting, which revealed a radioactive peak in fraction 14, the remainder of which (900 μL) was prepared for LC-MS as described in Chapter 2. This sample was then analysed by LC-MS on the Finnegan.

Results

Initial scintillation counting of 1-mL aliquots of extracts (Table 3.2) and feeding tubes (Table 3.3) revealed that ca. 88 % of the radioactivity supplied was taken up by the root material. The percentage substrate taken up by the roots was calculated thus:

—— ,

where x = 'total radioactivity of extract' and y = 'residual radioactivity in feeding tube'

Table 3.2 - Radioactivity of extracts of pea roots after [^{14}C]TAM feeding.

Sample	Radioactivity in 1 mL aliquot (DPM)	Total radioactivity (DPM)	% uptake of applied radioactivity
3.1e	2.36×10^4	5.32×10^6	88.93
3.2e	2.38×10^3	5.24×10^5	87.78
3.3e	8.50	2.76×10^3	

Table 3.3 - Residual radioactivity of feeding tubes, which were used to apply [^{14}C]TAM to pea roots.

Sample	Radioactivity in 1 mL aliquot (DPM)	Total radioactivity (DPM)
3.1ft	6.31×10^4	6.63×10^5
3.2ft	6.95×10^3	7.30×10^4
3.3ft	45.3	5.21×10^2
3.4ft	6.56×10^4	7.87×10^5

HPLC followed by scintillation counting of 3.1e, revealed three significant radioactive peaks (Figure 3.2). When 3.2e was analysed in a similar way, two radioactive peaks were observed (Figure 3.3). Similar treatment of 3.4ft revealed only one significant peak (Figure 3.4), indicating that the metabolite in fraction 21 was not produced when there was no root material present.

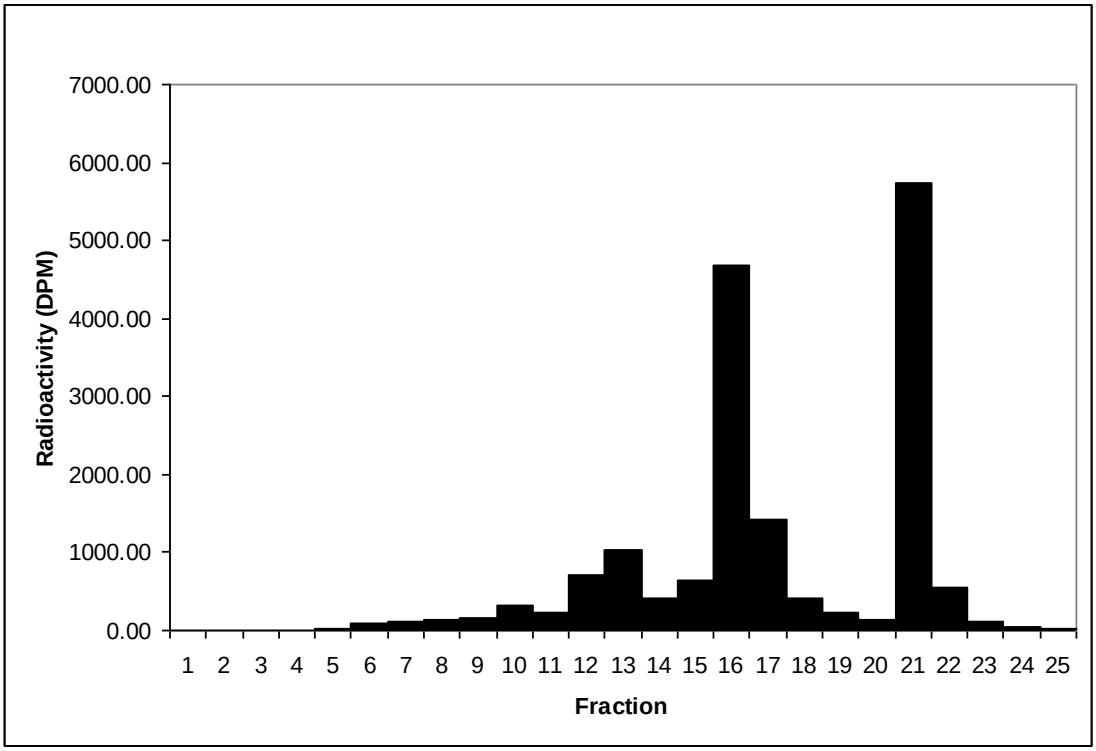

Figure 3.2 - Radioactivity of HPLC (Program 1) fractions of a pea root extract prepared after application of [^{14}C]TAM (3.1e).

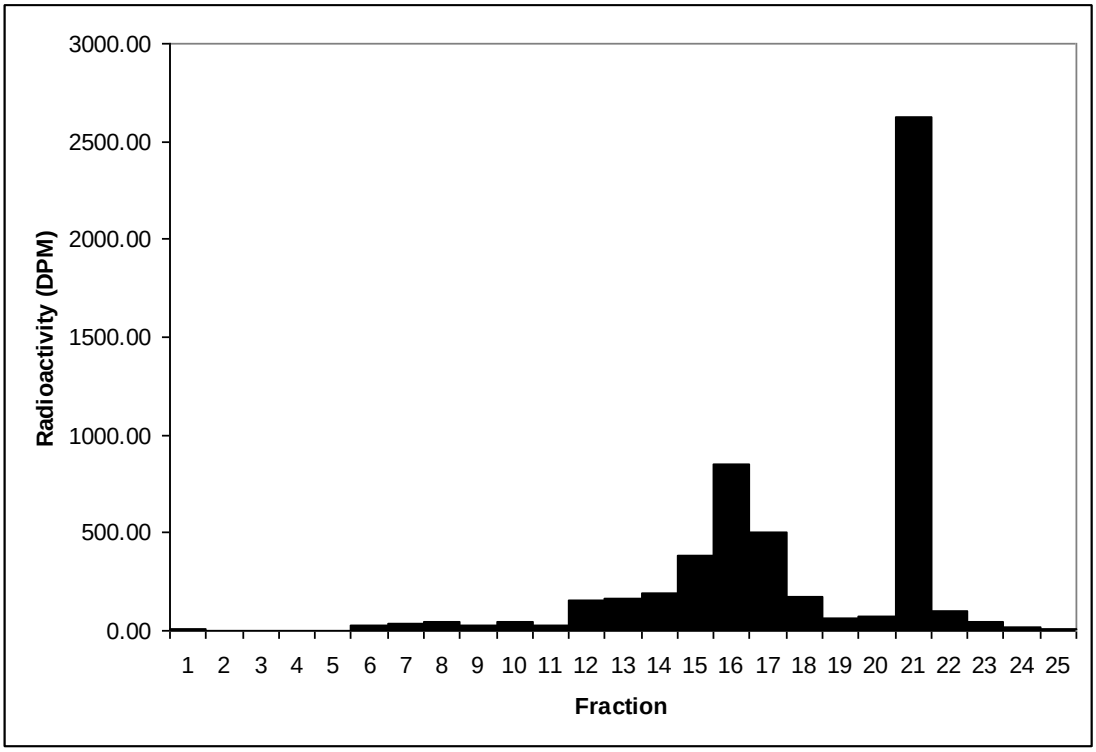

Figure 3.3 - Radioactivity of HPLC (Program 1) fractions of a pea root extract prepared after application of [^{14}C]TAM (3.2e).

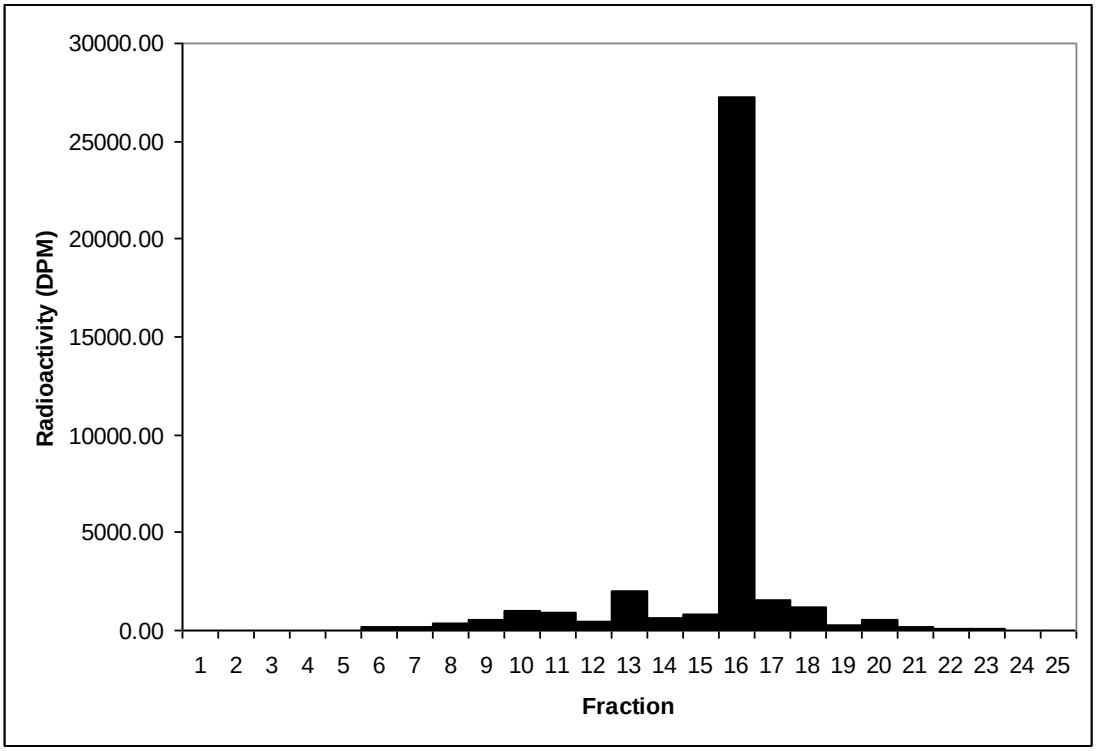

Figure 3.4– Radioactivity of HPLC (program 1) fractions of a [^{14}C]TAM feeding tube (3.4ft).

LC-MS was used to identify the three radioactive peaks in 3.1e. On the basis of full scan MS, the three compounds were identified as [^{14}C]HO-TAM (Figure 3.5), unmetabolised [^{14}C]TAM (Figure 3.6) and [^{14}C]NAcTAM (Figure 3.7) (Tivendale, 2008). The RT and MS fragmentation pattern of NHT (data not shown; see Chapter 4) did not match those of the [^{14}C]HO-TAM detected in this experiment. Although only two radioactive peaks were detected in extract 3.2e (see Figure 3.3), all three compounds were identified in the extract by LC-MS (Figure 3.8).

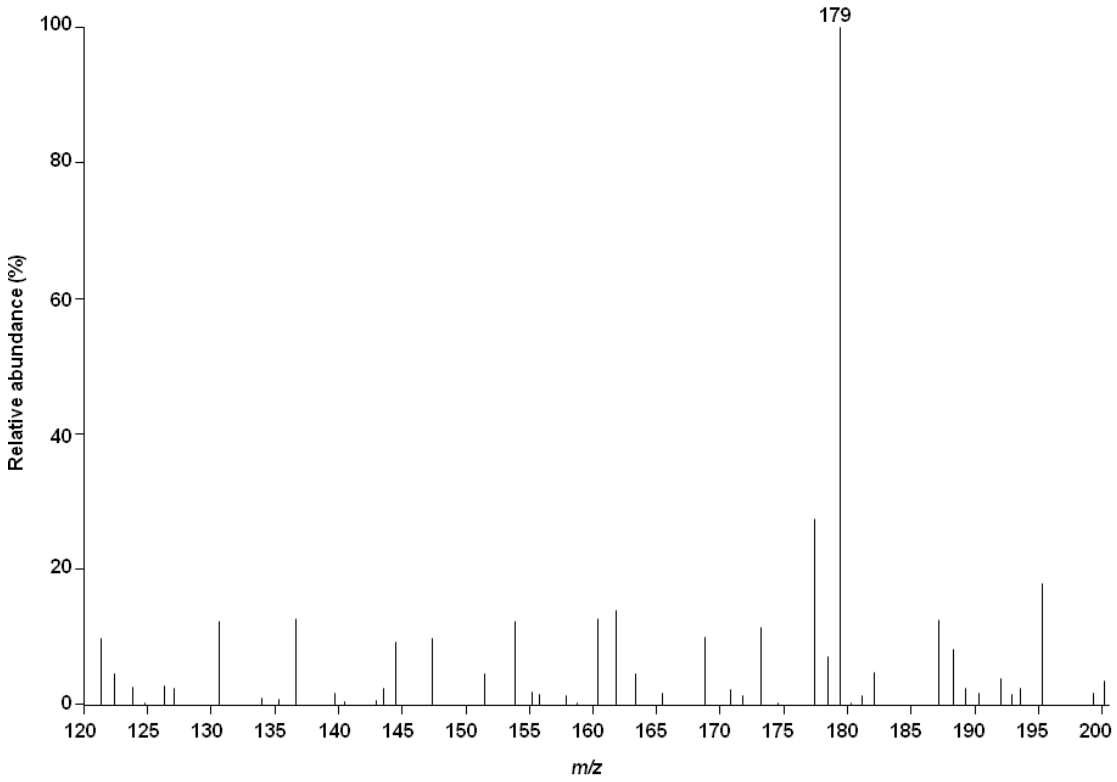

Figure 3.5 - MS of an unidentified [^{14}C]HO-TAM (obtained *via* LC-MS; RT: 8.95-9.00 min), from a pea root extract after administration of [^{14}C]TAM.

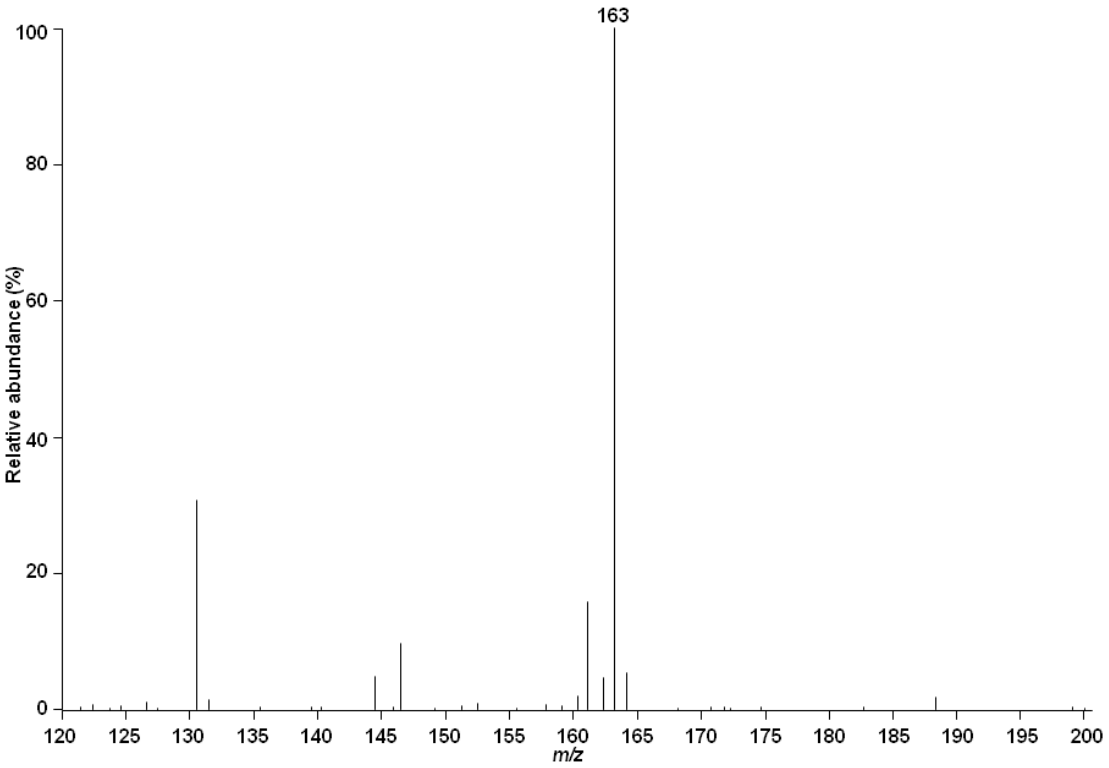

Figure 3.6 – MS of unmetabolised [^{14}C]TAM (obtained *via* LC-MS; RT 12.11-12.60 min), from a pea root extract after administration of [^{14}C]TAM.

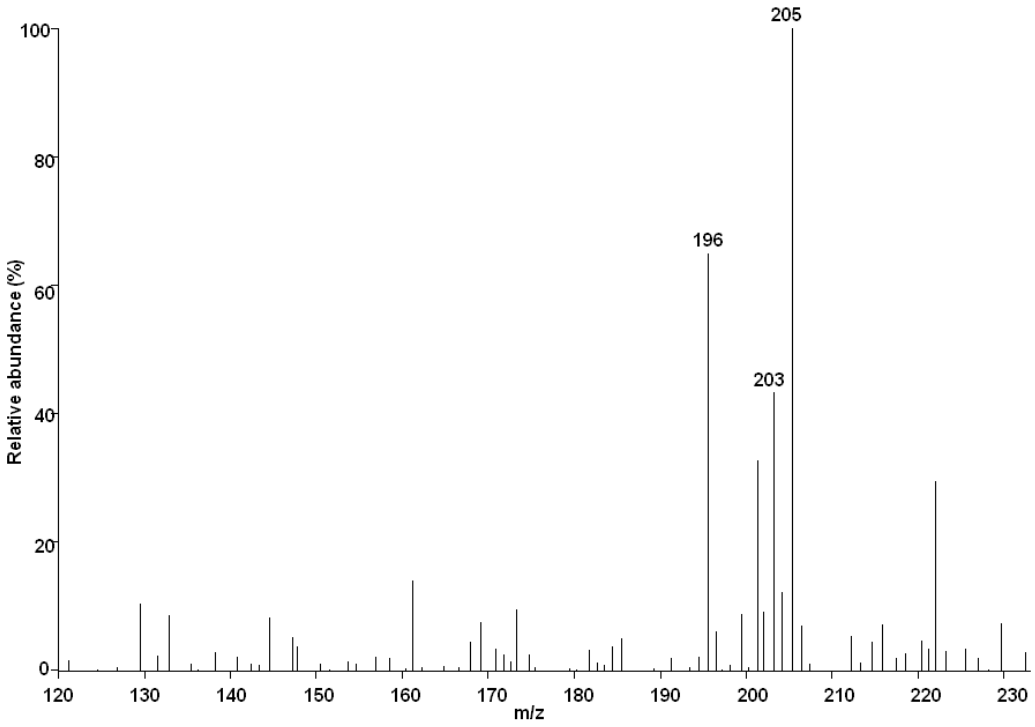

Figure 3.7 - MS of [^{14}C]NAcTAM (obtained *via* LC-MS; RT 17.16-17.28 min), from a pea root extract after administration of [^{14}C]TAM.

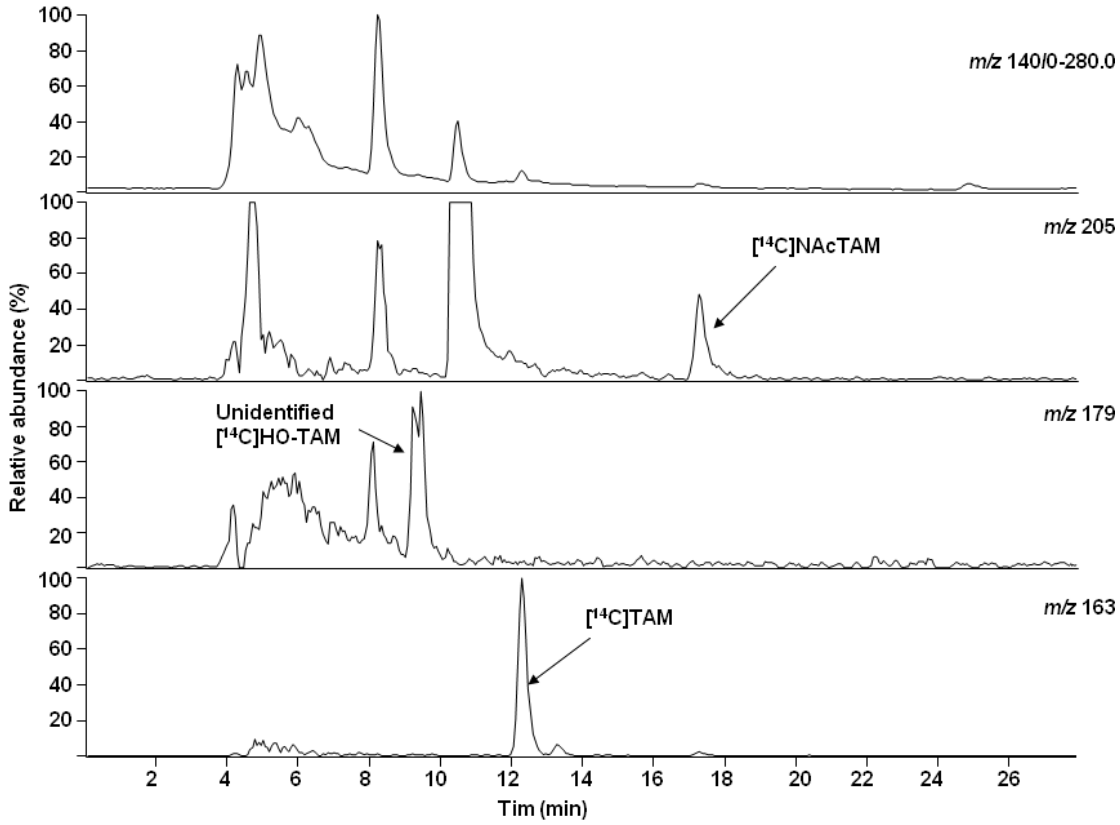

Figure 3.8 – LC-MS (SIM mode) analysis of a pea root extract (3.2e), after administration of [^{14}C]TAM.

Extract 4.1e was also analysed by LC-MS/MS, using extract 3.1e as a source of [^{14}C]NAcTAM as an internal standard. From the chromatograms of these separations (Figure 3.9 and Figure 3.10), the ratio of [^{14}C]NAcTAM to [^{12}C]NAcTAM was calculated. Analysis of 3.1e only revealed a ratio of 2.55, whereas analysis of 4.1e spiked with 3.1e revealed a ratio 2.56, thus indicating that the untreated root extract did not contain endogenous NAcTAM, or contained endogenous NAcTAM at a level below the limit of detection.

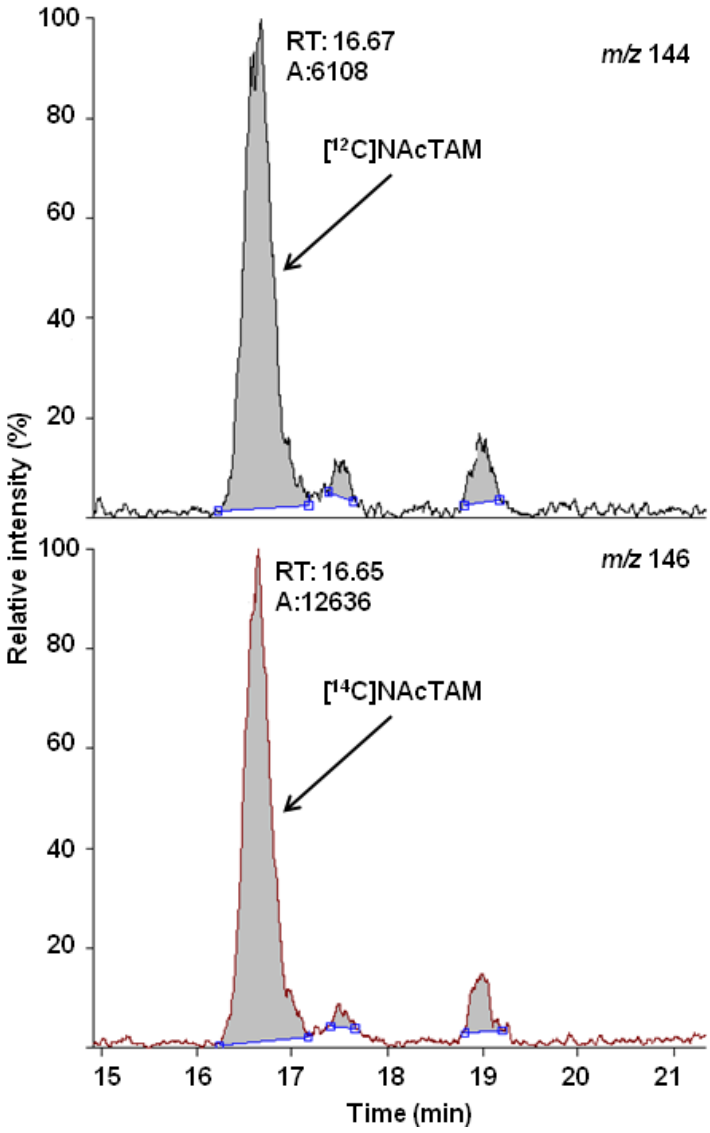

Figure 3.9- LC-MS (SIM mode) analysis of a pea root extract (3.1e), after administration of [^{14}C]TAM. Major peak was identified by MS as NAcTAM. The top channel represents [^{12}C]NAcTAM and bottom channel [^{14}C]NAcTAM.

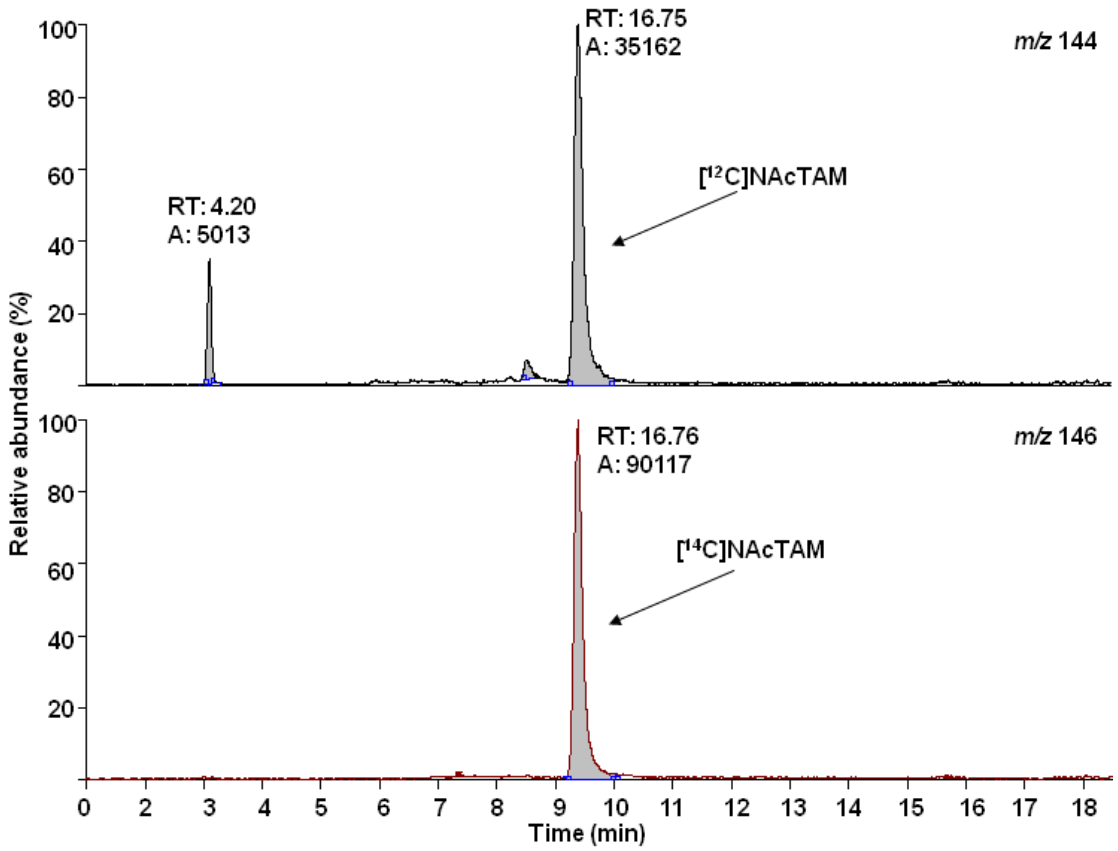

Figure 3.10 – LC-MS (SIM mode) analysis of a pea root extract (4.1e) spiked with another pea root extract (3.1e, prepared after administration of [^{14}C]TAM). The major peak was identified by MS as NAcTAM. The top channel represents [^{12}C]NAcTAM and bottom channel [^{14}C]NAcTAM.

To determine if TAM and NAcTAM exist in equilibrium in the plant, [^{14}C]NAcTAM was fed to pea roots. However, there was no detectable uptake of [^{14}C]NAcTAM by the roots (data not shown).

Discussion

In this series of experiments the metabolic fate of TAM in pea roots was examined using [^{14}C]TAM. Feeding of [^{14}C]TAM revealed several interesting findings. Firstly, pea roots appear to have a high capacity for uptake of TAM from their surrounding media; in this experiment, ca. 88 % of the applied TAM was taken up by the roots. This was the case when large or small amounts of TAM were applied. HPLC-radiocounting of two pea root extracts prepared after administration of [^{14}C]TAM revealed two major labelled compounds, which were identified by LC-MS as unmetabolised TAM and NAcTAM. Thus, it appears that when excess TAM is present in pea roots, it is diverted from the IAA pathway *via* conversion to NAcTAM. This may

explain the observation of Songstad et al. (1990), who report that transgenic tobacco plants that accumulate TAM do not accumulate IAA.

LC-MS also revealed the presence of a ^{14}C-labelled HO-TAM. One of the proposed IAA biosynthetic pathways contains the step TAM → NHT. However, the HO-TAM which incorporated ^{14}C-label in the current experiment had the wrong RT for NHT. From this experiment, it seems unlikely that NHT is involved in IAA biosynthesis; to the best of the author's knowledge, NHT has is yet to be identified as an endogenous compound in any plant species.

The endogenous level of NAcTAM in pea roots was determined by spiking aliquots of the untreated root extract with small amounts of the treated root extract, known to contain [^{14}C]NAcTAM. When the untreated extract was spiked with the treated root extract, LC-MS showed no change in $^{12}C/^{14}C$ ratio. Thus, there is no evidence that NAcTAM is an endogenous compound in pea roots under normal growing conditions. It appears that NAcTAM can be produced in pea roots but only under conditions where TAM is abundant.

From this series of experiments several conclusions can be drawn. Pea roots have a very high capacity for TAM uptake. However, even when TAM is abundant, this does not directly result in increased IAA production; rather TAM is converted to NAcTAM, which appears to be stable in the plant. NAcTAM may be converted back to TAM, and subsequently to IAA, if the plant becomes IAA deficient; however, when attempts were made to test this hypothesis, the roots did not take up the applied NAcTAM.

Chapter 4 Reassessing the role of YUCCAs in auxin biosynthesis[2]

Introduction

The TAM pathway for auxin biosynthesis (Figure 4.1) received particular attention in the 2000's, due to the identification of the *YUCCA* (*YUC*) genes (Zhao et al., 2001; Tobeña-Santamaria et al., 2002; Cheng et al., 2006, 2007; Expósito-Rodríguez et al., 2007; LeClere et al., 2010). The YUC proteins are homologous to known FMOs (Zhao et al., 2001). It has been reported that AtYUC1 (Arabidopsis; Zhao et al., 2001), and its homologues in tomato (Expósito-Rodríguez et al., 2007) and maize (LeClere et al., 2010), catalyse the formation of NHT from TAM. Both Zhao et al. (2001) and LeClere et al. (2010) based this conclusion on mass spectral identification of the product of *in vitro* assays, using recombinant YUC protein with TAM as the substrate. Expósito-Rodríguez et al. (2007), who isolated the *YUC* homologue *FZY*, provided no MS identification of their *in vitro* product, instead relying solely on HPLC co-elution of the product with synthetic 'NHT'. Zhao et al. (2001) and LeClere et al. (2010) did not present MS data for authentic NHT for comparison with their product and there are numerous differences between their published mass spectra for the putative NHT produced in their *in vitro* assays.

[2] Part of the study reported here has been published in the research article Tivendale ND, Davies NW, Molesworth PP, Davidson SE, Smith JA, Lowe EK, Reid JB, Ross JJ (2010) Reassessing the role of *N*-hydroxytryptamine in auxin biosynthesis. Plant Physiology **154:** 1957-1965 and the addendum Ross JJ, Tivendale ND, Reid JB, Davies NW, Molesworth PP, Lowe EK, Smith JA, Davidson SE (2011) Reassessing the role of YUCCAs in auxin biosynthesis. Plant Signaling and Behavior **6:** 437-439.

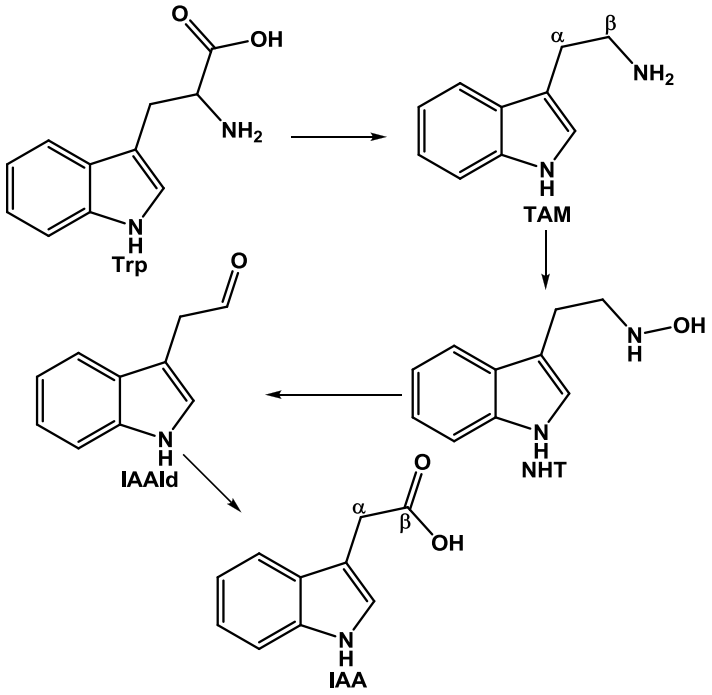

Figure 4.1 – Previously-proposed TAM-dependent IAA biosynthetic pathway, adapted from Zhao et al. (2001) and Zhao (2010).

Extensive mutant-based studies clearly show the importance of *YUC* genes for plant development (Cheng et al., 2006, 2007; Kim et al., 2007; Kim et al., 2011; Stepanova et al., 2011), and since these genes are supposedly linked to the TAM pathway by NHT, it is of paramount importance to definitively characterise this compound. At the outset of this study, this had not been achieved by ESI MS, the method used by Zhao et al. (2001) and LeClere et al. (2010) to identify reaction products. In this study, the TAM pathway is re-examined by exploiting our previously-synthesised NHT (Tivendale, 2008; Quittenden et al., 2009), and determining its mass spectral properties for comparison with the previously-published spectra for putative NHT and related compounds. In addition, the work of Zhao et al. and LeClere et al. is replicated to determine the true identity of the *in vitro* assay products.

Materials and Methods

Synthesis of NHT and LC-MS analysis of NHT, serotonin and TAM

NHT was synthesised as described previously (Tivendale, 2008; Quittenden et al., 2009) and analysed by LC-MS (Orbitrap) along with commercially-obtained serotonin (5-HT; Sigma-Aldrich Co.) and TAM.

AtYUC1 analysis

Cloning of *AtYUC1* and subsequent ligation into pMAL-c5X

cDNA of *AtYUC1* in pCHF3 plasmid was obtained from Dr Yunde Zhao (University of California, San Diego). The *AtYUC1*:pCHF3 construct was digested using SmaI and PstI (giving a blunt 5' end and a TGCA overhang at the 3' end). The vector, pMAL-c5X, was digested using XmnI and SbfI and purified using the Wizard SV gel and PCR Cleanup Kit (Promega) to remove the 54-base fragment and buffers and enzymes. The *YUC1* cDNA was then ligated into pMAL-c5X (pMAL) as described in the *Biolabs Extraction Method* manual, except the ligation method that gives the best yields at 4 °C overnight was used.

Transformation of *E. coli* with *YUC1* construct

JM109 *E. coli* were transformed with the *YUC1*:pMAL construct, using the heat shock method (Promega Corporation, 2000). To determine which colonies had been successfully transformed, a colony PCR was performed, using the following method: using a sterile wooden toothpick, a colony was picked off an agar plate and swirled in 5 μL of sterile H_2O. The toothpick was then streaked onto a numbered area on an LB plate. Sixteen replicates were performed for each of the three samples (Y3p1, Y5p1 and Y5Vp1). The samples were then denatured at 95 °C for 5 min. The master mix was prepared by mixing H_2O (36.75 μL), 10X Thermopol buffer (5 μL), dNTP (10 mM, 1 μL), forward primer (10 μM, 1 μL), reverse primer (10 μM, 1 μL) and Taq (NEB; 0.25 μL). To each sample was added 45 μL of master mix. The mixtures were then incubated at 94 °C for 2 min, after which the following temperature cycle was applied for 35 cycles: 94 °C for 15 s, 55 °C for 15 s, 72 °C for 2 min. After this, the mixtures were incubated at 72 °C for 5 min

and then cooled to 11 °C. 30 µL of each sample was separated on agarose gel. Samples that contained the correct insert were sequenced by Macrogen Inc., Korea.

AtYUC1 expression and purification

The AtYUC1-MBP fusion protein was expressed and purified using a method adapted from the *NEB pMAL Protein Fusion and Purification Instruction Manuel*, as described in Chapter 2.

***In vitro* assay using AtYUC1 and TAM**

The following method was adapted from Zhao et al. (2001) and LeClere et al. (2010). Purified AtYUC1 protein was divided into two 1.5-mL aliquots and one 100-µL aliquot. The two larger aliquots were placed in Eppendorf tubes, which contained 9.99 x 10^4 DPM of [^{14}C]TAM. The samples were concentrated under reduced pressure for 4 h after which the volumes were 130 µL. To these protein solutions were added 10 µL of $NADP^+$ (Sigma-Aldrich Co.; 14.8 $\mu g.\mu L^{-1}$), 10 µL of glucose-6-phosphate (5.2 $\mu g.\mu L^{-1}$), 15 µL of TAM (4.26 $\mu g.\mu L^{-1}$), 1.2 µL of glucose-6-phosphate dehydrogenase (Sigma-Aldrich Co.; suspension; 67.3 $units.\mu L^{-1}$) and 35 µL of sodium phosphate buffer (pH 8.4). To one of the mixtures was added 200 µL of methanol (control). The resulting mixtures were incubated at 37 °C for 3 h. After the incubation time, 200 µL of methanol was added to the test mixture and two 100-µL aliquots were taken from each sample and the solvent was removed under reduced pressure. One set of aliquots was transferred in 60 µL of 89:10:1 H_2O/ACN/acetic acid to auto-sampling vials for LC-MS analysis, and the other set were analysed by HPLC-radiocounting.

The experiment was repeated but the incubation time was increased to 20 h, as described by (LeClere et al., 2010).

The experiment was repeated once more but this time using crude protein extract and incubating once again for 3 h.

***In vitro* assay using AtYUC1 and IPyA**

The following method was adapted from Mashiguchi et al. (2011). *In vitro* assay mixtures consisted of: recombinant protein (AtYUC1-MBP or MBP; 350 $ng.\mu L^{-1}$), maltose (2 mM), NADPH (743 $ng.\mu L^{-1}$), FAD (Sigma-Aldrich Co.; 33 $ng.\mu L^{-1}$), and IPyA (20 $ng.\mu L^{-1}$) in K_2HPO_4/KH_2PO_4 buffer (10 mM pH 7.5). NPCs were also prepared by replacing the protein with

buffer. Three replicates of each assay were prepared and incubated at 30 °C for 30 min, after which the samples were removed from the bath and 10 µL of [$^{13}C_6$]IAA (10 ng.µL^{-1}), followed by 15 µL of MeOH was added to each. The samples were then analysed by UPLC-MS for IPyA, IAA and [$^{13}C_6$]IAA as described in Chapter 2.

ZmYUC analysis[3]

Expressing and purifying ZmYUC

ZmYUC1 was supplied by Prof. Prem Chourey (University of Florida, Gainesville, USA) as a pET41 (Novagen; Kanamycin resistance) construct in *E. coli* (BL21). The plasmid was prepared for sequencing (Promega Corporation, 2010), which was subsequently conducted by Macrogen Inc. (Seoul, Korea). Sequences were analysed to determine *ZmYUC* insert was in frame and contained both the Enterokinase and GST tags.

ZmYUC was expressed using the EnPresso Tablet Cultivation Set (BioSilta), adapting the following method from the manufacturer's instructions and using the antibiotic Kanamycin (100 µg.mL^{-1}). Cells were grown for 6 h at 37 °C in a pre-culture then inoculated and left shaking overnight (16 h) at 30 °C. Protein expression was then induced by addition of IPTG (final concentration 0.4 mM), after which the cultures were incubated (30 °C), with shaking, and harvested after 24 h. Cells were resuspended in 10 mL of GST Wash/Bind buffer (Novagen) with proteinase inhibitors (BioSilta) and 25 µl of stock PMSF (0.1 M) and cooled slowly to -20 °C and left at this temperature overnight. Cells were thawed in cold water, sonicated and rLysozyme (1 in 50 dilution of 50 mg.mL^{-1} stock using rLysozyme Dilution Buffer; both the rLysozyme stock and the dilution buffer were obtained from Novagen) was added to rupture any remaining intact cells. The sample was centrifuged (1.0 x 10^4 g, 20 min at room temp) and the supernatant (crude extract) was collected. RNase free DNase (23 µL; 20 U; Qiagen) was added to the crude extract, which was then divided into three fractions: one for SDS-PAGE, one to be purified by affinity chromatography, and one to be kept crude.

The column purification procedure was adapted from the Novagen GST·Bind Kits manual (Novagen, 2007) and LeClere et al. (2010). The GST·Bind Resin was poured into a chromatography column (2.5-cm ID); the protein was then loaded onto the column and the

[3] I thank Sam Cook for technical assistance with the analyses of ZmYUC.

column was washed as recommended by Novagen (2007), but rather than eluting with GST Elution Buffer, Recombinant Enterokinase (Novagen) was used to cleave ZmYUC from the GST tag (as described previously by LeClere et al., 2010). After the enterokinase was loaded, the column was left at room temperature for 1 h before the flow was resumed and 3-mL fractions were collected at the recommended flow rate. Bound protein was then eluted using GST Elution Buffer (Novagen) and collected in 3-mL fractions. Aliquots were taken from all samples and analysed by spectrophotometry to determine protein concentrations. All samples were stored at -70 °C, until needed.

In vitro assay using ZmYUC

Two protein samples were used: column purified ZmYUC and crude protein extract. To 140 µL of each sample was added 30 µL of TAM (final concentration 2 mM) and NADPH (final concentration 2 mM). An NPC was prepared in the same way but replacing the protein solution with K_2HPO_4/KH_2PO_4 buffer (pH 8.5; 10 mM). All four samples were incubated at 30 °C for 3 h. After this, acetic acid in methanol (5 % v/v) was added (final ratio 1:20:79 acetic acid/methanol/buffer) and the samples prepared for UPLC-MS as described in Chapter 2.

Results

Mass spectra of authentic NHT and serotonin

NHT was synthesised as described in Quittenden et al (2009), confirming its identity by ^{1}H and ^{13}C NMR [^{1}H (300 MHz; [D_6]DMSO) δ: 2.82 (t, *J* = 7.4 Hz, 2H), 2.99 (t, *J* = 7.4 Hz, 2H), 3.38 (bs, 2H), 6.95 (t, *J* = 7.2 Hz, 1H), 7.04 (t, *J* = 7.2 Hz, 1H), 7.11 (s, 1H), 7.31 (d, *J* = 8.1 Hz, 1H), 7.49 (d, *J* = 7.8 Hz, 1H), 10.77 (s, 1H); ^{13}C (75 MHz; [D_6]DMSO) δ: 23.6 (CH_2), 55.1 (CH_2), 112.0 (CH), 113.1 (C), 118.8 (CH), 118.9 (CH), 121.5 (CH), 123.3 (CH), 128.0 (C), 136.9 (C); see Hino et al. (1990) for ^{1}H NMR data for comparison] and MS. Synthetic NHT was analysed by LC-ESI MS (Figure 4.2A), along with commercially-obtained serotonin (Figure 4.2B) and TAM (Figure 4.3). The spectra were obtained using a Thermo LTQ ion trap/Orbitrap high resolution mass spectrometer combination to enable the assignment of empirical formulae to the ion-trap-generated product ions, based on mass measurements to 5 ppm accuracy. MS, MS/MS (MS^2) and MS/MS/MS (MS^3) were performed for all three compounds.

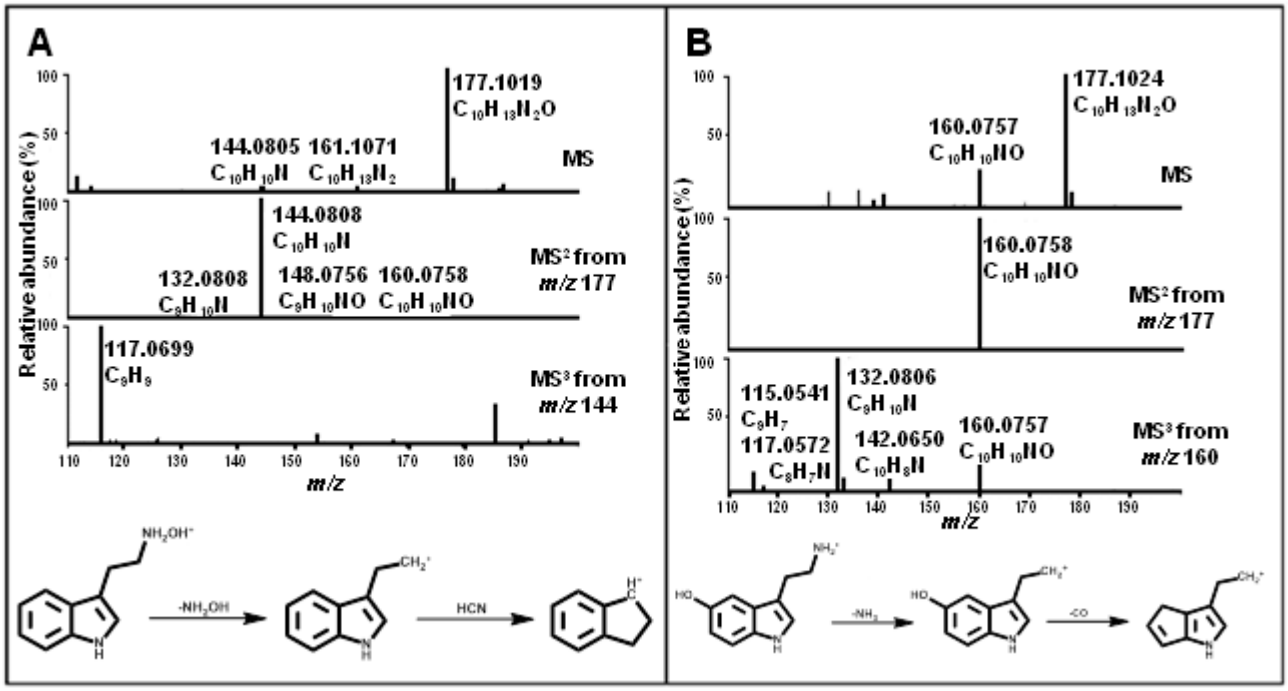

Figure 4.2 - MS, MS^2 and MS^3 data for (A) NHT and (B) serotonin and suggested fragmentation pathways for each. The collision energy for MS^2 and MS^3 was 35 %.

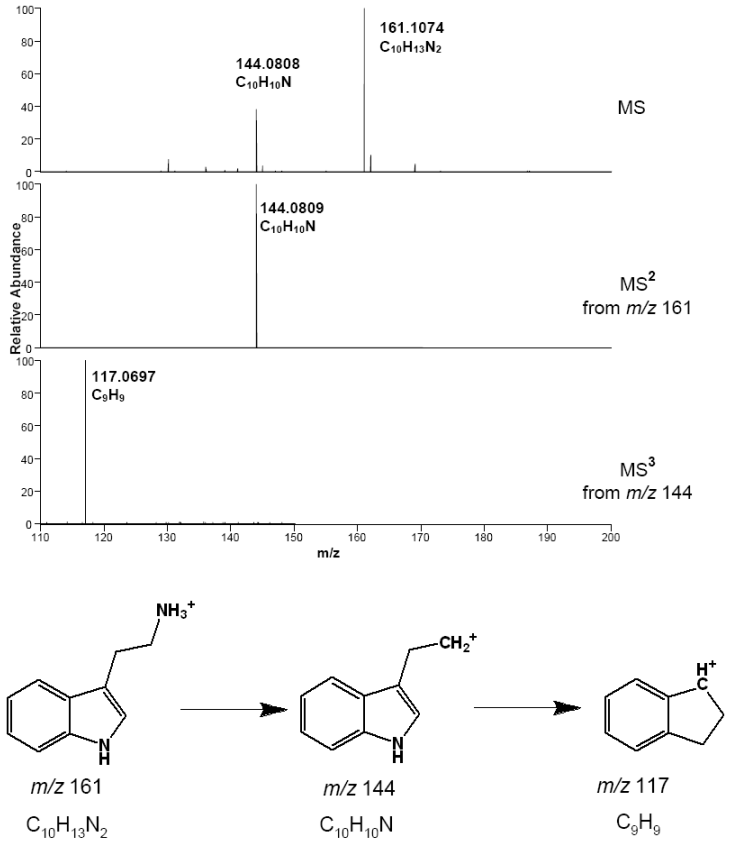

Figure 4.3 - MS, MS^2 and MS^3 data, with suggested fragmentation pattern, for TAM.

The mass spectrum of NHT revealed an intense $[M+H]^+$ ion at *m/z* 177 with a less abundant ion at *m/z* 144 (loss of NH_2OH). The predominant product ion of *m/z* 177 was *m/z* 144 (loss of NH_2OH; MS^2, Figure 4.2A) and the predominant product ion of *m/z* 144 was *m/z* 117 (loss of HCN; MS^3, Figure 4.2A). A peak at *m/z* 160 was detected in MS^2 but was very weak (1-3 % of *m/z* 144 depending on collision energy) and is not even visible in Figure 4.2A. In contrast, the mass spectrum of serotonin (also with an $[M+H]^+$ ion at m/z 177) revealed ions predominantly at *m/z* 160 (loss of NH_3) in MS^2 and *m/z* 132 (loss of CO) in MS^3. The losses of HCN (see Figure 4.2 and Figure 4.3) and CO (outlined in Figure 4.4) involve complex rearrangements and the likely formation of new rings (as proposed by McClean et al., 2002) and hence the charge and double bond distribution may not be localised exactly as shown.

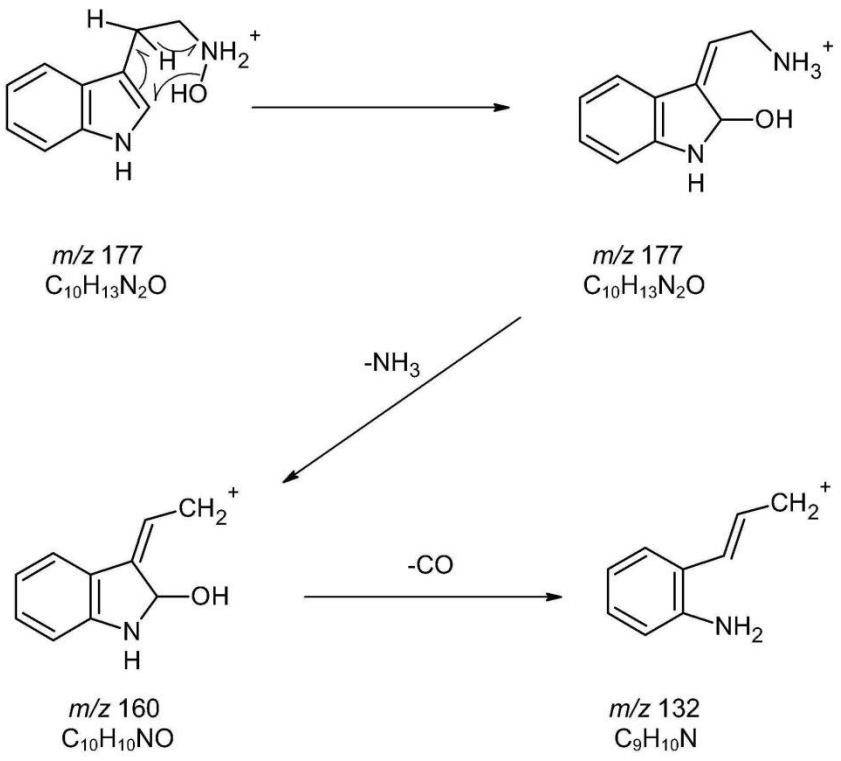

Figure 4.4 - Possible mechanism for the loss of NH_3 from NHT in MS^2 producing the very low abundance product ion at m/z 160, and the subsequent loss of CO in MS^3.

The NHT MS^2 spectrum revealed a very weak signal at *m/z* 160. With less accurate instrumentation, this loss of 17 Da from the $[M+H]^+$ (*m/z* 177) ion could be attributed to loss of either a hydroxyl radical or NH_3. However, mass data accurate to 5 ppm allow unequivocal determination of the empirical formula of the product ion and thereby the fragment lost. The $[M+H]^+$ ion had an exact mass of 177.1019 Da, while that of the product ion was 160.0758 Da. This measured loss of 17.0261 Da is NH_3 (17.0265 Da) rather than a hydroxyl radical (17.0077 Da; these masses were calculated on the basis of individual isotopes, not standard atomic weights). It is likely that in MS^2 an internal rearrangement transfers the hydroxyl group to the indole ring (Figure 4.4). MS^3 was also conducted on the *m/z* 160 ion from MS^2, which gave *m/z* 142.0650 and *m/z* 132.0807 as major product ions, due to losses of H_2O and CO, respectively. This indicates that the *m/z* 160 ion from NHT contained oxygen, confirming that it was not formed through loss of a hydroxyl radical (as NHT contains only one oxygen atom).

It is important to note that the synthetic NHT was quite labile on storage and readily converts to TAM. Consequently the sample analysed by LC-MS contained NHT with small to significant

amounts of TAM depending on the age of the standard. The small ion at *m/z* 161 in the mass spectrum of NHT (Figure 4.2A) was in fact derived from the tail of the TAM HPLC peak which eluted 1.3 min before NHT on reverse-phase LC, and not from NHT itself (NHT is less polar than TAM, as also shown by TLC analyses reported here; Figure 4.5). Another way in which artefact ions can be introduced in LC-MS analysis is through thermally-induced decomposition of the analyte. In APCI analyses of authentic NHT a strong *m/z* 161 ion was observed (data not shown) through the thermally-induced decomposition of NHT to TAM; in APCI mass spectra the *m/z* 161 ion was typically stronger than *m/z* 177.

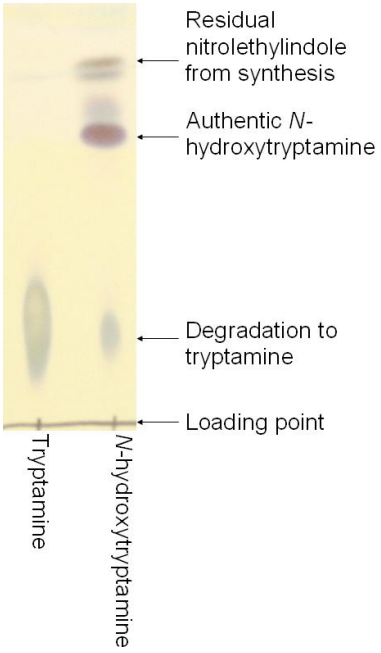

Figure 4.5 - TLC chromatogram of a mixture of NHT and TAM.

The spectra obtained here were compared with those of Zhao et al. (2001) and LeClere et al. (2010; adapted with permission in Figure 4.6) Both these groups also used ESI MS to identify the reaction products (in addition LeClere et al. included MS^2 and MS^3 data). The general appearance of our synthetic NHT MS (Figure 4.2A) was completely different from that obtained by Zhao et al. (see Figure 3C in Zhao et al., 2001) for AtYUC1 enzyme products. The Zhao et al. spectrum had a very unusual appearance for an ESI MS, due to the very weak putative $[M+H]^+$ ion at *m/z* 177 and an abundance of ions dominating the spectrum. ESI mass spectra are normally characterised by an intense signal for the protonated molecule (Smith et al., 1990) with little or

no fragmentation, as illustrated by both the data presented in this thesis and those presented by LeClere et al. (2010).

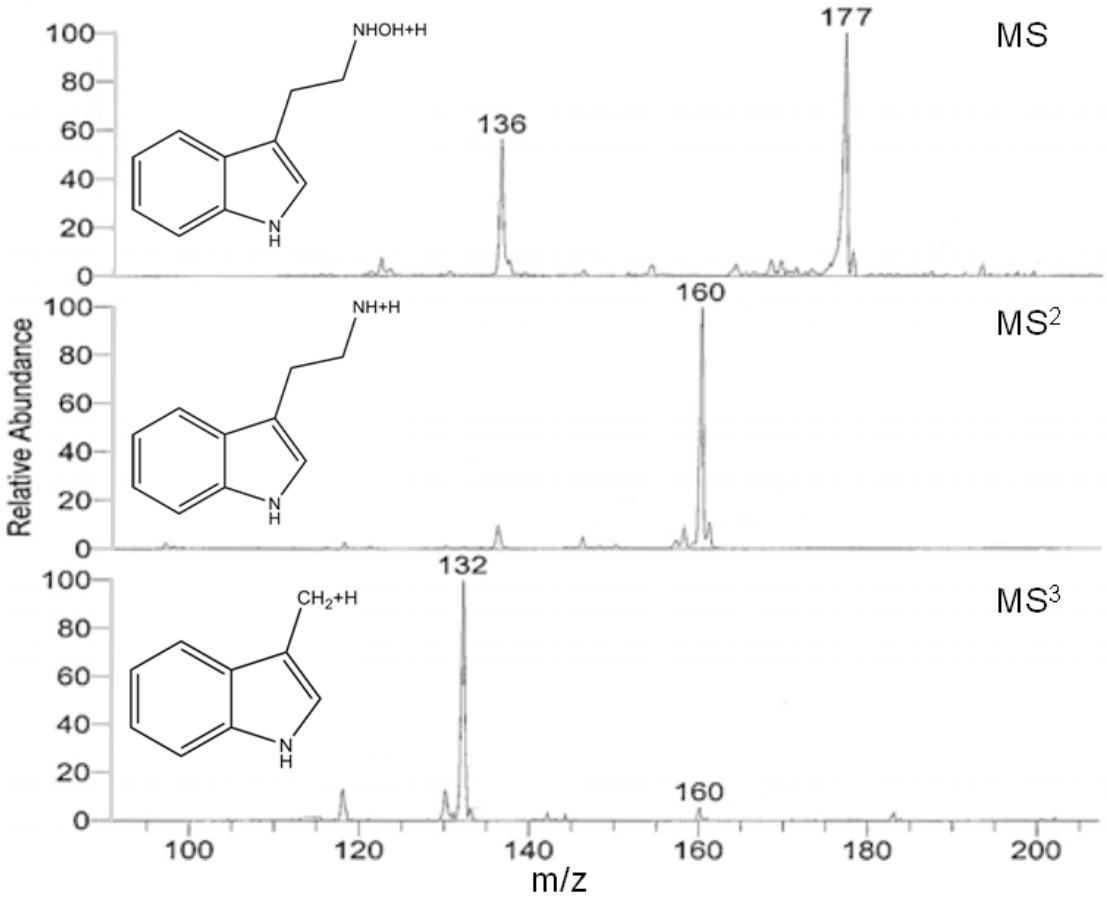

Figure 4.6 - MS^n data for putative NHT (adapted from LeClere et al. 2010 with permission).

MS^n data for authentic NHT (Figure 4.2A) were also completely different from those presented by LeClere et al. (2010) for their putative NHT (Figure 4.6). The LeClere et al. MS^2 result shows a large *m/z* 160 ion, whereas the MS^2 for authentic NHT showed predominantly *m/z* 144. On the other hand, the ring-hydroxylated TAM derivative, serotonin, generates spectra (Figure 4.2B) that closely resemble those shown by LeClere et al. (Figure 4.6). The same may also be true for other ring-hydroxylated tryptamines, and for α- and β-hydroxytryptamine (see Figure 4.1 for these positions). Serotonin had an intense *m/z* 160 ion in MS^2, caused by loss of NH_3, and an intense *m/z* 132 in MS^3, from subsequent loss of CO. Accurate mass data reported here support this previously proposed hypothesis (McClean et al., 2002) for the fragmentation of serotonin. Although NHT does undergo these same losses (Figure 4.2A), the relative abundance of the *m/z* 160 ion is extremely low.

Re-examining the function of AtYUC1

The MS analyses reported here show that YUC-like proteins may not catalyse the conversion of TAM to NHT. To investigate this further, the *AtYUC1* gene was obtained, expressed in *E. coli* (Figure 4.7A) and the recombinant protein purified by affinity chromatography (Figure 4.7B); the purified protein was then used for *in vitro* assays, using TAM as the substrate. However, no TAM metabolism was evident in this assay (Figure 4.8). Similarly the crude protein extract did not display any TAM metabolism activity (data not shown).

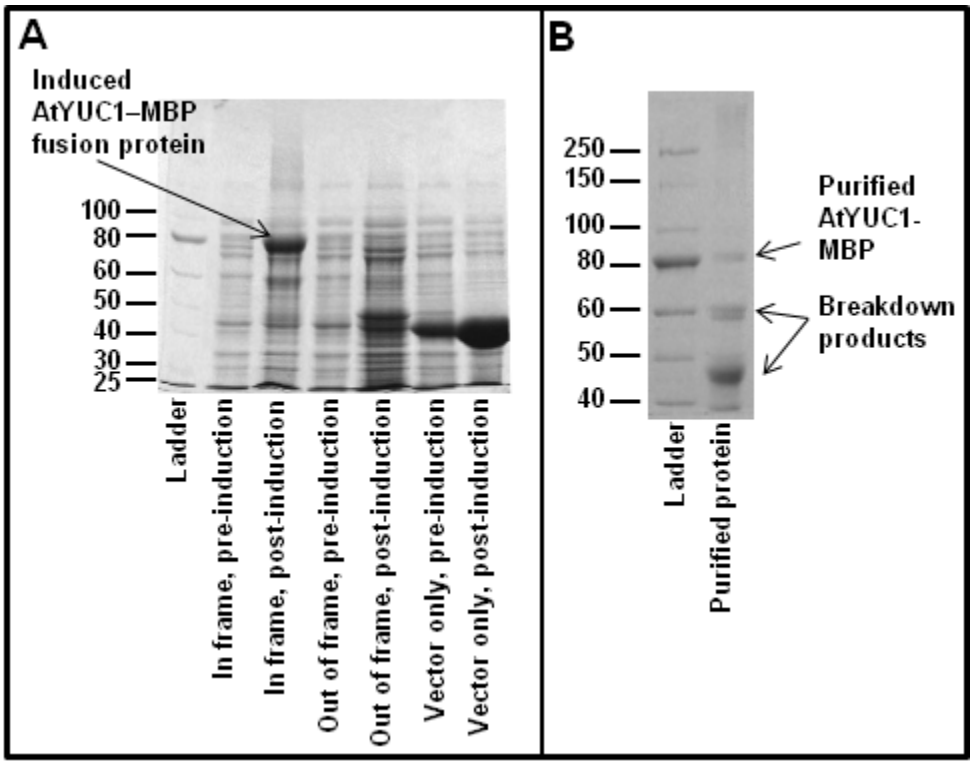

Figure 4.7 - SDS-PAGE photos showing (A) protein expression induction (AtYUC1-MBP fusion protein has a molecular weight of ca. 85 kDa; MBP has a molecular weight of ca. 40 kDa) and (B) purified AtYUC1-MBP fusion protein (85 kDa; other proteins detected in this sample are assumed to be AtYUC1-MBP breakdown products).

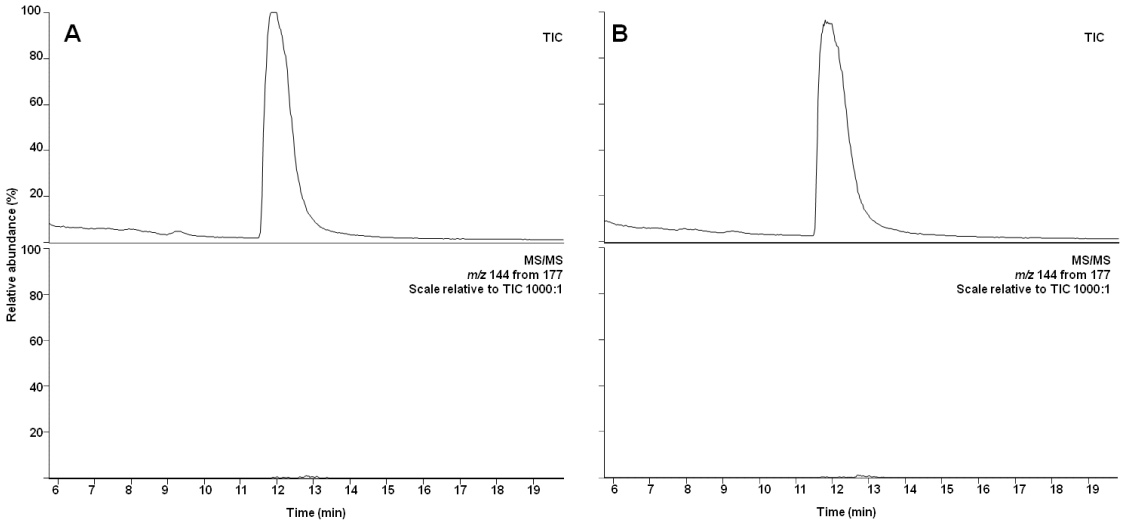

Figure 4.8 - LC-MS chromatograms of AtYUC1 *in vitro* assay reaction products. The upper channels show the TIC, the lower channels show MS^2 m/z 144 from m/z 177 (NHT). The large peak shown in the TIC is TAM. There is no difference between the test (A) and the control (B), indicating that AtYUC1 did not convert TAM to NHT.

The hypothesis that AtYUC1 catalyses the conversion of IPyA to IAA was also tested. The analysis showed no significant difference in IAA production between the tests and controls (Table 4.1). IAA is a physicochemical breakdown product of IPyA (Moore and Shaner, 1968; Gibson et al., 1972; Garcia-Tabares et al., 1987; Camilleri and Jouanin, 1991; Koga et al., 1992; Tam and Normanly, 1998).

Table 4.1 – Analysis of IAA produced from IPyA *in vitro*, as determined by UPLC-MS with a [$^{13}C_6$]IAA internal standard. AtYUC1 was used as a potential catalyst for this conversion; the other two sample sets were controls. Shown are means ± se.

Protein	IAA/[$^{13}C_6$]IAA
AtYUC1	0.30 ± 0.01
MBP	0.31 ± 0.01
No protein control	0.28 ± 0.01

Re-examining the function of ZmYUC

As further evidence that YUCs do not catalyse the conversion of TAM to NHT, several experiments similar to those described above were conducted using recombinant ZmYUC. This

analysis also showed no difference between the tests and controls and therefore provided no evidence for enzymatic conversion of TAM to NHT *in vitro*. However, two auto-oxidation products (or impurities present in the TAM) were detected in all the samples (Figure 4.9). The earlier-eluting compound had a mass spectrum (data not shown) consistent with 2-OT (see Chapter 5) and serotonin but its RT did not match either standard. The mass spectrum and RT of the later-eluting peak matched those of 2-OT (data not shown) and it was concluded that this compound was indeed 2-OT. Either of these compounds may have been the product analysed by LeClere et al. (2010). Both compounds showed a *m/z* 177 to *m/z* 160 transition, in common with the LeClere et al. product.

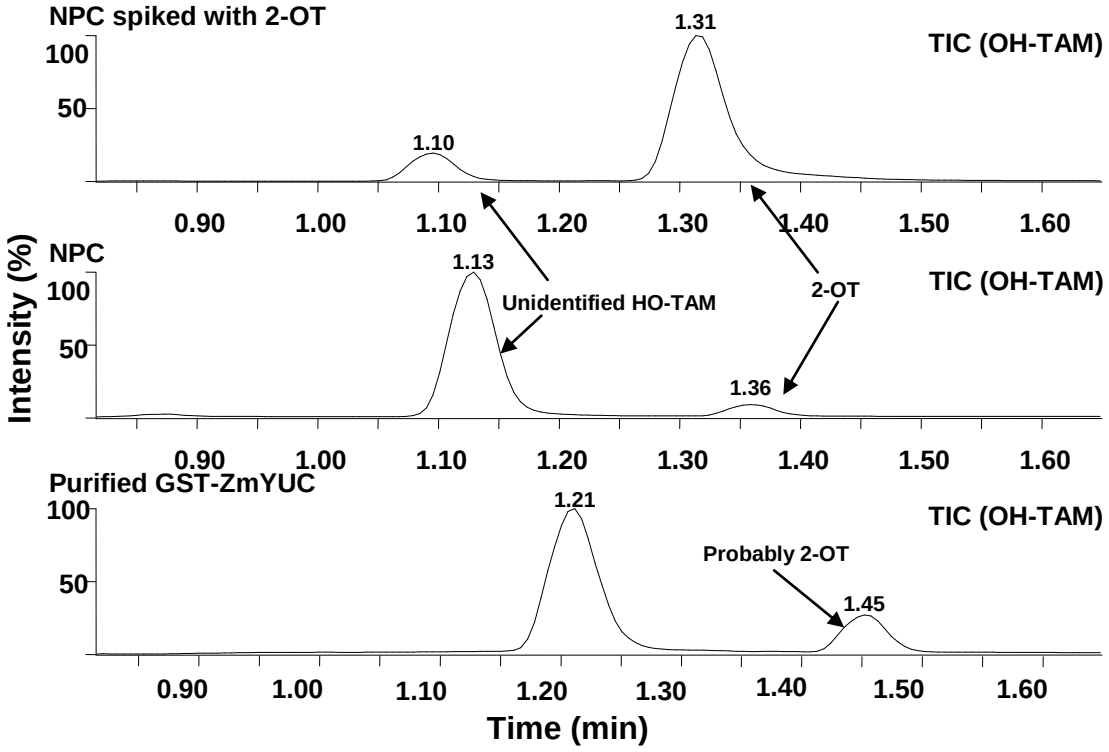

Figure 4.9 – UPLC-MS (SIR mode for HO-TAM) of several samples associated with an *in vitro* assay of recombinant purified ZmYUC. Sample names are shown on the left of each chromatogram. Through comparison with the RT and fragmentation pattern of synthetic 2-OT the peaks indicated on the chromatogram were identified. 2-OT was detected in the test case (bottom channel) and the NPC (top channel shows the NPC spiked with 2-OT and the second channel from the top shows the non-spiked NPC). The peak at 1.45 min in the 'Purified GST-ZmYUC' case is probably 2-OT and larger peak at 1.21 is probably the same unidentified HO-TAM as seen in the other samples.

Discussion

In this study the role of NHT in auxin biosynthesis was reassessed. In the first set of experiments NHT, suggested to be an important intermediate in auxin biosynthesis (Zhao et al., 2001), was characterised. A key aspect of the synthesised compound is that on ESI MS, the major MS^2 ion is *m/z* 144, not *m/z* 160. NHT is less polar than its supposed precursor, TAM, and is relatively labile. These findings, in particular the MS data, allow previous reports on the detection of NHT to be assessed. Zhao et al. (2001) reported that NHT is produced when TAM is supplied to AtYUC1 as an *in vitro* substrate and, as a result, most TAM pathway variants proposed after 2001 include the step TAM → NHT (e.g. Bartel et al., 2001; Ljung et al., 2002; Woodward and Bartel, 2005; Sugawara et al., 2009; Vanneste and Friml, 2009; LeClere et al., 2010; Normanly, 2010; Zhao, 2010). Zhao et al. (2001) used MS to identify the *in vitro* product as NHT; however, no standard was reported for comparison, and when compared with the spectra reported here (Figure 4.2A), their data do not definitively identify this compound. Zhao et al. proposed that the major fragment ions that they observed at *m/z* 160, 144 and 130 resulted from losses of a hydroxyl radical (17 Da), hydroxylamine (33 Da) and a neutral 'CH_2NH_2OH' (47 Da) species, respectively. However, the loss of the hydroxyl radical breaks the 'even-electron rule' (Karni and Mandelbaum, 1980) and here it was show that this loss does not occur from authentic NHT. The even-electron rule, a fundamental mass spectrometry principle, states that 'even-electron' species, such as the $[M+H]^+$ ion at *m/z* 177, should not produce energetically less favourable 'odd-electron' species by the loss of radicals through homolytic bond cleavage, but rather should form other even-electron species through the loss of neutral molecules. Exceptions to this rule in ESI MS and other 'even-electron' ionisation techniques are rare and the occasional odd-electron ions that do occur are of low relative intensity (Thurman et al., 2007). Given that Zhao et al. (2001) presented a mass spectrum without MS^2 data, there may not even be a direct link between the *m/z* 177, *m/z* 160 and *m/z* 144 ions in that spectrum (if, for example, more than one compound was present in their analyte). The presence of strong ions at *m/z* 160, 132 and 130 in their spectrum is difficult to reconcile with the data for authentic NHT (Figure 4.2A). Zhao et al. made no firmer statement than that their mass spectrum was 'consistent with' NHT. There is now strong evidence that the product obtained by Zhao et al. was not NHT and therefore AtYUC1 may not catalyse the conversion of TAM to NHT *in vitro*. Zhao (2010) also notes that due to the broad *in vitro* substrate specificity of FMOs, TAM may not be the primary AtYUC1 substrate.

Expósito-Rodríguez et al. (2007) cloned a *YUC*-like gene (*FZY*) from tomato into *E. coli* and used the expression product for an *in vitro* assay. These authors claim to have synthesised NHT and to have confirmed its identity using ^{1}H NMR. Although their ^{1}H NMR data are consistent with ours, they do not present ^{13}C NMR results and their electron ionisation MS data show an M^{+} ion at *m/z* 174, which is incorrect for NHT (MW = 176.0950). In the current LC-MS analysis of NHT, the $[M+H]^{+}$ ion was observed at *m/z* 177.1019, which implies a MW of 176.0941, in good agreement with the calculated value. Possibly Expósito-Rodríguez et al. analysed a synthetic by-product by MS. These authors claim that the product of their *in vitro* assay co-eluted with their synthesised 'NHT' on LC; however, this claim is rendered unconvincing by the very close retention times of TAM and the synthetic 'NHT' on their system (see Figure 4B in Expósito-Rodríguez et al., 2007). These authors provided no MS identification of their product and therefore may not have obtained NHT. Therefore, FZY may not catalyse the conversion of TAM to NHT *in vitro*.

Most recently, LeClere et al. (2010) isolated a gene from maize, ZmYUC, which is 40% homologous to AtYUC1, at the protein level. This group also performed an *in vitro* assay, using TAM as a substrate, and claim to have obtained NHT as a product. As shown by their TLC result, there was strong conversion to a product, and they presented good MS data (Figure 4.6). However, these data clearly indicate that their *in vitro* product was not NHT. In particular, NHT does not give an intense ion at *m/z* 160 in MS^{2}, as their compound did (Figure 4.6), but rather an intense ion at *m/z* 144 (Figure 4.2A). Differences in collision energy can create different relative ion abundances in MS^{2} spectra (LeClere et al. do not report the collision energy used); however, a range of collision energies were tested and in all cases the major product ion in MS^{2} for NHT was *m/z* 144, and the *m/z* 160 signal was never more than a few percent relative to *m/z* 144. LeClere et al. explain their large *m/z* 160 and 132 ions in terms of losses of OH and CH_2NH, respectively, but there are at least two problems with this scheme. Firstly, these losses give rise not to *m/z* 132 in MS^{3} but *m/z* 131 (177-17-29 = 131). Secondly, the even-electron rule (Karni and Mandelbaum, 1980) is broken by the suggested loss of OH from NHT in MS^{2}. Instead the observed ions at *m/z* 160 and *m/z* 132 in their MS^{2} and MS^{3} spectra for their reaction product may be due to losses of NH_3 and CO, respectively, entirely analogous with the observations for serotonin (Figure 4.2B), 2-OT (see Chapter 5) and with the NH_3 loss for TAM (Figure 4.3).

Hence, the data presented by LeClere et al. (2010) unequivocally show that the ZmYUC reaction product was not NHT, when compared to authentic NHT. Instead their data indicate the possibility of hydroxylation either on the indole ring or the α-carbon of the side chain. Their product was not serotonin, since on TLC the R_f of serotonin is less than that of TAM (data not shown), inconsistent with the LeClere et al. results. Nevertheless, if hydroxylation of the α- or 2-carbon reduces polarity (see Chapter 5), both the R_f value and the spectrum observed might be explained. It should be noted that FMOs are usually thought to catalyse oxidation of heteroatoms, but there are exceptions involving oxidation of carbon (e.g. Driscoll et al., 2010).

Even though it is unlikely that the YUCs catalyses conversion of TAM to NHT, both Zhao et al. (2001) and LeClere et al. (2010) obtained a product when TAM was supplied as an *in vitro* substrate. One of the aims of this study was to identify this product (see Chapter 5 for analysis of other possible products of YUC). However, the results presented here clearly show little difference between the test and control assays, using AtYUC1 (Figure 4.8) or ZmYUC (Figure 4.9), indicating that these proteins do not use TAM as a substrate under the conditions used here, or the protein degraded to inactive breakdown products during or prior to the assay. The latter is unlikely for several reasons: firstly, SDS-PAGE showed that, although the pure protein did degrade (probably sometime during purification), there was still sufficient protein of the size corresponding to AtYUC1; secondly, a functional assay was conducted using the crude extract, which showed reasonable proportions of AtYUC1, and obtained similar results. The lack of observable metabolism of TAM may have been due to deviation from incubation times or other assay conditions described by Zhao et al. (2001) and LeClere et al. (2010), but it is unlikely that small changes such as these would result in the results observed.

Thus, the evidence for the supposedly 'rate-limiting' step of the TAM pathway is unconvincing. The data presented by Zhao et al. (2001) and Expósito-Rodríguez et al. (2007) do not provide enough evidence to identify the product, while those of LeClere et al. (2010) show that the product is not NHT. Reproduction of the work of Zhao et al. (2001) and LeClere et al. (2010) was attempted, but the alleged product was undetectable. There is little evidence that this conversion happens *in vitro* and no evidence that it happens *in vivo*, as there have been no successful labelling experiments performed using plant systems, nor any clear identification of endogenous NHT. The detailed analysis of the role of NHT and the YUCs in auxin biosynthesis

reported here also highlights the importance of collaboration between plant biologists and analytical and organic chemists. It was through collaboration with experts in the relevant fields that problems with the published mass spectra for NHT were identified, and thus the role of this compound in auxin biosynthesis was called into question.

However, the findings presented here do not necessarily mean that YUC proteins are not involved in IAA biosynthesis. One scenario that still places YUC in the TAM pathway to IAA involves it catalysing the β-hydroxylation of TAM. However, this hypothesis would be difficult to test as the β-hydroxylated product would be unstable, hydrolysing to IAAld immediately in the presence of water. This expected instability implies that the abundant reaction product obtained by LeClere et al. (2010) was not β-hydroxytryptamine. A second possibility, which is currently gaining widespread support, is that the YUCs are involved in IPyA-dependent IAA biosynthesis, acting downstream of the TAA family (Kriechbaumer et al., 2011; Mashiguchi et al., 2011; Stepanova et al., 2011; Won et al., 2011), although the cursory *in vitro* analysis reported here does not support this hypothesis. A third possibility is that *in vivo* the YUC proteins tested catalyse a step, or several steps, leading to a compound (or compounds) other than IAA, as first suggested by Tobeña-Santamaria et al. (2002). This compound may be an auxin or auxin-like compound, in view of the auxin-related phenotypes of *yuc* mutants (Cheng et al., 2006), and this explanation would account for the observations that mutants with reduced YUC activity typically do not contain less IAA than the wild-type (Tobeña-Santamaria et al., 2002) and YUC1 over-expression does not result in a significant increase in IAA content (Stepanova et al., 2011; also see Chapter 6).

Chapter 5 Synthesis of alternate YUCCA oxidation products

Introduction

In the previous chapter, strong evidence against reports that AtYUC1 and ZmYUC catalyse the conversion of TAM to NHT *in vitro* was provided (Zhao et al., 2001; Expósito-Rodríguez et al., 2007; LeClere et al., 2010)

. However, both Zhao et al. (2001) and LeClere et al. (2010) showed the presence of a product in their *in vitro* assays. Both these groups incorrectly identified this product as NHT (Tivendale et al., 2010; see also Chapter 4). Although other roles for the YUCs have been reported (Kriechbaumer et al., 2011; Mashiguchi et al., 2011; Stepanova et al., 2011; Won et al., 2011), these studies have problems of their own (see Chapter 6) and if the *in vitro* product detected by Zhao et al. (2001) and LeClere et al. (2010) could be identified, it may help further the understanding of the role of YUCs in plants. It has already been shown (see Tivendale et al., 2010 and also Chapter 4) that, while the mass spectral data for 5-HT (Figure 5.1A) are similar to those presented by LeClere et al. (2010), on TLC 5-HT is more polar than TAM and therefore unlikely to be the oxidation product obtained by Zhao et al. (2001) and LeClere et al. (2010), which was less polar than TAM. The other phenolics—1-HT (Figure 5.1B), 4-HT (Figure 5.1C) and 6-HT (Figure 5.1D)—should behave similarly to 5-HT on TLC. However, hydroxylation on the 2-position or α-carbon of the side-chain will not produce a phenol and therefore may result in a compound that is less polar than TAM and gives a mass spectrum consistent with those of LeClere et al. (2010). The aim of this series of experiments is to synthesise 2-OT (Figure 5.2A) and α-HT (Figure 5.2B) for analysis.

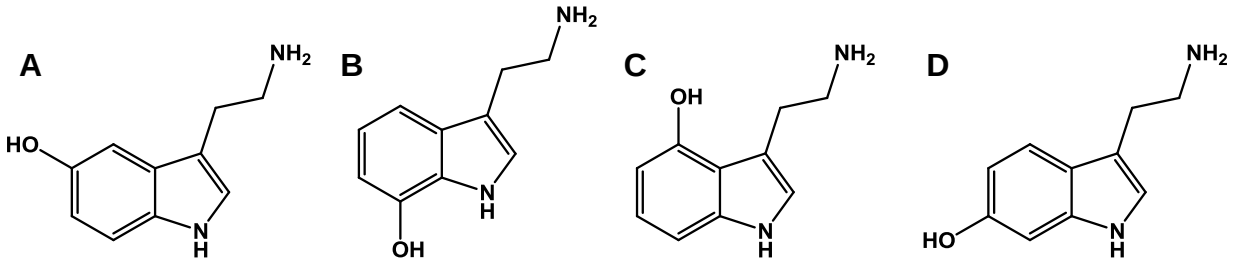

Figure 5.1 – Structural formulae of (A) 5-HT, (B) 1-HT, (C) 4-HT and (D) 6-HT.

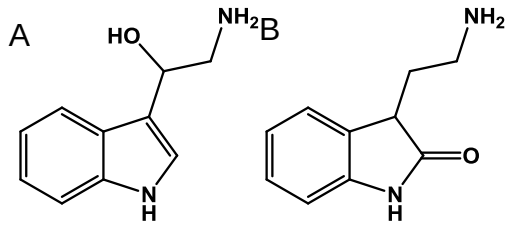

Figure 5.2 – Structural formulae of (A) α-HT and (B) 2-OT.

Materials and methods

Synthesis of α-hydroxytryptamine

Synthetic methods were adapted from Satoh et al. (1969), Miyake et al. (2000a), Miyake et al. (2000b) and Roy et al. (2006).

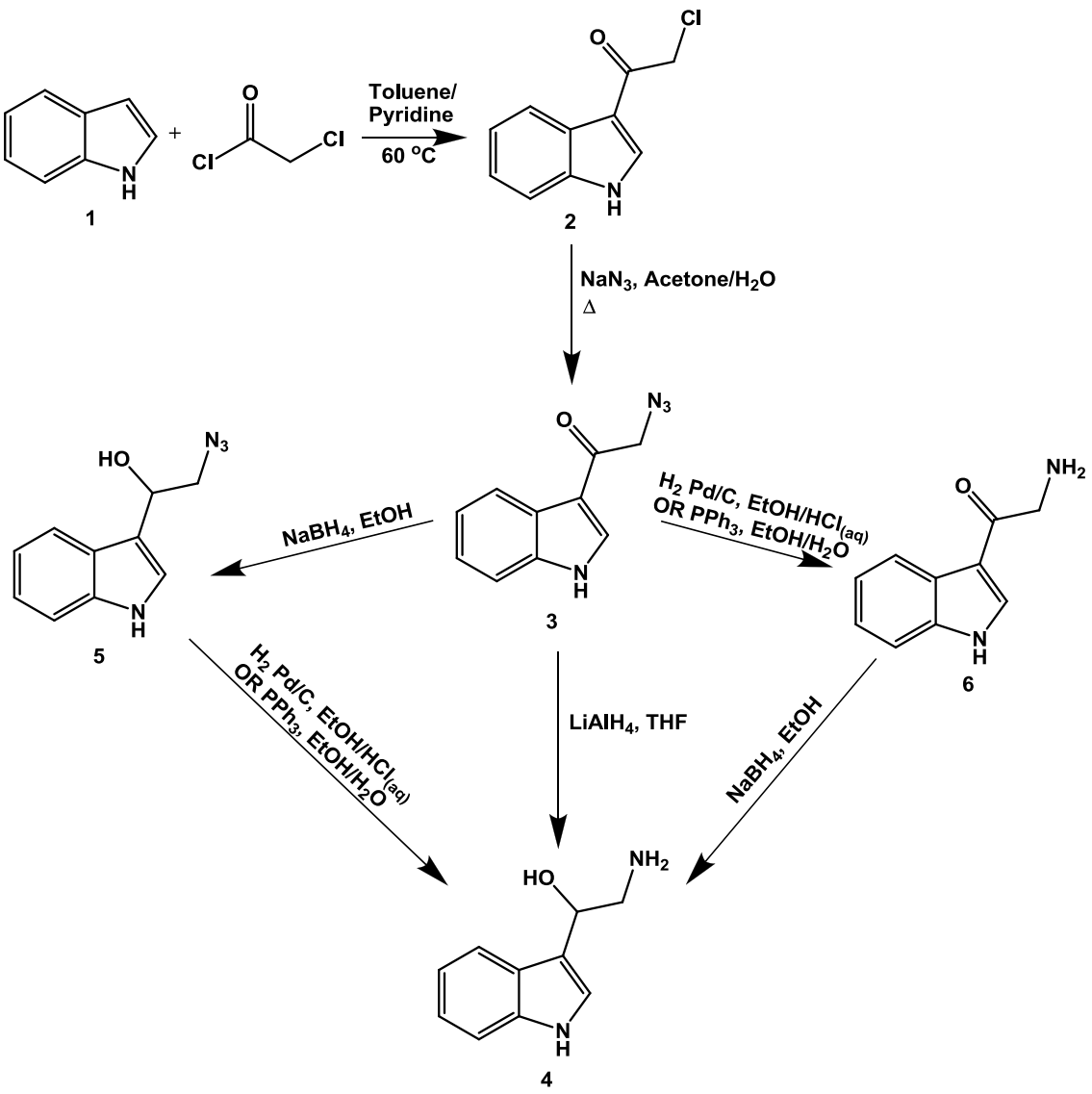

Figure 5.3 – Synthetic scheme for α-HT (4).

Indole (**1**, 2.0026 g, 17 mmol) was stirred at room temperature in a mixture of toluene (50 mL) and pyridine (2 mL). Chloroacetylchloride (1.35 mL, 17 mmol) was added over ca. 30 min, and then the mixture was heated to 60 °C and stirred at this temperature for 2 h. The mixture was then cooled to room temperature and H_2O (50 mL) and methanol (10 mL) were added to it, after which it was stirred for an additional hour at room temperature. The precipitate was collected by filtration and was recrystallised from ethanol to give **2** [896.3 mg, 4.6 mmol, 27 % yield; ^{1}H NMR ($CDCl_3$ + 1 drop [D_6]DMSO, 300 MHz) δ: 4.47, (s, 2H), 7.16 (m, 2H), 7.35 (m, 1H), 7.87 (d, *J* = 3.3 Hz, 1H), 8.20 (m, 1H), 11.18 (bs, 1H); ^{13}C NMR ($CDCl_3$, 75 MHz) δ: 46.3

(CH_2), 112.2 (CH), 114.5 (C), 122.2 (CH), 122.8 (CH), 123.8 (CH), 125.9 (C), 133.0 (CH), 137.0 (C), 186.6 (C); these spectra are consistent with those presented in Roy et al. (2006) for this compound]. The α-chloroketone, **2** (300 mg), and NaN_3 were dissolved in acetone (40 mL) and H_2O (20 mL) and the resulting mixture was stirred at reflux for 19 h, before cooling to room temperature. H_2O (17 mL) was then added and the mixture extracted with DCM (3 x 10 mL). The organic extracts were combined and dried over Na_2SO_4, before the solvent was removed under reduced pressure, to give the crude product **3** [182 mg; ^{1}H NMR ($CDCl_3$, 300 MHz) δ: 4.26 (s, 2H), 7.08-7.14 (m, 2H), 7.26-7.32 (m, 1H), 7.76 (d, *J* = 3.0 Hz, 1H), 8.13-8.16 (m, 1H), 11.24 (bs, 1H); these chemical shifts are consistent with those presented in Roy et al. (2006) for this compound, however their NMR analyses were conducted in [D_6]DMSO].

$LiAlH_4$ (17 mg, 0.44 mmol) was added to a stirred solution of **3** (crude mixture, 44 mg, 0.22 mmol) in THF (5 mL) under an atmosphere of N_2. The mixture was stirred at room temperature for 1.5 h before the reaction was quenched with ethyl acetate (3 mL), followed by H_2O (0.25 mL). The solvents were removed under reduced pressure to give a bright red solid. The crude ^{1}H NMR spectrum showed reduction of the ketone [^{1}H (CD_3OD, 300 MHz) δ: 3.53 (dd, *J* = 4.2 Hz, 12.6 Hz), 3.64 (dd, *J* = 7.9 Hz, 12.4 Hz), 4.65 (dd, *J* = 4.3 Hz, 8.0 Hz)] and the IR spectrum revealed the absence of the azide (present in **3**). The desired $[M+H]^+$ ion (*m/z* 177) was observed by ESI MS; however it was only ca. 25 % of the most intense ion produced: *m/z* 175.

Three alternatives to the method described above were used in an attempt to obtain **4**. In the first alternative $NaBH_4$ (8 mg, 0.2 mmol) was added to a stirred solution of **3** (crude mixture, 20 mg, 0.2 mmol) in EtOH and the mixture was left at room temperature for 1.5 h, after which a further portion of $NaBH_4$ (12 mg) was added. After 10.5 h, the starting material was no longer visible by TLC (ethyl acetate), IR showed that the azide group still remained, ESI MS showed molecular mass of 202 (as the $[M+Na]^+$ ion: 225) and ^{1}H NMR and IR analyses of the crude reaction mixture [^{1}H NMR ($CDCl_3$, 300 MHz) δ: 3.62 (dd, *J* = 4.1 Hz, 12.45 Hz, 1H), 3.71 (dd, *J* = 7.9 Hz, 12.45 Hz, 1H), 5.22 (dd, *J* = 4.1 Hz, 7.9 Hz, 1H), 7.09-7.37 (m, 3H), 7.38 (d, *J* = 7.8 Hz, 1H), 7.70 (d, *J* = 8.1 Hz, 1H), 8.32 (bs, 1H); IR ν (cm^{-1}): 1011, 1045, 1095, 1231, 1262-1276, 1338, 1419-1437, 1457, 1550, 2104 (—N_3), 3222-3391] showed the desired product (**5**).

Half of the crude mixture (**5**) was dissolved in EtOH (10 mL) and 2 M HCl (1 mL) and Pd/C (11 mg) were added to the mixture under an atmosphere of N_2. The mixture was then stirred under an atmosphere of H_2 for 1 h. The mixture was then filtered through Celite and the solvent evaporated under reduced pressure. However, the crude ^{1}H NMR (D_2O or CD_3OD) showed decomposition.

The other half of the crude mixture (**5**) was reduced using the Staudinger reaction. The azidoalcohol, **5**, was dissolved in CD_3OD/D_2O (9:1) in an NMR tube. Triphenylphosphine (PPh_3; 13 mg, 0.05 mmol) was added and the reaction was monitored by ^{1}H NMR. After 120 min, the chemical shifts had not changed. A few drops of the mixture were taken for MS analysis. There was some evidence of the expected mass for **4** (176; as the $[M+Na]^+$ ion: 199), but the starting material still remained (molecular weight 202; $[M+Na]^+$ 225). After 1 week, ^{1}H NMR indicated decomposition.

In the second alternative (see Figure 5.3), the order of the two final steps was reversed. The azidoketone, **3**, (crude mixture; 20 mg 0.999 mmol) was dissolved in EtOH (10 mL) and HCl was added (1 mL; 2 M). The mixture was then degassed and put under an atmosphere of N_2, prior to the addition of Pd/C (15 mg), after which it was stirred under an atmosphere of H_2 for 18 h. The mixture was filtered through Celite, and the solvent evaporated under reduced pressure. ESI MS analysis of the crude mixture showed the expected mass (175) and fragmentation by MS^2, and ^{1}H NMR showed the desired product [**6**; 1H NMR (D_2O, 300 MHz) 4.20 (s, 2H), 7.11 (m, 2H), 7.32 (m, 1H), 7.89 (m, 2H)], which was then reduced with $NaBH_4$ (24 mg) in EtOH (10 mL) for 12 h, before analysis by ^{1}H NMR (D_2O or $CDCl_3$). The NMR spectrum contained limited evidence for the desired product (**4**) and ESI MS revealed primarily a mass of 174.

In a separate experiment, using PPh_3 rather than H_2 to reduce the azide, PPh_3 (26 mg, 0.10 mmol) was added to a stirred solution of **3** (crude mixture; 20 mg, 0.10 mmol) in EtOH/H2O (75 % v/v; 10 mL). After stirring at room temperature for 1 h, $NaBH_4$ was added and the mixture was stirred at room temperature for a further 1 h. The solvent was removed under reduced pressure and the crude ^{1}H NMR [$CDCl_3$, 300 MHz; δ: 3.52 (dd, J = 4.1 Hz, 12.5 Hz), 3.65 (dd, J = 7.8 Hz, 12.6 Hz), 5.17 (dd, J = 4.1 Hz, 8.0 Hz); the aromatic signals were obscured by the phenyl groups of PPh_3 and Ph_3PO] indicated the presence of the desired product (**4**; the

^{1}H NMR signals are similar, but not identical to those, produced by **5**), the mixture was subject to flash chromatography, eluting with ethyl acetate in hexanes (45 % v/v), followed by ethyl acetate. The column was then stripped with TEA/MeOH/ethyl acetate (1:1:18). ^{1}H NMR spectra of purified fractions indicated that decomposition had occurred.

The third alternative method was adapted from Wang and Chen (2007). In this method (Figure 5.4), oxalyl chloride (1.7 mL, 19.8 mmol) was added drop-wise to a stirred solution of **1** (2.0309 g, 17.1 mmol) in diethyl ether, under an atmosphere of N_2 at 0 °C. The mixture was stirred for 3 h after which it was allowed to warm to room temperature over 1 h. The solvent was removed under reduced pressure to give **7** [^{1}H NMR (CD_3OD, 300 MHz) 7.16-7.23 (m, 2H), 7.37-7.41 (m, 1H), 8.26-8.29 (m, 1H), 8.57 (d, J = 3.6, 1H), 11.47 (bs, 1H); this spectrum is comparable to spectra previously reported for this compound by Aubry et al. (2009), although, their analyses were conducted in [D_6]DMSO]. A portion of this solid (988 mg) was dissolved in methanol (2 mL) and chilled to 0 °C. Ammonia in H_2O (28 % v/v; 1 mL) was added and the mixture, which was then stirred for ca. 2 h at room temperature. H_2O (30 mL) was then added to the mixture, which was subsequently extracted with ethyl acetate (3 x 30 mL). The combined organic layers were washed with brine (10 mL) and dried over $MgSO_4$, filtered and the solvent was evaporated under reduced pressure to give **8** as a solid [696 mg, 78 % yield; ^{1}H NMR (CD_3OD, 300 MHz) 7.22-7.29 (m, 2H), 7.49 (m, 1H), 8.30 (m, 1H), 8.72 (s, 1H)]. The solid α-ketoamide (**8**) was compared to the starting material (**7**) by TLC to ensure the reaction was complete.

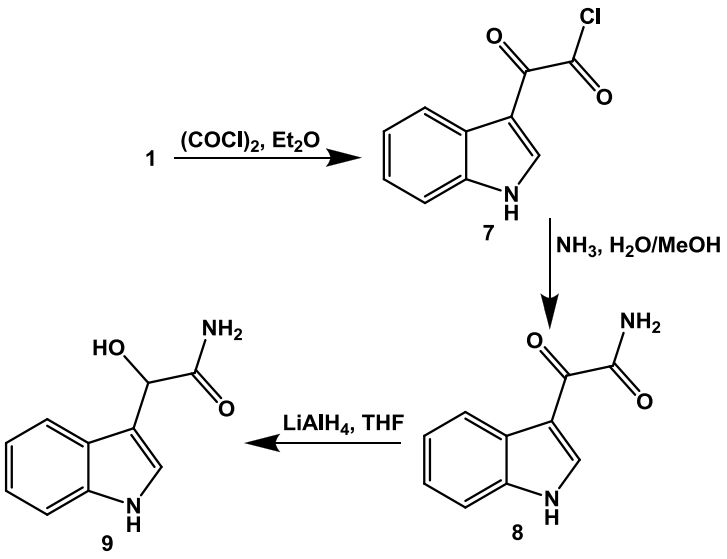

Figure 5.4 – Synthetic scheme for indole-3-ethanolamide (9).

8 (200 mg, 1.064 mmol) was dissolved in THF (10 mL) under an atmosphere of N_2 and chilled on ice. Excess $LiAlH_4$ was added and the mixture was stirred at room temperature for 3 h. The reaction was quenched by careful addition of ethyl acetate followed by $NaHCO_3$ (20 mL). The mixture was extracted with ethyl acetate (3 x 10 mL), the combined layers washed with brine (10 mL) and dried over $MgSO_4$. The mixture was filtered and the solvent evaporated under reduced pressure to give indole-3-glycolamide, **9** [^{1}H NMR (300 MHz, CD_3OD) δ: 5.32 (s, 1H), 6.99-7.13 (m, 3H), 7.35 (dt, J = 8.1 Hz, 0.9 Hz, 1H), 7.72 (dt, J = 8.0 Hz, 0.9 Hz, 1H)] as a solid. The ^{1}H NMR clearly shows reduction of the ketone, but the amide remained intact. Hypothetically, **4** is a possible reduction product of **8**, but this could not be detected. Stronger conditions may have achieved reduction of the amide to the amine, but would probably also result in the loss of the α-hydroxyl group.

Synthesis of **4** by $LiAlH_4$ reduction of indole-3-cyanomethanone (**10**; Figure 5.5) as described by Miyake et al. (2000b) was also attempted, but without success.

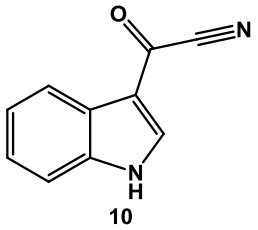

10

Figure 5.5 – Structural formula for indole-3-cyanomethanone.

Synthesis and analysis of 2-oxytryptamine

Synthetic method was adapted from Pham et al. (2005).

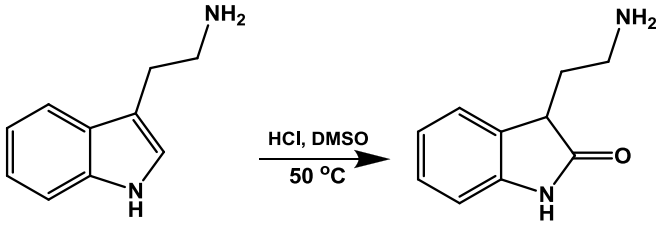

Figure 5.6 – Synthetic scheme for 2-OT.

TAM (245 mg, 1.5 mmol) was dissolved in DMSO (520 µL) and the mixture was heated to 50 °C; concentrated HCl (400 µL) was then added, drop-wise. The mixture was stirred at 50 °C for 6 h and then cooled to room temperature; the product was collected by filtration and washed with ethanol (2 mL), to give 2-OT as a white solid (112 mg, 42 % yield), which was analysed by ^{1}H and ^{13}C NMR spectrometry, [^{1}H ([D_6]DMSO, 300 MHz) δ: 2.05 (m, 2H), 2.92 (m, 2H), 3.58 (t, *J* = 6.7 Hz, 1H), 6.84 (d, *J* = 7.5 Hz, 1H), 6.97 (td, *J* = 7.5 Hz, 1.0 Hz, 1H), 7.16-7.25 (m, 2H), 8.02 (bs, 2H), 10.52 (s, 1H); ^{13}C (DMSO), 75 MHz δ: 28.7 (CH2), 37.0 (CH), 43.4 (CH_2), 110.1 (CH), 122.2 (C), 124.7 (CH), 128.7 (CH), 129.5 (CH), 143.2 (C), 179.0 (C); these chemical shifts are comparable to those presented by (Pham et al., 2005)], IR spectroscopy [ν (cm^{-1}): 3233, 3134, 2894, 2160, 2032, 1698, 1614, 1481, 1467, 1389, 1337, 1298, 1210, 1178, 1118, 1097, 958, 853, 755, 666], EI MS [*m/z*: 176 (M^+, 30 %), 159 (42 %), 146 (100 %), 133 (43 %), 128 (37 %), 117 (27 %)], TLC and UPLC-ESI MS/MS.

Results

Synthesis of α-HT

Synthesis of α-HT (**4**) proved difficult. Synthesis by reduction of the α-ketoamide (**8**) or the α-ketonitrile (**10**) was unsuccessful. The synthetic methods from the azidoketone (**3**) were more successful: after reduction of **3** with $LiAlH_4$, ^1H NMR of the crude reaction mixture produced a spectrum consistent with **4** and IR analysis showed the azide and the carbonyl had been reduced. MS analysis revealed the desired molecular weight (176) but the final product could not be purified by flash column chromatography indicating its instability, as previously reported by Ames et al. (1956).

Some success was also achieved using other methods of reduction adapted from Roy et al. (2006). The individual steps—reduction of the ketone by reaction with $NaBH_4$ and reduction of the azide by hydrogenation or *via* the Staudinger reaction—yielded the desired intermediates (**5** and **6**, respectively). However, upon reduction of the azide group in **5** (either by hydrogenation or the Staudinger reaction) or the ketone group in **6**, there was only limited evidence by ^1H NMR, IR and/or MS for the formation of **4** in the crude mixtures and the pure product could not be isolated by flash column chromatography.

Synthesis and analysis of 2-OT

2-OT was successfully synthesised, using a method adapted from Pham et al. (2005) and identified using ^1H and ^{13}C NMR spectrometry, MS and IR spectroscopy. However, as the method contained few details, some experimentation was required to adapt it to a smaller scale here. Using the exact ratios of solvents to reagents and physical conditions described by Pham et al. (2005), primarily starting material was obtained in the solid portion. The solvent volume, reaction time and reaction temperature were all doubled to obtain the desired product. The yield obtained was reasonable (42 %), considering the product was obtained by precipitation and the method was scaled-down.

TLC and MS/MS analyses of the compound proved interesting. When 2-OT and TAM were analysed by TLC (15:4:1 DCM/MeOH/TEA; Zhao et al., 2001), 2-OT had a higher R_f than TAM (Figure 5.8), indicating that it was less polar. MS^n data (Figure 5.7) for this compound revealed

an intense $[M+H]^+$ ion at *m/z* 177.2. In MS^2 the principal signal observed was at *m/z* 160.1 and *m/z* 132.1 was the main ion in MS^3. Suggested losses that produce these ions are shown in Figure 5.7.

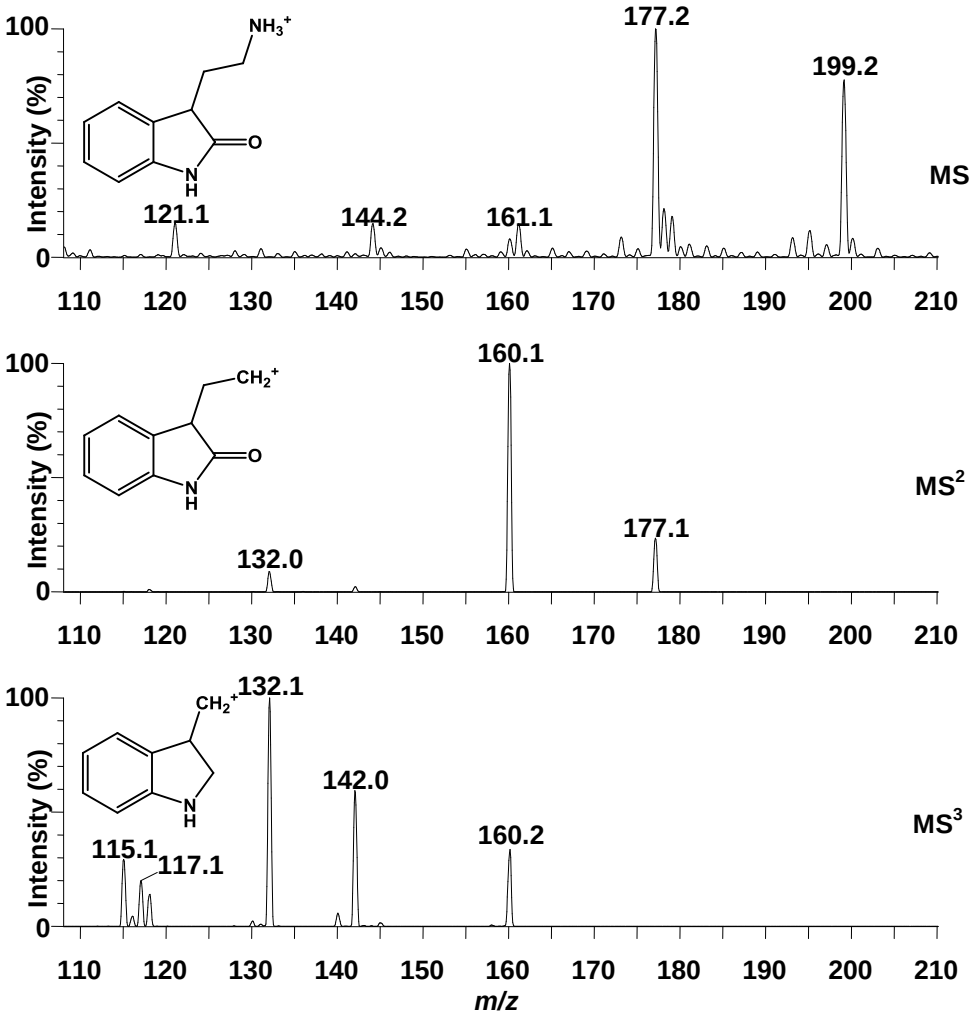

Figure 5.7 – MS, MS^2 and MS^3 analyses of 2-OT. Suggested losses that generate the most intense ions at each level of fragmentation are shown on the left.

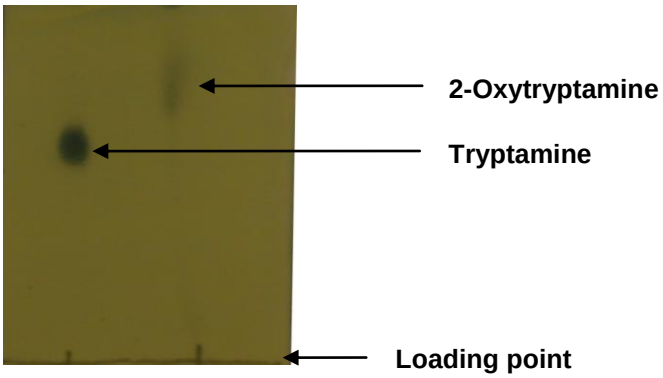

Figure 5.8 – TLC (using 15:4:1 DCM/MeOH/TEA) of TAM (left) and 2-OT (right).

Discussion

The publication of two papers (Zhao et al., 2001; LeClere et al., 2010) incorrectly identifying NHT as an *in vitro* assay product highlights the importance of meticulousness in analytical methods. As was discussed earlier in this thesis, the greatest deficiency in the characterisations of the *in vitro* product was lack of an authentic standard for comparison. Low resolution MS does not allow for definitive identification of a compound without a standard. It was shown definitively that the product LeClere et al. (2010) detected from their *in vitro* assay was not NHT and there was insufficient evidence to determine the true identity of the product obtained by Zhao et al. (2001) (Tivendale et al., 2010; Chapter 4). However, this immediately raises the question of the true identity of the LeClere et al. (2010) product. Hence, the aim of this series of experiments was to synthesis α-HT and 2-OT, two alternative TAM oxidation products.

At least one group has reported the synthesis of α-HT (from indole-3-cyanomethanone; Miyake et al., 2000b), although no MS data was reported for this compound and their synthesis could not be replicated here. $LiAlH_4$ reduction of **3** appeared to give the desired product, by ^1H NMR and IR, and the desired mass was evident by MS, but α-HT could not be isolated as a pure product. The methods adapted from Roy et al. (2006) also proved difficult. Reduction of azides and ketones are reasonably well documented steps (e.g. Bretschneider and Hörmann, 1953; Engin et al., 2007); indeed the azide or the ketone of **3** were successfully reduced to produce the desired intermediates (**5** and **6**). However, attempts to reduce both the azide and the ketone of **3** in sequential steps to produce α-HT as a pure product were unsuccessful, probably due to instability (Ames et al., 1956). Due to the unsuccessful attempts to synthesise α-HT as a pure

product, it is not possible to make any strong comment on the likelihood of this compound as a YUC oxidation product. Nevertheless, given the apparent instability of α-HT, it is unlikely that this was the abundant product obtained by LeClere et al. (2010). Nevertheless, α-HT has been reported as the *in vitro* product of indolyl-3-alkane α-hydroxylase—an enzyme isolated in crystalline form from soil isolate organisms *Pseudomonas XA*—supplied with TAM (Roberts and Rosenfeld, 1977). This enzyme also hydroxylated the α-carbon of Trp methyl-ester, IEt, indole-3-propanoic acid or indole-3-butyric acid.

Analysis of 2-OT revealed several interesting findings. After its identification by ^{1}H and ^{13}C NMR, IR spectroscopy, EI MS and ESI MS^n, the compound was analysed by TLC. TLC utilises a polar stationary phase (silica) so polar compounds will move relatively slowly up the plate and have lower R_f values than non-polar compounds (Poole, 2003). On TLC, using the conditions described by Zhao et al. (2001; 15:4:1 DCM/MeOH/TEA), the R_f of 2-OT was greater than that of TAM, indicating that it was less polar. The difference in R_f values for 2-OT and TAM we observed ($\Delta R_f = 0.1$) was comparable to those reported by Zhao et al. (2001 $\Delta R_f = 0.2$) and LeClere et al. (2010; $\Delta R_f = 0.3$). The differences in R_f-values may be accounted for by differences in moisture content in the silica plates or the solvents used. Most importantly, the mass spectra produced by 2-OT on ESI MS^n (Figure 5.7) were remarkably similar to those reported by LeClere et al. (2010). Intense ions at *m/z* 177 in MS, *m/z* 160 in MS^2 and *m/z* 132 in MS^3 were observed, just as LeClere et al. reported for the product of their *in vitro* assay. These ions are most likely due to loss of ammonia to give *m/z* 160 and subsequent loss of carbon monoxide to give *m/z* 132, as previously found for 5-HT. Hence it may be that this compound, rather than NHT, was the *in vitro* product of ZmYUC supplied with TAM. However, replication of the work of LeClere et al. (2010; see Chapter 4) revealed no metabolism of TAM was observed, although 2-OT was detected as an auto-oxidation product of TAM.

Chapter 6 The importance of the PsTAR family in auxin biosynthesis[4]

Introduction

The evidence for each of the proposed auxin biosynthetic pathways is incomplete (reviewed in Bartel et al., 2001; Woodward and Bartel, 2005; Normanly, 2010; Zhao, 2010). However, recently there have been advances in the understanding of the IPyA pathway (Stepanova et al., 2008; Tao et al., 2008; Yamada et al., 2009; Chourey et al., 2010; He et al., 2011; Mashiguchi et al., 2011; Phillips et al., 2011; Stepanova et al., 2011; Won et al., 2011). This pathway is known to operate in certain microorganisms (Koga et al., 1991a; Koga et al., 1991b; Koga et al., 1994; Patten and Glick, 1996; Pedraza et al., 2004; Vandeputte et al., 2005; Spaepen et al., 2007; Tsavkelova et al., 2007; Malhotra and Srivastava, 2008; Quyet-Tien et al., 2008; Van Puyvelde et al., 2011) but until recently was largely uncharacterised in plants (for reviews, see Bartel et al., 2001; Ljung et al., 2002; Vanneste and Friml, 2009; Lehmann et al., 2010; Normanly, 2010; Zhao, 2010). However, it is thought to be widespread throughout the plant kingdom, as potential intermediates have been isolated from a range of species (Cooney and Nonhebel, 1991; Koga, 1995; Tam and Normanly, 1998; Mashiguchi et al., 2011). Study of the IPyA pathway is somewhat complicated as IPyA is notoriously unstable and degrades to IAA at room temperature (Moore and Shaner, 1968; Gibson et al., 1972; Garcia-Tabares et al., 1987; Camilleri and Jouanin, 1991; Koga et al., 1992; Tam and Normanly, 1998), making it difficult to demonstrate that the conversion of IPyA to IAA is enzymatically controlled (Koga et al., 1992). Theoretically, in the IPyA pathway Trp is converted by an aminotransferase to IPyA, which is subsequently converted by a decarboxylase to IAAld, and finally to IAA by an aldehyde oxidase. Recently, three groups identified and isolated the long-awaited Trp aminotransferase from *Arabidopsis* (Stepanova et al., 2008; Tao et al., 2008; Yamada et al., 2009) and two groups identified Trp aminotransferases from maize (Chourey et al., 2010; Phillips et al., 2011).

[4] The majority of the study reported here has been published in the research article Tivendale ND, Davidson SE, Davies NW, Smith JA, Dalmais M, Bendahmane A, Quittenden LJ, Sutton L, Bala RK, Le Signor C, Thompson R, Horne J, Reid JB, Ross JJ (2012) Biosynthesis of the halogenated auxin, 4-chloroindole-3-acetic acid. Plant Physiology **159:** 1055-1063

Tao et al. (2008) were examining the shade avoidance syndrome in *Arabidopsis* and identified mutant alleles of the *SAV3* gene, which encodes a protein with an alliinase C-terminal/aminotransferase class I and II domain. *sav3* mutants are unable to respond to changes in R:FR ratio (i.e. they cannot avoid shade). Using various lines of evidence (including an *in vitro* assay), Tao et al. demonstrated that SAV3 catalyses the conversion of Trp to IPyA. To reflect this function, they renamed the non-mutant allele *TRYPTOPHAN AMINOTRANSFERASE OF ARABIDOPSIS 1* (*TAA1*). Under normal conditions, *taa1* mutants contain 60% of WT levels of free IAA and when they are transferred to the shade, the rate of IAA biosynthesis in mutant plants does not increase, as it does in WT plants. This indicates that synthesis of auxin *via* this pathway is rapidly deployed to increase IAA levels upon exposure to shade (Tao et al., 2008).

Stepanova et al. (2008) also isolated this gene, and several others related to it, during a study on the relationship between ethylene and IAA biosynthesis. The ethylene insensitive mutant *weak ethylene insensitive 8* (*wei8*), like *sav3* mutants, contains a mutation in *TAA1*. *wei8* (*taa1*) mutants have no obvious phenotypic defects, aside from root-specific ethylene insensitivity. Sequence analysis revealed four genes closely related to *TAA1*, referred to as *TRYPTOPHAN AMINOTRANSFERASE RELATED1* to *4* (*TAR1* to *4*). This group also conducted an *in vitro* assay using TAA1 as the enzyme and Trp as the substrate and obtained IPyA as the product. Further analysis of the *TAR*s revealed overlapping expression and functions of TAA1 and TAR2 in auxin biosynthesis. Indeed, the double mutant *taa1 tar2* showed a significant reduction in auxin-mediated gravitropism compared to the *taa1* mutant. In addition, Stepanova et al. (2008) found the level of free IAA in roots and hypocotyls of dark-grown 3-day-old *taa1 tar2* mutants to be half that of the WT. This group showed that *TAA1* and *TAR2* are up-regulated in response to ethylene, indicating that auxin biosynthesis mediates tissue-specific ethylene responses. Furthermore, TAA1 and TAR2 are required for meristem maintenance, differential growth in apical hooks and proper gynaecium development (Stepanova et al., 2008).

Yamada et al. (2009) report characterisation of an auxin biosynthesis gene called *TRANSPORT INHIBITOR RESPONSE 2* (*TIR2*) in *Arabidopsis*. Compared to the WT, the *tir2* mutants display many auxin-related defects, including shorter root hairs, fewer lateral roots, decreased IAA content at higher temperatures and, like the *taa1 tar2* mutant, reduced gravitropic response (Stepanova et al., 2008). The *tir2* mutant phenotype could be rescued by exogenous application of IAA or IPyA (Yamada et al., 2009), indicating that the phenotype may be due to auxin

deficiency. However, sequence analysis showed that *TIR* was not a new gene but is identical to *TAA1*. As further evidence for this, Yamada et al. introduced *TAA1* cDNA (under control of the *CaMV 35S* promoter) into *tir2* mutants, and the phenotype was rescued.

Chourey et al. (2010) examined the *mn1* mutant (the *Mn1* gene that codes for an endosperm-specific cell wall invertase, INCW2) which has impaired sugar metabolism and decreased IAA content (both free acid and IAA-sugar conjugates). This group characterised a *TAA1* homologue from maize and named it *ZmTAR1*. Phillips et al. (2011) report positional cloning and characterisation of another *TAA1* homologue, *vanishing tassel2* (*vt2*), from maize. This group constructed a *vt2 spi1* (sparse inflorescence1, a monocot-specific member of the YUC gene family; Gallavotti et al., 2008) double mutant that had only a slightly more severe phenotype than the *vt2* mutant and no further reduction in IAA content compared to the *vt2* or *spi1* single mutants. Phillips et al. (2011) interpret these results as evidence that the *TAA* and *YUC* families may function in the same pathway, as previously suggested by Strader and Bartel (2008), rather than separate pathways.

Serious doubts about the original proposed role for YUCs were raised (Tivendale et al., 2010; see Chapter 4), and the hypothesis that the *YUC* and *TAA* families act in the same pathway was borne out in four subsequent studies (Kriechbaumer et al., 2011; Mashiguchi et al., 2011; Stepanova et al., 2011; Won et al., 2011). Mashiguchi et al., Stepanova et al. and Won et al. report synergistic interaction between the YUC and TAA families. It was reported that the main phenotypic traits associated with *taa* mutants were also observed in *yuc* mutants and loss of up to four *YUC* genes on the *wei8-1 tar2-1* mutant background had no additional auxin-related phenotypic effects beyond those of the parental line (Stepanova et al., 2011; Won et al., 2011). It was also shown that endogenous IPyA levels are reduced in 3-week-old *Arabidopsis wei8-1 tar2-1* double mutant seedlings and IPyA levels are elevated in comparable *yuc1/2/4/6* quadruple mutants (Mashiguchi et al., 2011). Furthermore, an increase in levels of IAA metabolites (oxIAA, IAAsp and IAGlu; see Figure 6.1) was observed upon expression of the *TAA1:YUC1* construct (i.e. *YUC1*, under the control of the *TAA1* promoter), on a WT background, and the increase was not observed when this construct was expressed on the *wei8-2 tar2-1* double mutant background (Stepanova et al., 2011). Moreover, IAA levels were not increased and the typical auxin overproduction phenotypes were not apparent when the *35S::YUC1* construct was expressed on the double mutant background (Won et al., 2011). Mashiguchi et al. (2011) report

enzymatic production of IAA when IPyA is supplied to YUC2 *in vitro*, and Kriechbaumer et al. (2011) report that the same is true for YUC4 (but they observed no activity when TAM was supplied as the substrate; cf. Chapter 4). Taken together, these observations indicate that TAA1/TAR2 enzymes catalyse conversion of Trp to IPyA, which is subsequently converted to IAA by YUC1/2/4/6. Mashiguchi et al. (2011), Stepanova et al. (2011) and Kriechbaumer et al. (2011) provide evidence against the involvement of IAAld and, by extrapolation, the aldehyde oxidase enzymes in the TAA/YUC pathway. However, IAAld spontaneously degrades to IAA upon standing at room temperature (Quittenden et al., 2009) so it is possible that the *in vitro* product of the YUC2 assay was in fact IAAld, which subsequently degraded to IAA.

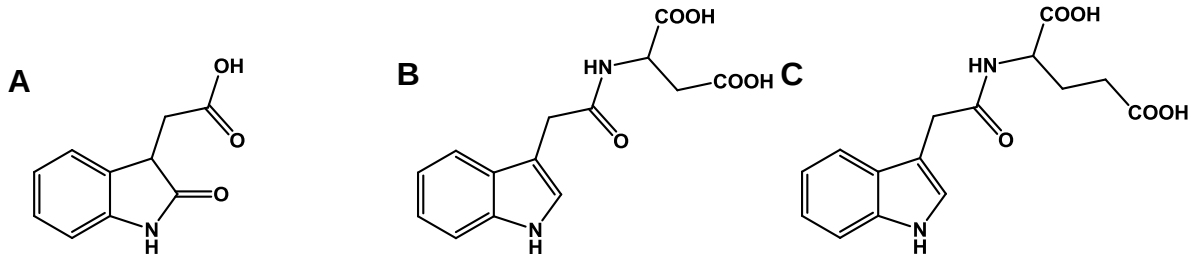

Figure 6.1 – Structural formulae for IAA metabolites (A) OxIAA, (B) IAAsp and (C) IAGlu.

However, there are some data presented that reveal the possibility of an interpretation slightly more complicated than the TAA/YUC linear pathway. Mashiguchi et al. (2011) report that lateral root formation (a typical auxin overproduction phenotype) is significantly enhanced in *TAA1ox yuc1D* double mutants relative to *yuc1D* plants (*TAA1ox* and *yuc1D* are auxin overproduction mutants), and claim that this additive effect indicates TAA1 and YUC1 act in the same pathway. However, this observation is also consistent with TAA1 and YUC1 acting in separate pathways, thus nullifying their inference. In fact, Stepanova et al. (2011) assert that additive auxin overproduction in the *sur2 YUCox* double mutant (relative to the single mutants; the *sur2* mutation results in CYP79B2/3 hyperactivity (Barlier et al., 2000)) indicates that CYP79B2/3 and the YUCs act in separate pathways (this inference may be correct, but if one step is rate-limiting then overproduction mutations would have an additive effect even if both enzymes were acting in the same pathway). In addition when *YUC1* was expressed in WT plants (driven by either *CaMV 35S* or *TAA1* promotion), high auxin phenotypes were observed (Stepanova et al., 2011; Won et al., 2011), but Stepanova et al. (2011) showed that levels of free IAA in these plants were similar to those in the WT, although the levels of oxIAA, IAAsp and IAGlu were

dramatically elevated. Therefore, the observed phenotypes may be due to production of another auxin or auxin-like compound as previously suggested (Tobeña-Santamaria et al., 2002; Tivendale et al., 2010; see also Chapter 4).

As part of their analyses, Tao et al. (2008), Stepanova et al. (2008) and Mashiguchi et al. (2011) conducted *in vitro* assays using their gene products as potential catalysts. *In vitro* assays are a crucial aspect for determining the biochemical function of a gene product; properly utilised, they allow for accurate identification of the substrate(s) for and product(s) of a protein. Both Tao et al. and Stepanova et al. obtained IPyA as the primary product from Trp, which provides evidence that this protein is involved in the IPyA branch of Trp-dependent IAA biosynthesis. Similarly, when IPyA was supplied to YUC2 or YUC4 *in vitro*, IAA was detected (Kriechbaumer et al., 2011; Mashiguchi et al., 2011). The other groups (Yamada et al., 2009; Chourey et al., 2010; Phillips et al., 2011; Stepanova et al., 2011; Won et al., 2011) did not perform *in vitro* assays as part of their studies, but rather inferred the function of the gene by sequence homology and mutant analysis, which can sometimes lead to incorrect characterisation.

Although IAA is the most widespread auxin, it is not the most potent (Ali et al., 2008). The halogenated auxin, 4-Cl-IAA, which is largely restricted to the Fabeae tribe of the Fabaceae family (Reinecke, 1999), but has also been reported in seeds of *Pinus sylverstris* (Ernstsen and Sandberg, 1986), is considered to be more active than IAA in some bioassays (Reinecke, 1999). Organohalogens are found in a range of organisms, especially in the marine environment, and include compounds with important biological roles (Gribble, 1998), such as antibiotics. Many organisms use organohalogens in chemical defence, as pheromones, or as regulatory compounds (e.g. thyroxin in humans), but these compounds are relatively rare in flowering plants (Gribble, 1998). Nevertheless, in seeds of some key legumes, such as *Lens culinaris* Medik., *Lathyrus latifolius* L., *Vicia faba* L. (fava bean) and pea, the levels of 4-Cl-IAA are among the highest reported for any auxin in plant tissues (Engvild et al., 1980, 1981; Katayama et al., 1988; Manabe et al., 1999; Reinecke, 1999). However, little is known about the role of auxins in regulating the late stages of seed development, and therefore the final yield of these agriculturally important species. In pea, it has been reported that 4-Cl-IAA moves from young seeds into the pod, where it is required for normal elongation (Reinecke et al., 1999; Johnstone et al., 2005; Ozga et al., 2009). This inference is based on the observation that deseeded pericarps fail to elongate, a phenotype that may be rescued by application of exogenous 4-Cl-IAA

(Reinecke et al., 1999; Ozga et al., 2009). Nevertheless, no mutant has been available to aid understanding of the biosynthesis and roles of 4-Cl-IAA, and there is limited physicochemical evidence on the origin of this compound (Reinecke, 1999). Currently, there is only limited evidence of biosynthesis of 4-Cl-IAA from 4-Cl-Trp and 4-Cl-indole in fava bean (Manabe et al., 1999); apart from these, no intermediates or genes from this pathway have been isolated or characterised. The pathways of auxin biosynthesis are starting to be revealed, but knowledge of the biosynthesis of 4-Cl-IAA is almost non-existent.

In this study, IPyA-dependent auxin biosynthesis is investigated further, through characterisation of two newly identified aminotransferases from pea, and examination of IPyA and 4-Cl-IPyA, a novel auxin biosynthesis intermediate.

Materials and methods

Characterisation of IPyA by UPLC-MS and ^{1}H and ^{13}C NMR

Standard IPyA was dissolved in methanol and analysed by UPLC-MS. This analysis was repeated but the IPyA was initially dissolved in H_2O.

Synthetic IPyA was analysed by ^{1}H and ^{13}C NMR and UPLC-MS. NMR analyses of IPyA were conducted in CD_3OD, DMSO, 1:1 CD_3OD/D_2O, $NaHCO_3$ in D_2O (pH 9), NaOH in D_2O (pH 12) and KH_2PO_4/K_2HPO_4 buffer (pH 8.5 or pH 6.5 in D_2O), heated to 40 °C for 3 h prior to analysis, roughly mimicking certain *in vitro* assay conditions (Stepanova et al., 2008; Tao et al., 2008). Water-suppression ^{1}H NMR and multiplicity-edited ^{13}C-^{1}H HSQC NMR was also performed on IPyA in phosphate buffer (pH 6.5 or 8.5).

UPLC-MS analysis was undertaken on IPyA samples dissolved in H_2O or MeOH, as described in Chapter 2. MRM transitions are also detailed in Chapter 2. When required, full scans were acquired from *m/z* 60 to *m/z* 500, with a cycle time of 0.25 s. In some cases (e.g. the data shown for IPyA) both full scan MS and MRM data were acquired simultaneously. Full scan product ion spectra for ICA and the unknown were obtained over the range *m/z* 50 to *m/z* 250 from the precursor ion at *m/z* 146.1, with a cycle time of 0.4 s, cone voltage 15 V and CE 18 V. Full scan product ion spectra for IPyA were obtained over the range *m/z* 80 to *m/z* 250 with a cycle time of 0.4 s from the precursor ion at *m/z* 204.1, with cone voltage 18 V and CE 15 V.

To test the sensitivity of IPyA to light and different solvents, a solution of IPyA was made up in methanol (167 ng.μL^{-1}) and four 1.2 µL aliquots were taken. All four aliquots were made up to 50 µL, two with methanol and two with H_2O. One of the methanol solutions and one of the H_2O solutions was covered with Al-foil and all four treatment samples were left at room temperature for two days before analysis for IPyA, IAA and ICA by UPLC-MS.

Synthesis and characterisation of 4-Cl-IPyA

The 4-Cl-IPyA synthesis method was adapted from Politi et al. (1996).

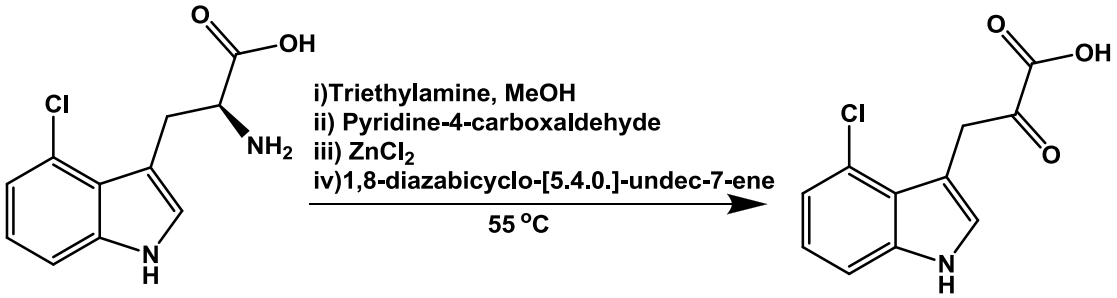

Figure 6.2 – Synthesis of 4-Cl-IPyA.

Triethylamine (76 µL) was added to a suspension of DL-4-Cl-Trp (102 mg) in methanol (1.7 mL), under an atmosphere of N_2 at room temperature. After stirring for 10 min, pyridine-4-carboxaldehyde (80 µL) was added and the mixture was stirred for a further 10 min, after which $ZnCl_2$ (anhydrous; 42 mg) was added to the mixture, which was stirred for a further 10 min. Total dissolution was achieved when 1,8-diazabicyclo-[5.4.0.]-undec-7-ene (164 µL) was added to the mixture, which was then stirred for a further 3 h, under N_2, after which it was quickly added drop-wise to HCl (2M, 5 mL), preheated to 50 °C. After 10 min, the temperature was increased to 55 °C and the mixture was left for another 25 min, after which it was slowly cooled to room temperature and stood for 16 h. The resulting brown precipitate was collected by vacuum filtration, air-dried overnight and then dried in a desiccator. The precipitate was identified as the target compound (47 mg, 46 % yield) by ^{1}H and ^{13}C NMR [^{1}H (CD_3OD, 300 MHz) δ: 7.06 (m, 2H), 7.33 (dd, *J* = 2.4 Hz, 3.9 Hz, 1H), 7.72 (s, 1H), 8.12 (d, *J* = 2.1 Hz, 1H), 11.18 (bs, 1H); ^{13}C (CD_3OD, 75 MHz) δ: 105.4 (CH), 110.5 (C), 110.4 (CH), 120.9 (CH), 122.1 (CH), 122.9 (C), 125.9 (C), 129.4 (CH), 137.1 (C), 137.8 (C), 167.5 (C)]. The product was analysed by UPLC-MS.

Expression and purification of PsTAR1 and PsTAR2

Dr Sandra Davidson and Lily Sutton isolated, from pea, three Trp aminotransferase genes, which they named *TRYPTOPHAN AMINOTRANSFERASE RELATED 1 to 3* (PsTAR1 to 3; Sutton, 2009). The sequences of PsTAR1 and PsTAR3 are very similar to each other and 51 % homologous to TAA1 at the protein level. However, PsTAR2 is more closely aligned to the *Arabidopsis* TAR2 (56 % identity). Recombinant PsTAR1 and PsTAR2 were expressed and purified, as described in Chapter 2.

In vitro assays of PsTAR1 and PsTAR2, using Trp and 4-Cl-Trp as substrates

It was first determined whether PsTAR2 could use Trp as an *in vitro* substrate. To obtain a global picture of Trp metabolism by this enzyme, carbon-14 labelled Trp was used. *In vitro* assay mixtures consisted of recombinant MBP-PsTAR2 (2.2 $\mu g.\mu L^{-1}$), [^{14}C]Trp (10^5 DPM), sodium pyruvate (4.3 $\mu L.\mu L^{-1}$), and PLP (1.6 mM) in K_2HPO_4/KH_2PO_4 buffer (pH 8.5; 10 mM). The total volume was 190 µl. Purified reverse-orientation PsTAR2 was used as a control. Both samples were incubated 37 °C for 3 h. After this, ACN was added to each sample to give a final ratio of 90:10 sample/ACN and both samples were analysed by HPLC-radiocounting (Program 2).

Next the identity of the product when PsTAR1 and PsTAR2 were supplied with Trp or 4-Cl-Trp as substrates was determined. *In vitro* assay reaction tubes contained purified recombinant protein (0.20 $\mu g.\mu L^{-1}$), substrate (either Trp or 4-Cl-Trp; 34 $ng.\mu L^{-1}$), sodium pyruvate (4.8 $g.L^{-1}$), PLP (1.2 mM) and maltose (4.1 mM), in K_2HPO_4/KH_2PO_4 buffer (10 mM, pH 8.5). The total reaction volume was 174 µL. Controls were also prepared, by replacing the protein with buffer solution (NPC) or MBP (0.20 $\mu g.\mu L^{-1}$). Three replicates of each sample type were prepared. All samples were incubated at 37 °C for 3 h, after which the reaction was stopped by the addition of acetic acid in methanol (5 % v/v) to give an 80:19:1 buffer/MeOH/acetic acid mixture. These mixtures were then analysed by UPLC-MS.

In addition, an *in vitro* assay in which the product level was measured at regular intervals through the incubation was conducted. A fraction of purified PsTAR2 (ca. 2 $\mu g.\mu L^{-1}$) was concentrated under reduced pressure to ca. 90 µL. To this was added 116 µL of [D_4]Trp (50 $ng.\mu L^{-1}$), 12.5 µL of PLP (20 mM; final concentration 1 mM) and 25 µL of sodium pyruvate

(500 mM; final concentration 50 mM), to give a final volume of 243.5 µL. An NPC was prepared using the same components but replacing the protein with KH_2PO_4/K_2HPO_4 buffer (pH 8.55). Both samples were incubated at 35 °C for 3 h. 20 µL aliquots were taken from each sample every 15 min for the first hour, and every 30 min thereafter. Immediately after removal from the incubation tube, each aliquot was treated with 10 µL of acetic acid in water (1 % v/v), centrifuged at 1.3 x 10^4 rpm and the supernatant was analysed by UPLC-MS for Trp, IPyA and IAA.

PsTAR1 and PsTAR2 *in vitro* assays using IPyA and 4-Cl-IPyA as substrates

Next it was determined whether or not PsTAR1 or PsTAR2 could use IPyA or 4-Cl-IPyA as substrates. *In vitro* assay mixtures consisted of purified recombinant protein (0.20 $\mu g.\mu L^{-1}$), substrate (34 $ng.\mu L^{-1}$), sodium pyruvate (4.74 $mg.mL^{-1}$), PLP (1.2 mM) and maltose (4.7 mM), in K_2HPO_4/KH_2PO_4 buffer (10 mM, pH 6.5). MBP was used as a control and an NPC was also prepared. Three replicates of each sample type were prepared.

Time-course *in vitro* assays using IPyA as a substrate were also conducted. The solvent of three aliquots of purified PsTAR2, each containing 350 µg of protein, was removed under reduced pressure and the residue redissolved in 125 µL of K_2HPO_4/KH_2PO_4 buffer (pH 6.5). Three aliquots (4.81 µL each) of purified MBP (fraction 4) were made up to 125 µL with the same buffer. To each of these was added IPyA (250 $ng.\mu L^{-1}$, 24 µL, 6 µg total), PLP (10 mM, 16.6 µL, final concentration = 1 mM). An NPC was also prepared by replacing the protein solution with 125 µL of buffer. These nine samples were incubated at 37 °C for a total of 3 h. Every 15 min for the first hour and every 30 min for the subsequent 2 h, 20-µL aliquots were taken from each treatment replicate. Immediately after removal, the aliquots were treated with 10 µL of acetic acid in methanol (5 % v/v) and 10 µL of [$^{13}C_6$]IAA (10 $ng.\mu L^{-1}$). This mixture was centrifuged (1.3 x 10^4 rpm) for 2 min and the supernatant was analysed by UPLC-MS for IAAld, IEt and IAA.

Determining endogenous levels of IAA and 4-Cl-IAA over the course of seed development

Seeds at several different stages of development were harvested into MeOH/BHT (Table 6.1). [$^{13}C_6$]IAA (20 ng) and [D_3]4-Cl-IAA (70 ng) were added to each of the extracts, which were then

analysed by UPLC-MS. Comparable seeds from the same pods were harvested into liquid N_2 for analysis of *PsTAR1, PsTAR2* and *PsTAR3* mRNA expression by Dr Sandra Davidson.

Table 6.1 – Fresh weights of Pisum sativum seeds, harvested at various stages of development. Shown are mean FW ± se (n = 3).

DPA	Average FW per seed (mg)
5-8	3.8 ± 0.4
12	54 ± 4
14-17	199 ± 10
20-22	293 ± 8
25-28	432 ± 27
35-38	459 ± 12

Results

Characterisation of IPyA by UPLC-MS and ^{1}H and ^{13}C NMR

Authentic IPyA was analysed by ^{1}H and ^{13}C NMR and UPLC-MS. NMR analyses of IPyA in CD_3OD [^{1}H, (300 MHz) δ: 6.92 (s, 1H), 7.09 (m, 2H), 7.36 (d, *J* = 4.2 Hz, 1H), 7.68 (d, *J* = 7.5 Hz, 1H), 7.93 (s, 1H); ^{13}C, (75 MHz) δ: 104.4 (CH), 110.2 (C), 111.2 (CH), 117.8 (CH), 119.5 (CH), 121.7 (CH), 127.1 (C), 127.4 (CH), 136.2 (C), 137.5 (C), 137.4 (C)], DMSO [^{1}H, (300 MHz) δ: 6.76 (s, 1H), 7.08 (m, 2H), 7.38 (d, *J* = 8.1 Hz, 1H), 7.68 (d, *J* = 7.8 Hz, 1H), 7.84 (s, 1H), 8.73 (s, 1H), 11.39 (s, 1H)], 1:1 CD_3OD/D_2O [^{1}H, (300 MHz) δ: 6.98 (s, 1H), 7.18 (m, 2H), 7.45 (d, *J* = 7.8 Hz, 1H), 7.72 (d, *J* = 6.9 Hz, 1H), 7.96 (s, 1H)], $NaHCO_3$ in D_2O (pH 9) [^{1}H, (300 MHz) δ: 6.60 (s, 1H), 7.06 (m, 2H), 7.34 (d, *J* = 8.1 Hz, 1H), 7.66 (d, *J* = 7.2 Hz, 1H), 7.73 (s, 1H)] and NaOH in D_2O (pH 12) [^{1}H, (300 MHz) δ: 6.12 (s 1H), 6.85 (m, 2H), 7.15 (d, *J* = 8.1 Hz, 1H), 7.45 (d, *J* = 7.8 Hz, 1H) 7.65 (s, 1H); ^{13}C (75 MHz) δ: 93.2 (CH), 111.6 (C), 113.2 (CH), 118.6 (CH), 118.8 (CH), 121.8 (CH), 122.6 (C), 126.4 (CH), 135.3 (C), 155.3 (C), 178.6 (C)] all indicated the presence of mainly the enol tautomer of IPyA (see Figure 6.3), although cross-peak integration ratios indicated the possibility of dual-state IPyA. When

synthetic IPyA was dissolved in methanol and analysed by UPLC-MS (MRM mode) one peak (Figure 6.4) was observed in the IPyA channels along with breakdown products IAA and ICA (Figure 6.5) in their respective channels. Reanalysis after 24 and 72 h by ^{1}H NMR showed little change to the sample and the UPLC-MS showed an increase in the proportion of IAA. Hence, the evidence indicates that the peak at 4.5 min was IPyA in the enol tautomer.

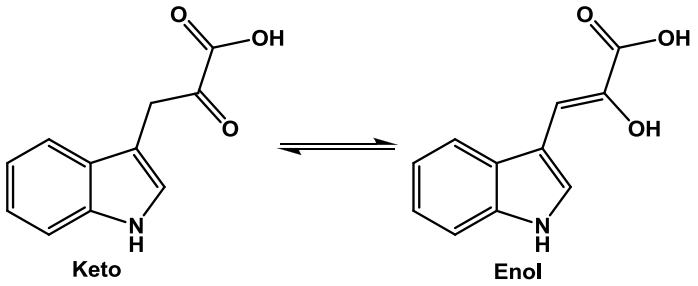

Figure 6.3 – Keto-enol tautomerisation of IPyA.

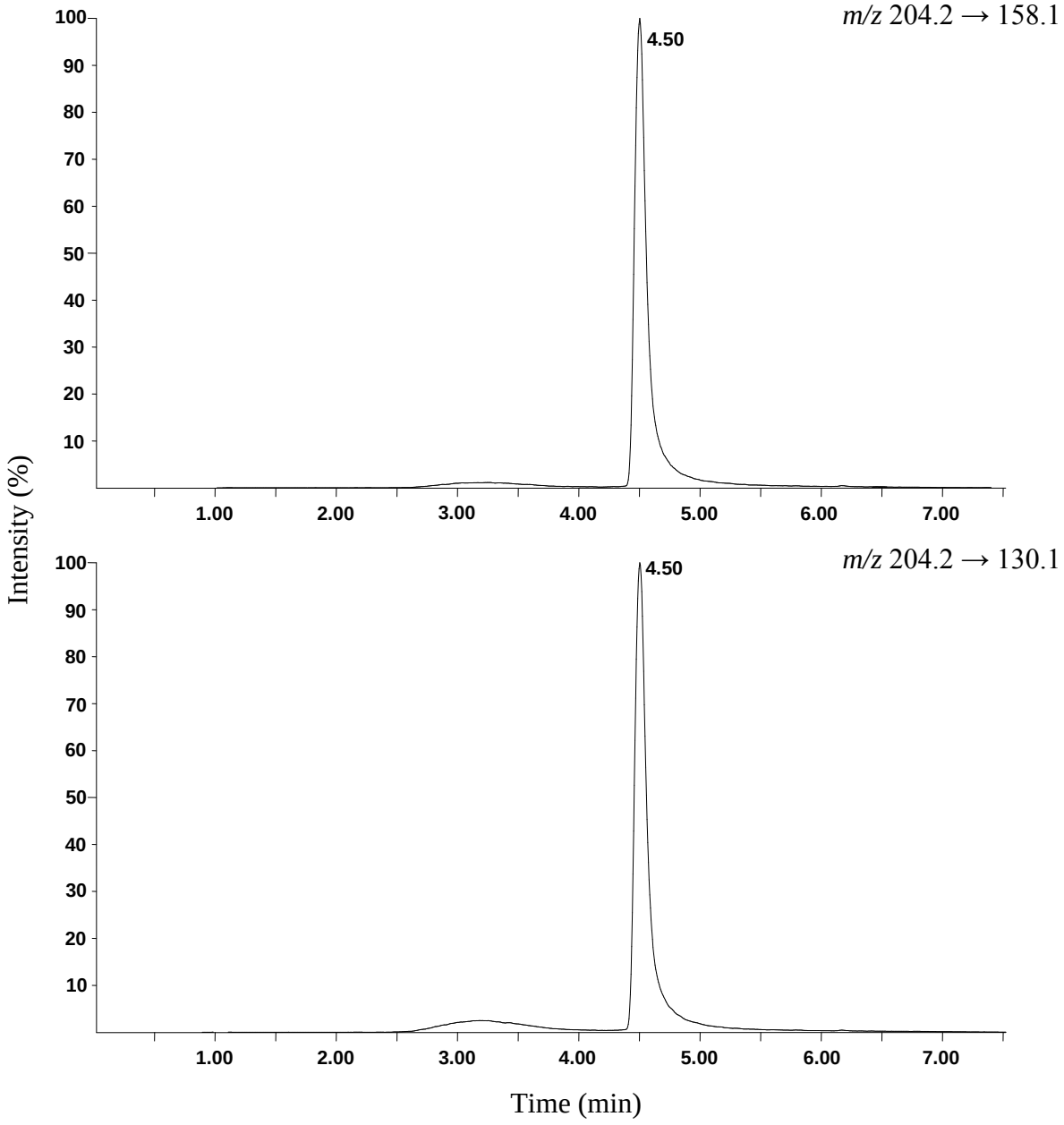

Figure 6.4 – UPLC-MS chromatogram (MRM for IPyA; acetic acid program) of authentic IPyA in methanol, showing the later peak, determined by ^{1}H and ^{13}C NMR to be enol-IPyA, dominating the chromatogram.

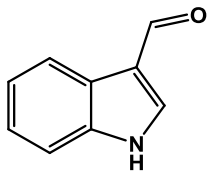

Figure 6.5 - Structural formula for ICA.

IPyA was also dissolved in KH_2PO_4/K_2HPO_4 buffer (pH 8.5 in D_2O) and heated to 40 °C for 3 h (roughly mimicking the *in vitro* assay conditions) prior to analysis by ^1H NMR [(300 MHz) δ: 4.04 ('d' 2H), 6.61 (s, 1H), 6.97-7.14 (m, 13H), 7.34-7.39 (m, 6H), 7.49 (d, J = 6.9 Hz, 2H), 7.75 (s, 1H)] and UPLC-MS. The ^1H NMR spectrum had a strange appearance due to the curious integration ratios, the diminishing of the signal at 6.63 ppm and the appearance of an abnormal 'doublet' (in a regular doublet the two peaks are of equal area and height; the observed abnormal 'doublet' consisted of a larger peak with a smaller one beside it). The unusual appearance of this signal is most likely due to equilibrium between the keto and enol tautomers (Figure 6.3); when the enol tautomer changes to the keto, it will incorporate a hydrogen atom from the solvent, and since the solvent was deuterated, this exchange results in replacement of the aliphatic protons with deuterium nuclei. The unusual integration ratio is probably due to the presence of both keto and enol tautomers, which give slightly different chemical shifts. Repetitions of this experiment using H_2O rather than D_2O and water-suppression NMR revealed primarily the keto tautomer in both pH 6.5 and pH 8.5 buffer after heating [^1H (400 MHz) δ: 4.1 (s, 2H) 7.0-7.2 (m, 3H), 7.4 (dd, J = 8.23 Hz, 8.45 Hz 2H); ^{13}C (100 MHz) δ: 40.9 (CH_2), 110.9 (C), 117.1 (CH), 123.7 (CH), 124.6 (CH), 127.1 (CH), 130.5 (CH), 132.0 (C), 141.4 (C), 175.7 (C), 209.5 (C)], with small amounts of the degradation product IAA. While the main compound detected was keto-IPyA, cross-peak volume integrals once again did not match expected single-tautomer peak ratios, indicating the presence of low amounts of enol-IPyA. The treatment described above also changed the behaviour of IPyA on UPLC-MS. Under these conditions a peak with a considerable tail was observed at 2.4 min, whereas in other solvents the peak for IPyA was at 4.5 min. There were substantial similarities in the MS^2 spectra produced from the solution in CD_3OD and the solution in KH_2PO_4/K_2HPO_4 buffer (pH 8.5), both consistent with IPyA [early peak *m/z*: 115 (8 %), 118 (8%), 130 (100 %), 142 (8 %), 158 (63 %); later peak *m/z*: 103 (6 %), 130 (100 %), 144 (7 %), 158 (82 %)]. Heating IPyA in H_2O or leaving it a room temperature for 3 h in the aforementioned buffer gave a mixture of the two tautomers (Figure 6.6); there was a significant increase in the keto tautomer after 24 h in the buffer (Figure 6.6) but it appears that both conditions (heat and a pH within 1.5 units of neutral) are necessary to produce the keto tautomer.

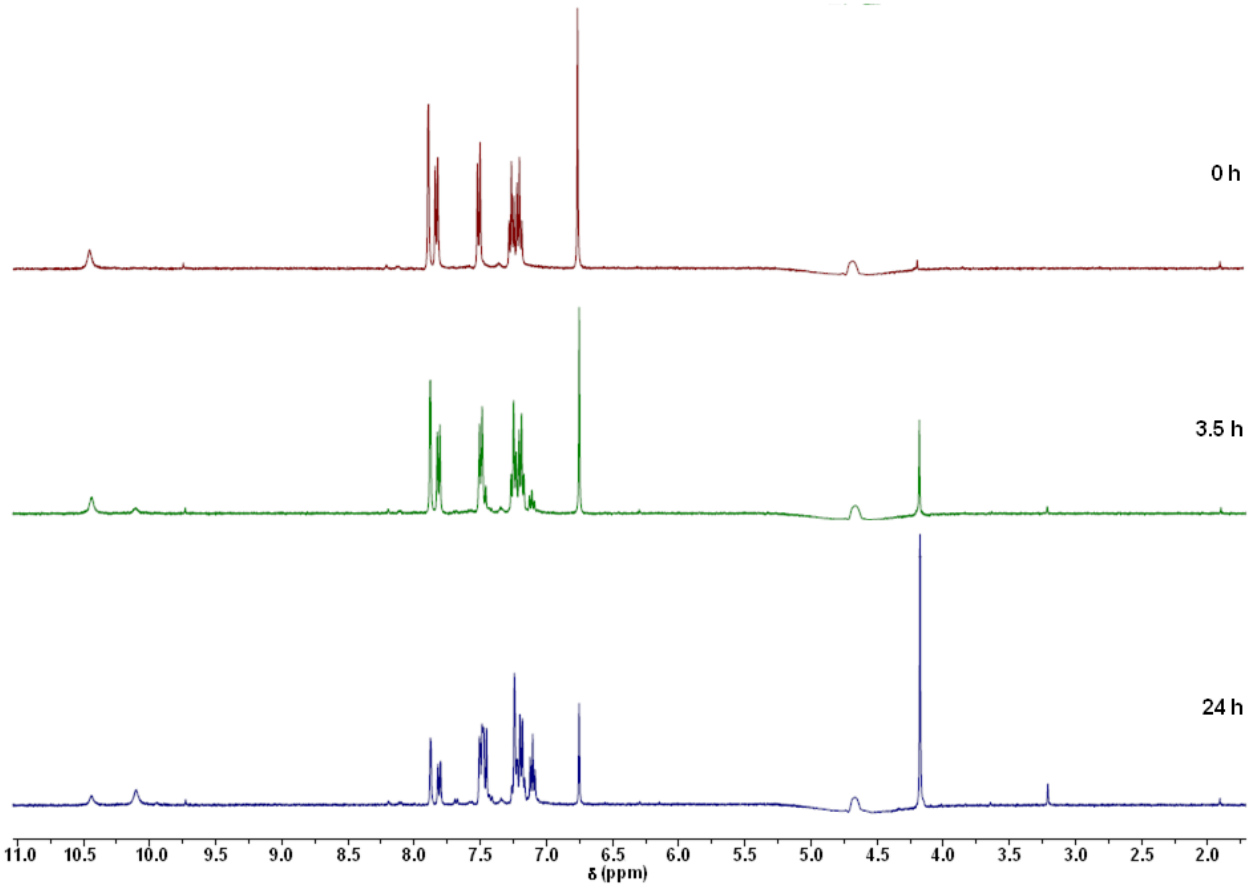

Figure 6.6 – ^{1}H NMR spectra of authentic IPyA in aqueous KH_2PO_4/K_2HPO_4 buffer (pH 8.5), at three time points after dissolution. The appearance of the singlet at 4.1 ppm and disappearance of the singlet at 6.7 indicate transition from the enol to the keto tautomer over 24 h.

As further evidence that the early peak was in fact IPyA, an IPyA solution was prepared such that primarily the early peak was observed on UPLC-MS (Figure 6.7), and the sample was reduced with $NaBH_4$ and analysed again by UPLC-MS (Figure 6.8). The product observed on UPLC-MS was ILA (confirmed by comparison with a standard), indicating that the early peak did in fact represent IPyA. As further evidence that early peak represented keto IPyA HSQC NMR was performed on an IPyA sample prepared in KH_2PO_4/K_2HPO_4 buffer (pH 8.5 in H_2O) and heated to 40 °C for 3 h. This revealed the presence of five aromatic CH groups and one aliphatic CH_2 (Figure 6.9). Combining these findings with the ^{1}H and ^{13}C NMR results, which clearly indicate the presence of a carbonyl group (209.5 ppm) and a carboxylic acid group (175.7 ppm), it was concluded that the early-eluting peak was the keto tautomer of IPyA.

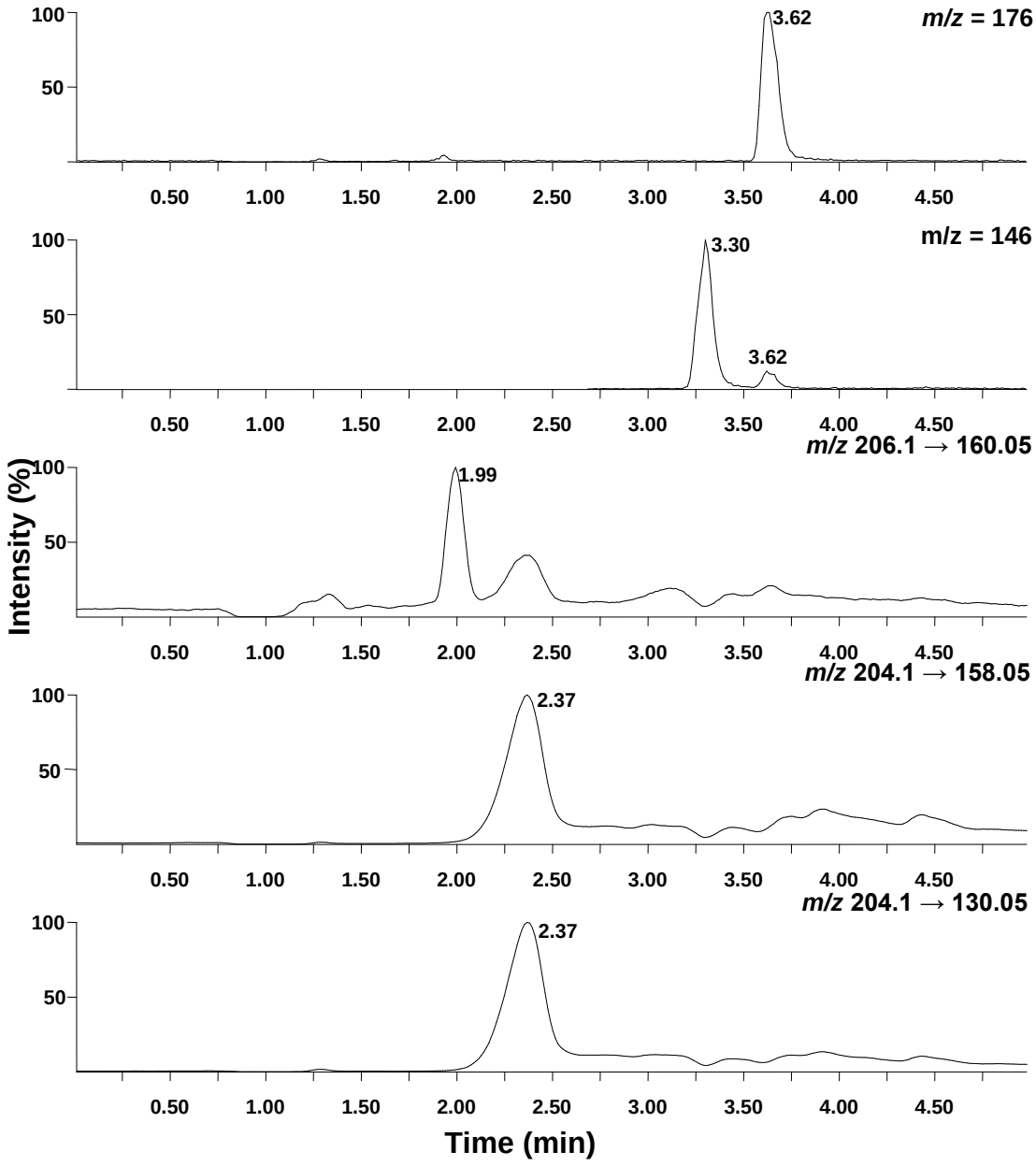

Figure 6.7 – UPLC-MS (pH 5.4 program) chromatogram of synthetic IPyA (dissolved in K_2HPO_4/KH_2PO_4 buffer and heated to 40 °C for 3 h) prior to reduction with $NaBH_4$, showing *m/z* 176 (IAA, RT: 3.62 min), *m/z* 146 (ICA, RT: 3.30 min) and keto-IPyA (*m/z* 204.1 → 158.1 and 204.1 → 130.1, RT: 2.37 min). ILA was not detected (*m/z* 206.1 → 160.05; expected RT: 2.84 min).

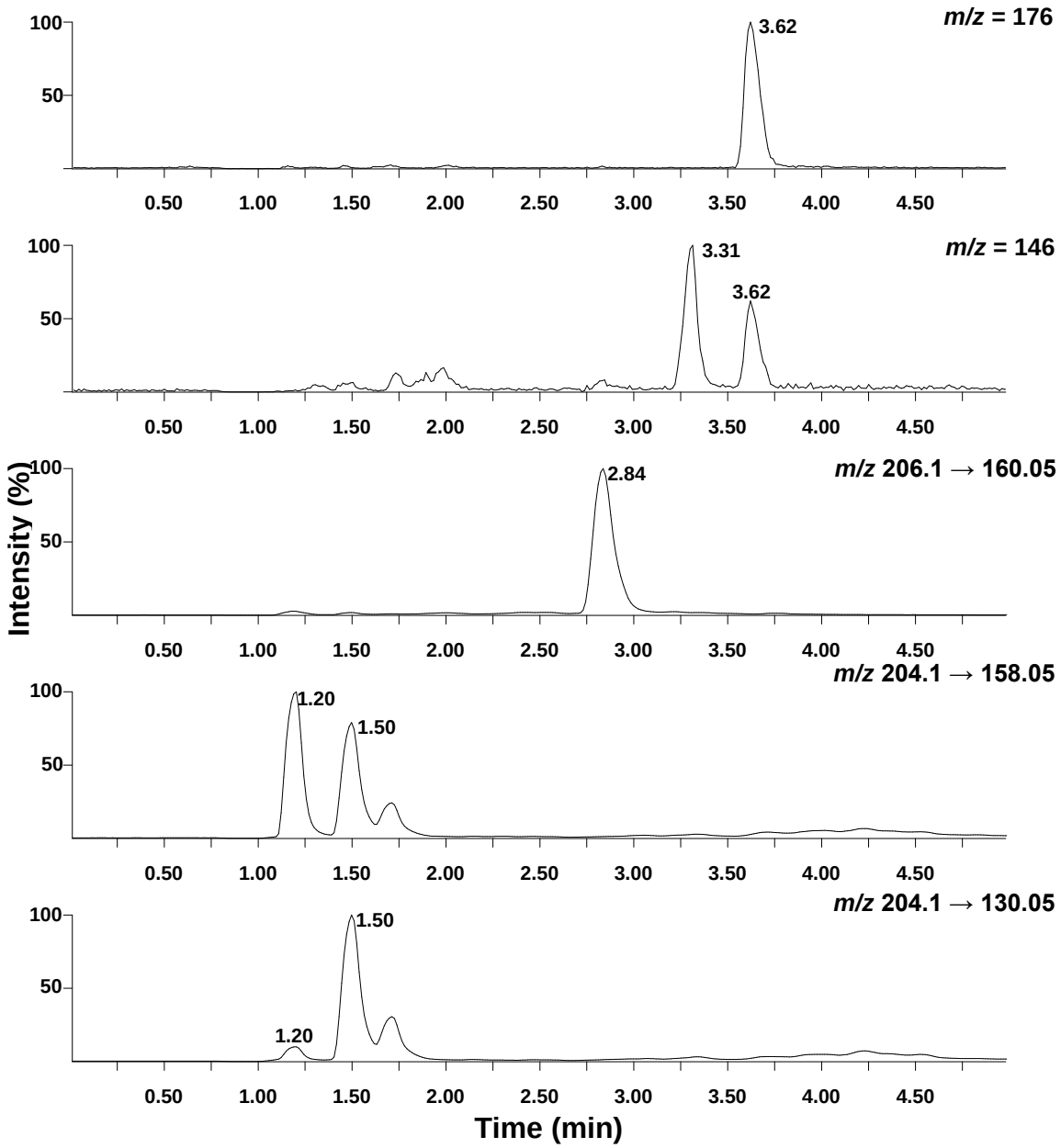

Figure 6.8 - UPLC-MS (pH 5.4 program) chromatogram of synthetic IPyA (dissolved in K_2HPO_4/KH_2PO_4 buffer and heated to 40 °C for 3 h) after reduction with $NaBH_4$, showing *m/z* 176 (IAA, RT: 3.62 min), *m/z* 146 (ICA, RT: 3.30 min) and ILA (*m/z* 206.1 → 160.05, 2.84 min). Keto-IPyA (*m/z* 204.1 → 158.1 and 204.1 → 130.1, expected RT: 2.37 min) was not detected.

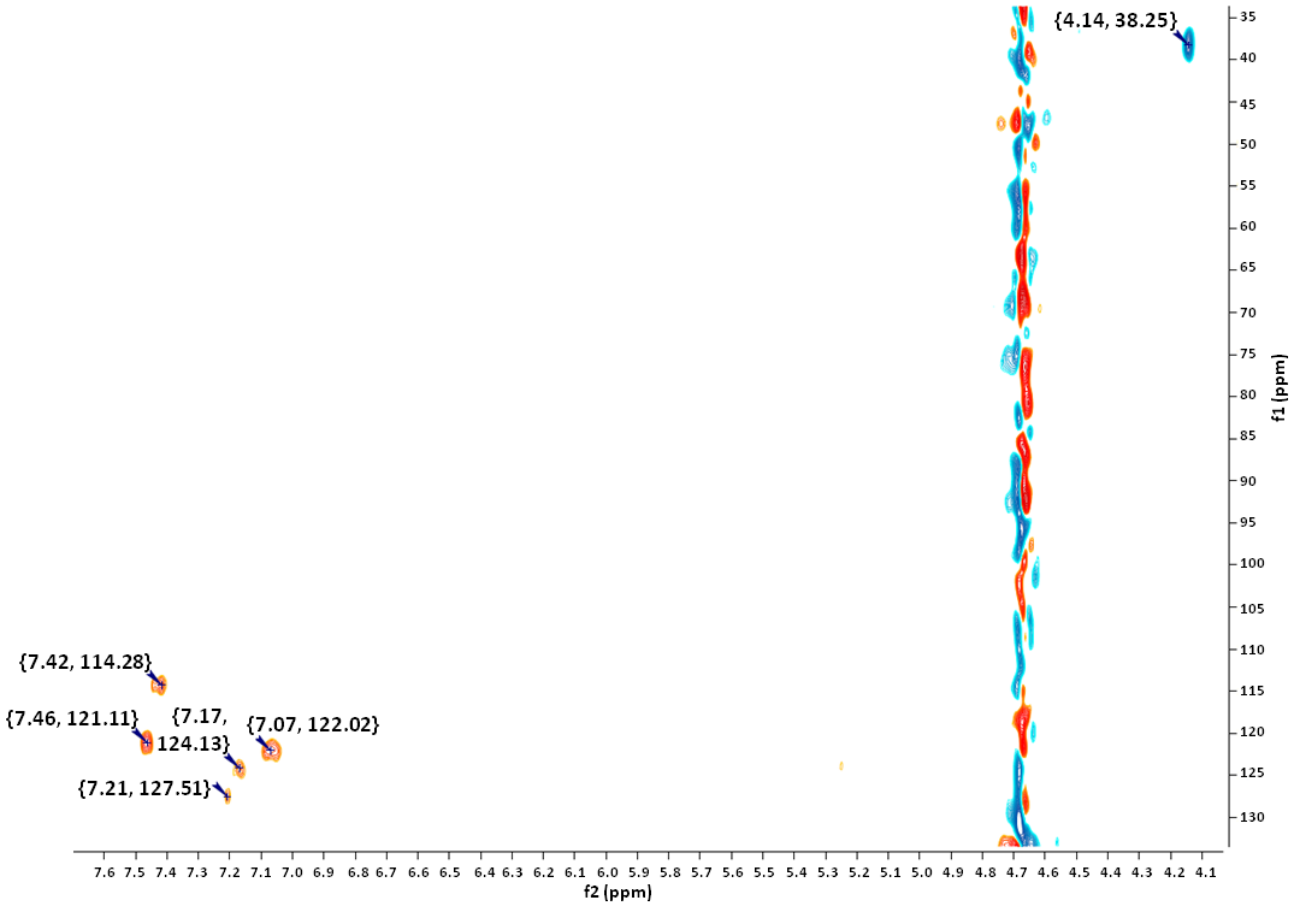

Figure 6.9 - HSQC NMR of standard IPyA.

When both tautomers of IPyA were visible on UPLC-MS, a substantial tail was often observed on the early peak (Figure 6.10). This was most likely due to keto-enol tautomerism occurring during the chromatography. A major difference between the mass spectra of the two tautomers is the ratio of *m/z* 158 to *m/z* 130. The enol tautomer produces a much greater percentage of *m/z* 158 than the keto tautomer. There was an exponential increase in the *m/z* 158 to *m/z* 130 ratio moving across the chromatogram from the early peak to the later peak. This indicates that the tail is due to inter-conversion of both tautomers rather than conversion of one tautomer to the other, which would produce a constant *m/z* 158 to *m/z* 130 ratio across the chromatogram.

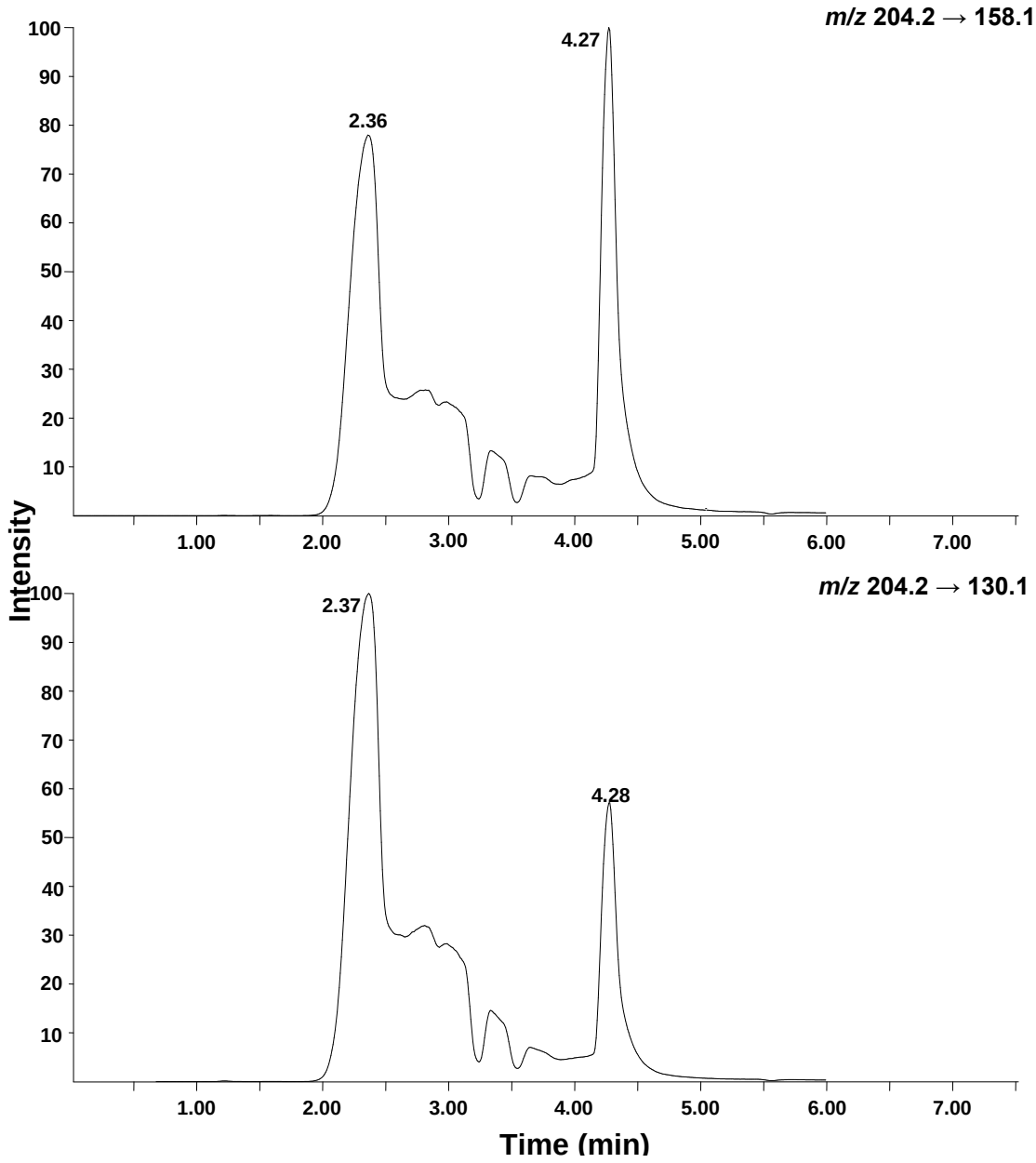

Figure 6.10 – UPLC-MS (MRM for IPyA) chromatogram of authentic IPyA, showing the keto (RT 2.37 min) and enol (RT 4.28) tautomers.

The stability of IPyA under various conditions was also tested. Previously it has been reported that IPyA is sensitive to light and moisture (IPyA container, Sigma-Aldrich). This theory was partially borne out when the stability of IPyA was tested at room temperature in the dark and under a mixed white light source (natural daylight and fluorescent light) in H_2O or MeOH (Table 6.2). In terms of relative abundance of IAA (breakdown product) compared to IPyA, more breakdown was observed in the light than in the dark in either solvent. This theory was also

supported by the observed increased breakdown to ICA in the light compared to the dark in methanol. Conversely, breakdown to ICA in H_2O was increased, albeit minimally, in the dark compared to the light. Taken together, these observations indicate that light may increases the rate of breakdown of IPyA to IAA and ICA. In terms of breakdown to ICA, no discernible trend was evident when comparing the effects of different solvents. However, there appeared to be some increase in breakdown to IAA in H_2O compared to methanol.

Table 6.2 – IPyA/IAA and IPyA/ICA ratios as determined by UPLC-MS for an IPyA standard after two days at room temperature with or without exposure to light.

IPyA/IAA				**IPyA/ICA**			
methanol		H_2O		methanol		H_2O	
Dark	Light	Dark	Light	Dark	Light	Dark	Light
0.3313	0.2338	0.3190	0.2791	0.0511	0.0067	0.0257	0.0555

Synthesis and characterisation of 4-Cl-IPyA

The target compound was successfully synthesised, in a reasonable yield (46 %), considering the product was obtained by precipitation and the method was scaled-down. When the compound was analysed by UPLC-MS, two peaks were observed. These most likely represented the keto and enol tautomers of the compound, as is the case with IPyA.

Expression and purification of PsTAR1

The IPTG-induced protein expression and affinity chromatography purification of the MBP-PsTAR1 and MBP-PsTAR2 fusion proteins was successful (PsTAR1 is shown in Figure 6.11). However, there was evidence of some breakdown in the crude extract and the purified fractions (the fusion protein should be ca. 80 kDa).

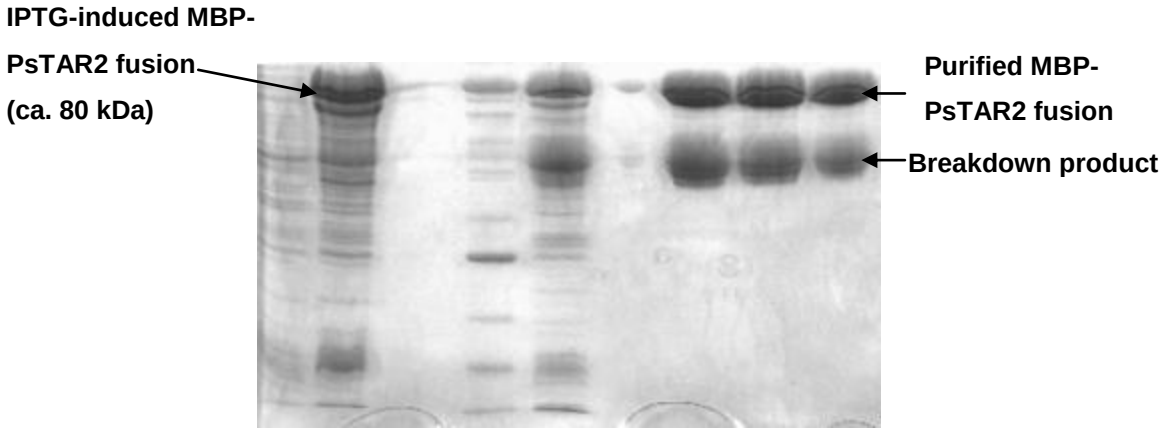

Figure 6.11 – SDS-PAGE of samples taken at various time-points throughout the expression and purification of recombinant PsTAR1 in *E. coli*. Samples are –IPTG (far left), +IPTG, blank, NEB protein ladder, crude protein extract, TB growth medium, purified fractions 6-8.

In vitro assays of PsTAR1 and PsTAR2, using Trp and 4-Cl-Trp as substrates

Analysis of *in vitro* single-time-point assay mixtures by HPLC-radiocounting showed that PsTAR2 could use Trp as a substrate (Figure 6.12), and Trp was not metabolised in either control (Figure 6.13 and Figure 6.14).

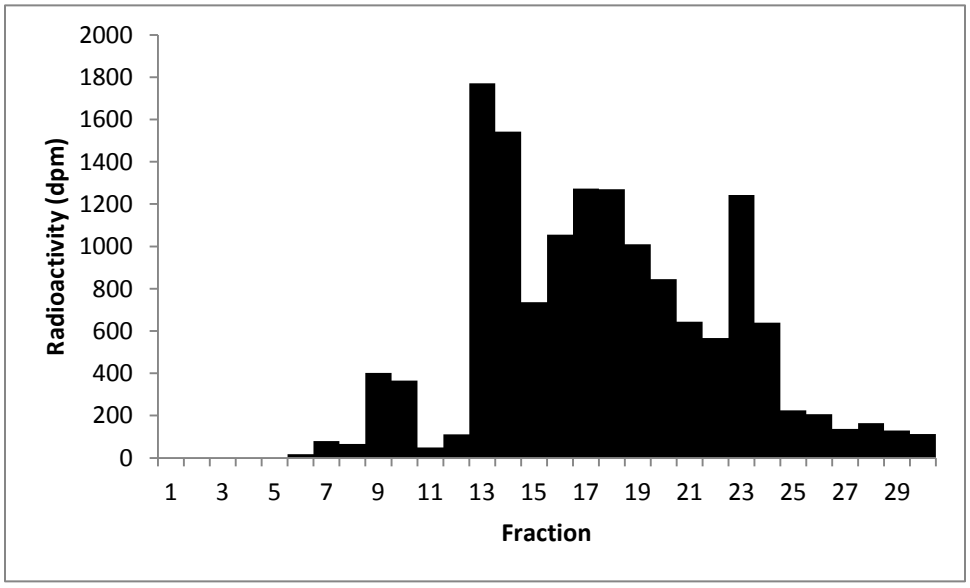

Figure 6.12 – HPLC-radiocounting histogram, showing the amount of radioactivity in each HPLC fraction, from an *in vitro* assay mixture using recombinant MBP-PsTAR2 as the catalyst and [^{14}C]Trp as the substrate.

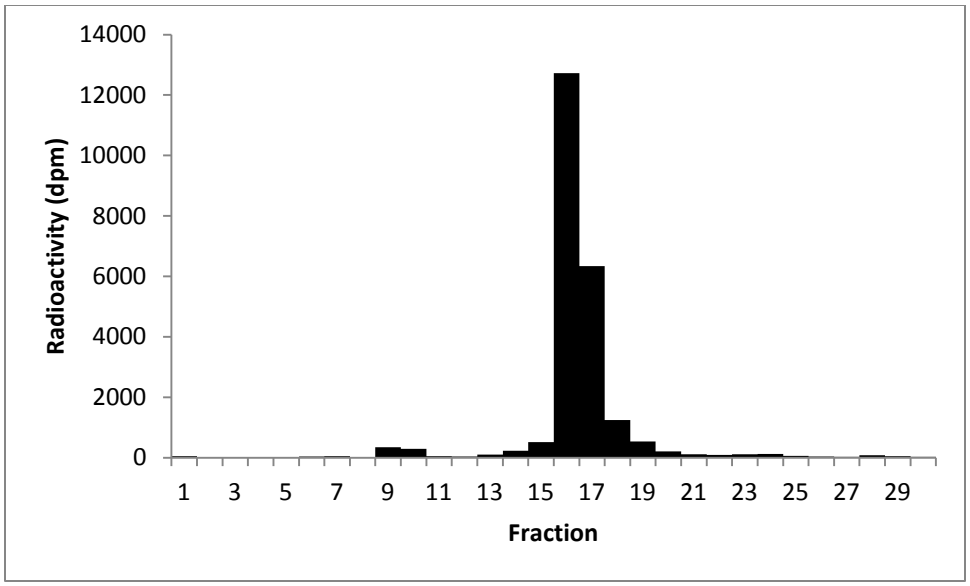

Figure 6.13 – HPLC-radiocounting histogram, showing the amount of radioactivity in each HPLC fraction, from an *in vitro* assay mixture using reverse-orientation recombinant MBP-PsTAR2 as the enzyme and [^{14}C]Trp as the substrate. This is a control for the result presented in Figure 6.12.

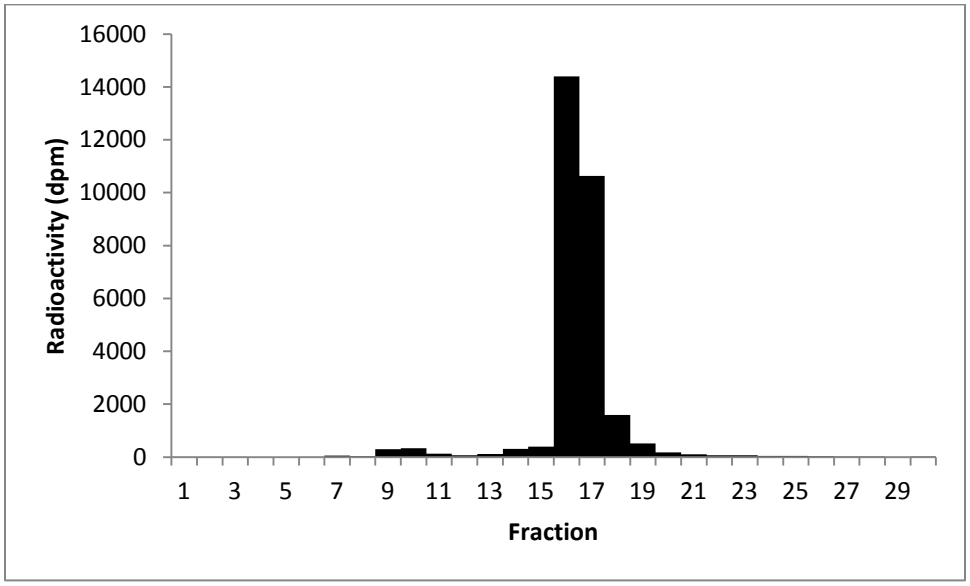

Figure 6.14 - HPLC-radiocounting histogram, showing the amount of radioactivity in each HPLC fraction, from an *in vitro* assay control mixture containing no protein catalyst and [^{14}C]Trp as the substrate. This is a control for the result presented in Figure 6.12.

The products of *in vitro* single-time-point assays, using PsTAR1 or PsTAR2 and Trp or 4-Cl-Trp, were identified by UPLC-MS as IPyA and 4-Cl-IPyA, respectively (Figure 6.15); the identity of the products was confirmed by comparison of RTs and mass spectra to those of authentic 4-Cl-IPyA (Figure 6.16) and IPyA (data not shown). IPyA was not detected in the

controls (data not shown). These results show that both proteins have aminotransferase activity, for both Trp and its 4-chlorinated derivative. While both enzymes strongly preferred Trp over 4-Cl-Trp (Table 6.3), the extent of this preference, in terms of percentage conversion, was less marked for PsTAR2 than PsTAR1. However, using the conditions described here, PsTAR1 was clearly the more effective enzyme, converting more than 95% of the Trp substrate to IPyA (Table 6.3).

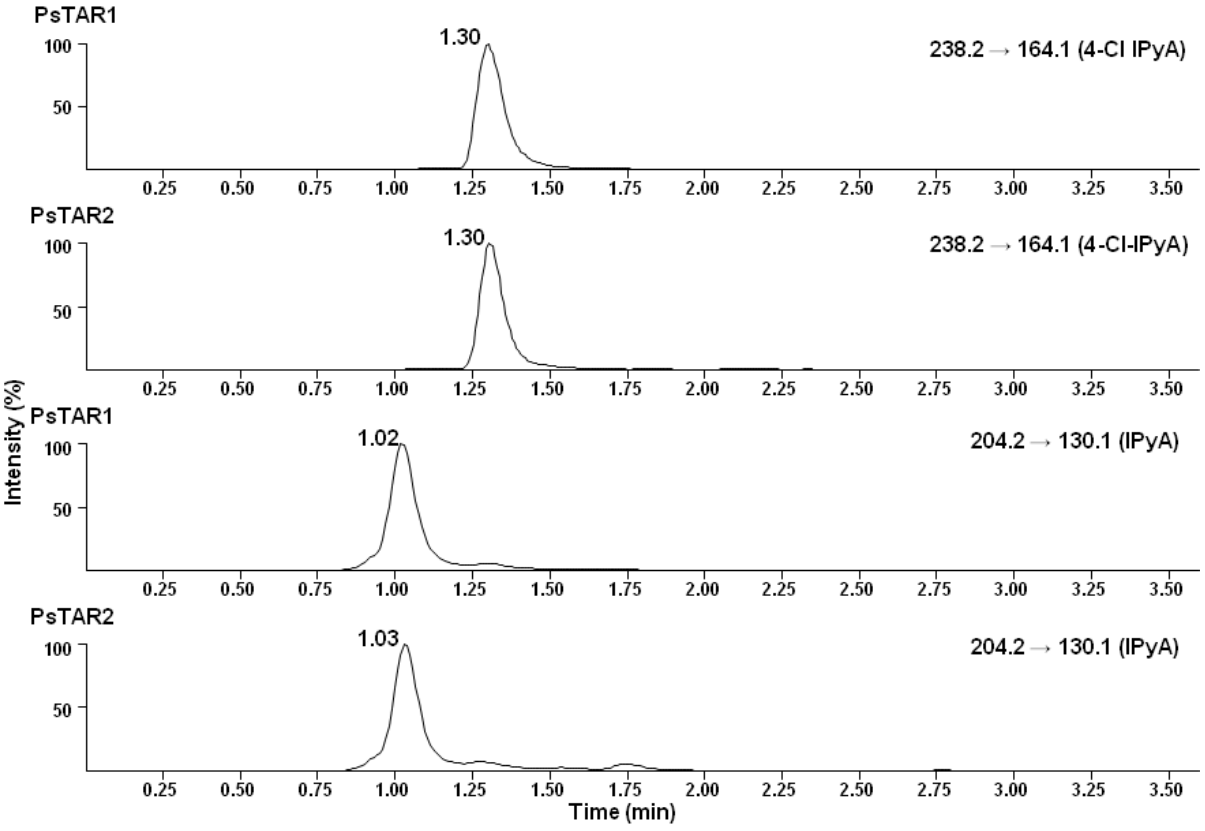

Figure 6.15 - UPLC-MS (MRM mode; pH 5.4 program) chromatograms, showing *in vitro* production of keto 4-Cl-IPyA (1.30 min) and keto IPyA (1.02 and 1.03 min) by PsTAR1 and PsTAR2 supplied with 4-Cl-Trp or Trp, respectively. The products were identified by comparing the retention times and mass spectra with those of authentic 4-Cl-IPyA and IPyA.

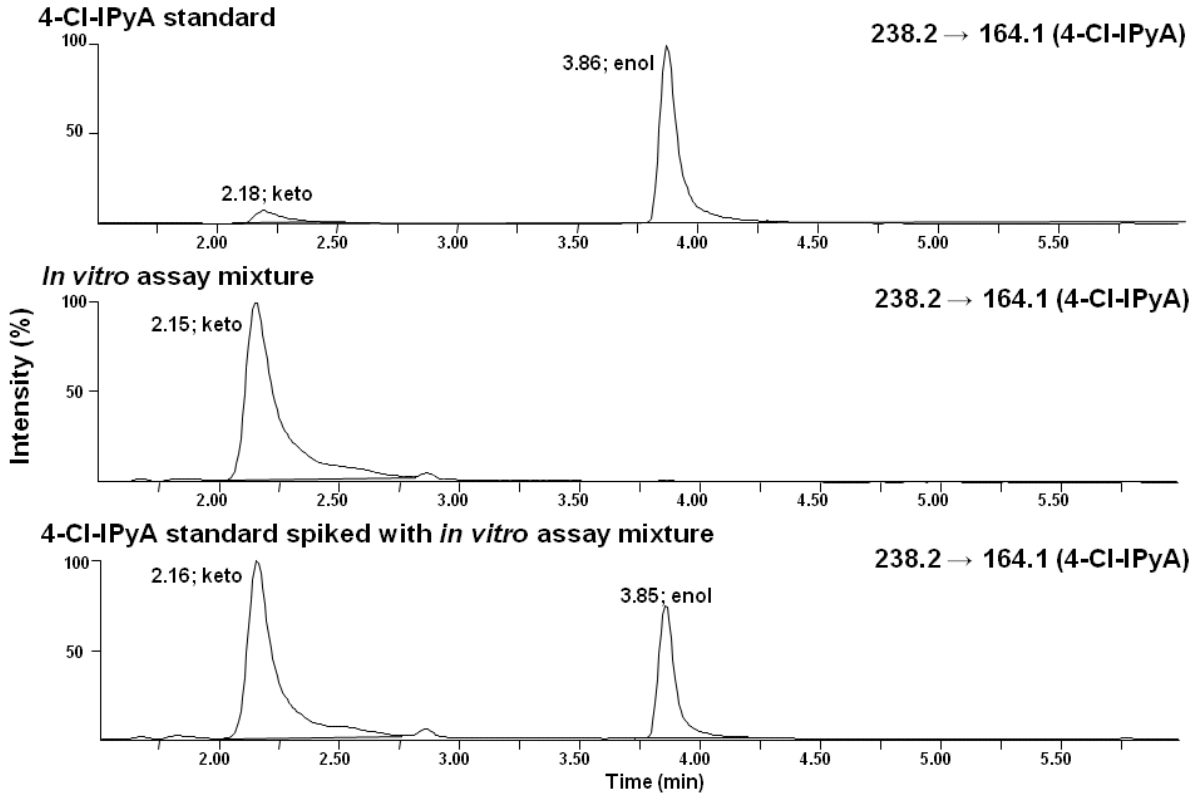

Figure 6.16 - UPLC-MS chromatograms (MRM mode; acetic acid program) of 4-Cl-IPyA standard (top channel), an *in vitro* assay mixture using PsTAR1 as the enzyme and 4-Cl-Trp as the substrate (middle channel) and a mixture of the two samples (bottom channel). Co-elution of the product with the standard confirms its identity as keto 4-Cl-IPyA.

Table 6.3 - *In vitro* conversion of Trp to IPyA and 4-Cl-Trp to 4-Cl-IPyA by PsTAR1 and PsTAR2 as determined by UPLC-MS. IPyA and Trp peak areas were used to determine the conversion as the percentage of product relative to the sum of product and residual Trp. Shown are means ± se (n = 3).

	Conversion to product (%)			
Substrate	PsTAR1	PsTAR2	MBP	NPC
Trp	96.0 ± 0.4	5.5 ± 0.3	0.005 ± 0.001	0.011 ± 0.003
4-Cl-Trp	3.98 ± 0.06	0.96 ± 0.04	0.00 ± 0.00	0.00 ± 0.00

The above results were also borne out in *in vitro* time-course assays (using Trp as a substrate), which showed a significantly greater increase in IAA (relative to Trp) in the test (Figure 6.17) compared to the control (Figure 6.18) throughout the incubation time. Notable amounts of keto-IPyA were also detected in the 'in frame' replicates (based on previous results, it is unlikely that

the enol tautomer was also produced, but the UPLC runs were cut short so it is impossible to be definitive on this point from these particular experiments), but not in the control replicates. The ratio of IPyA peak areas to Trp peak areas provided a good measure of the extent of conversion at each time point. Similarly, IAA peak areas were compared to Trp peak areas.

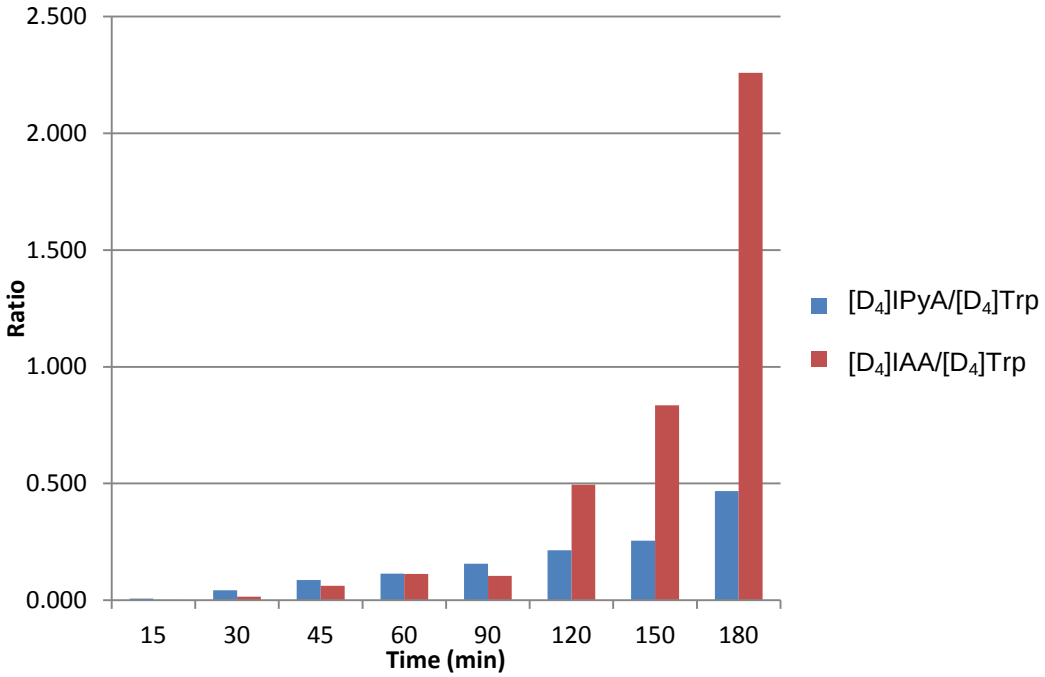

Figure 6.17 – Ratio of [D_4]IPyA to [D_4]Trp and [D_4]IAA to [D_4]Trp, obtained by UPLC-MS analyses (MRM mode) of an *in vitro* assay mixture using PsTAR2 as the enzyme and [D_4]Trp as the substrate, over 3 h. The ratio of the peak areas for [D_4]IPyA (product) to the peak areas for [D_4]Trp (reagent) were used as a measure of conversion.

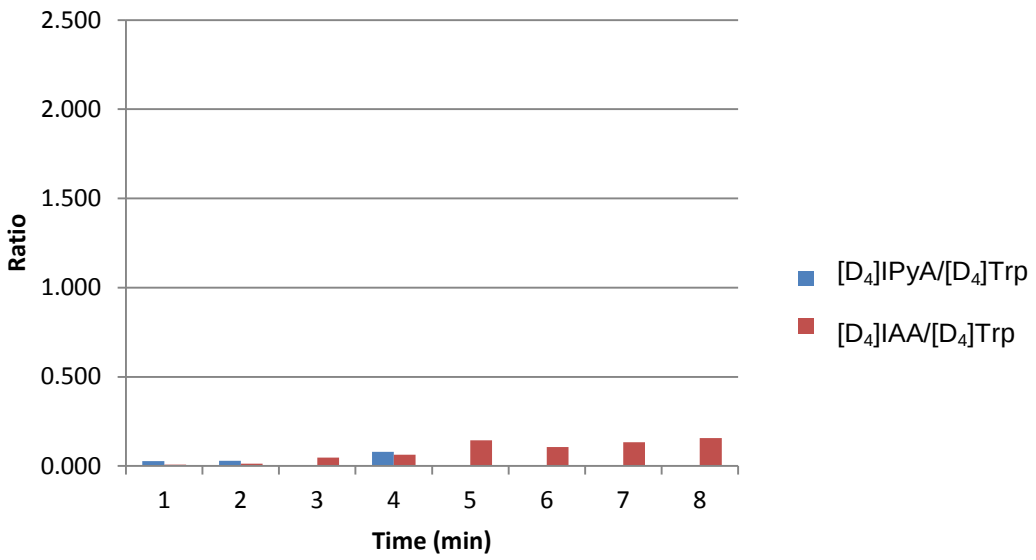

Figure 6.18 - Ratio of [D_4]IPyA to [D_4]Trp and [D_4]IAA to [D_4]Trp, obtained by UPLC-MS analyses (MRM mode) of an *in vitro* assay mixture using reverse orientation PsTAR2 as the enzyme and [D_4]Trp as the substrate, over 3 h.

PsTAR1 and PsTAR2 *in vitro* assays using IPyA and 4-Cl-IPyA as substrates

In both PsTAR1 and PsTAR2 *in vitro* assays, 4-Cl-IAA and IAA were detected in significant amounts, when 4-Cl-Trp and Trp, respectively, were supplied. *In vitro* assays using 4-Cl-IPyA or IPyA as the substrate showed no significant increase in 4-Cl-IAA or IAA production, relative to the controls (Table 6.4), thereby indicating that the 4-Cl-IAA and IAA detected was due to spontaneous, rather than enzymatic, conversion of the initial enzyme products, 4-Cl-IPyA and IPyA. However, this conversion is reportedly enzymatic in *Arabidopsis* (Kriechbaumer et al., 2011; Mashiguchi et al., 2011; Stepanova et al., 2011; Won et al., 2011).

Table 6.4 – IAA/[$^{13}C_6$]IAA and 4-Cl-IAA/[D_3]4-Cl-IAA ratios of two sets of *in vitro* assay mixtures, as determined by UPLC-MS. The substrates in these assays were IPyA and 4-Cl-IPyA respectively. Shown are means ± se (n = 3).

Protein	IAA/[$^{13}C_6$]IAA	4-Cl-IAA/[D_3]4-Cl-IAA
PsTAR1	0.47 ± 0.02	0.74 ± 0.04
PsTAR2	0.41 ± 0.08	0.29 ± 0.02
Vector only	0.43 ± 0.03	0.83 ± 0.05
NPC	0.44 ± 0.02	0.69 ± 0.05

Determining endogenous levels of IAA and 4-Cl-IAA over the course of seed development

Auxin levels, and the expression of *PsTAR1* and *PsTAR2*, were measured over the course of seed development (detailed in full in Tivendale et al., 2012). It was found that the level of 4-Cl-IAA increased dramatically from 7 to 12 DPA and then steadily declined until the completion of seed development. Conversely, IAA levels were initially high but decreased markedly from 7 to 16 DPA, and remained low thereafter (Figure 6.19A). qRT-PCR showed that *PsTAR1* is strongly expressed early in seed development (7 DPA) when IAA levels are maximal and *PsTAR2* is strongly expressed at later stages (16-28 DPA) when 4-Cl-IAA levels are high, although past their peak (Figure 6.19B).

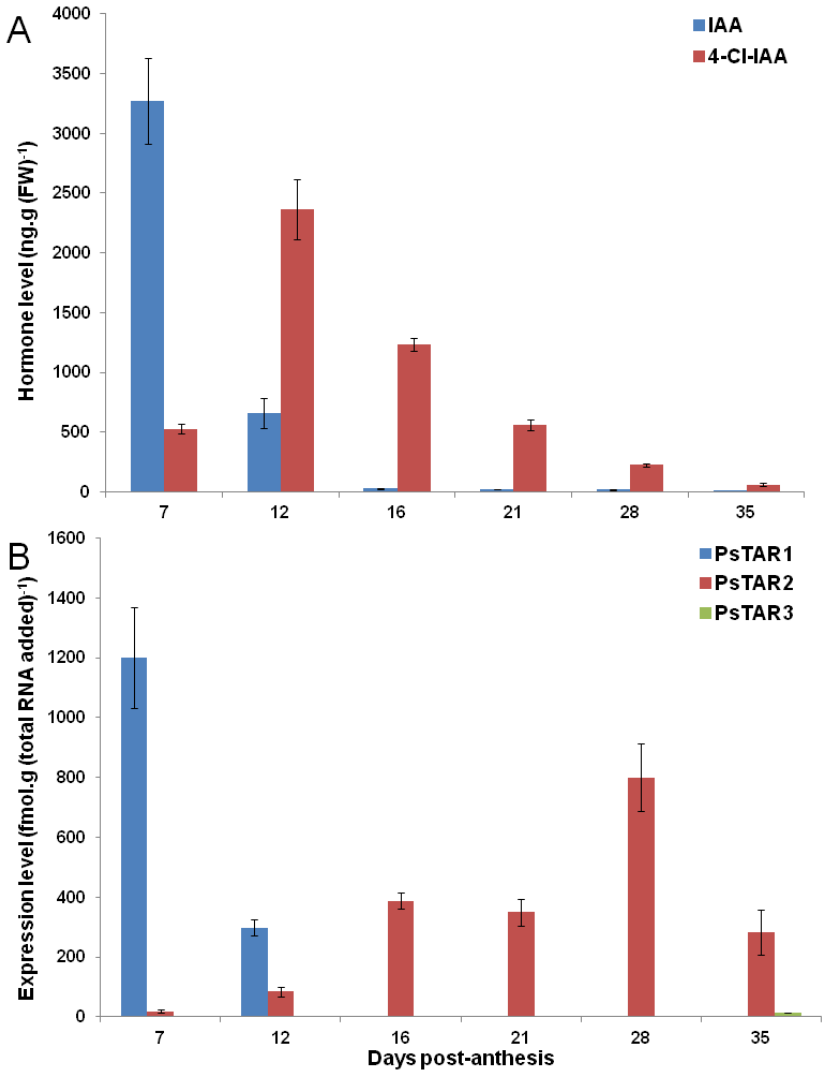

Figure 6.19 - (A) IAA and 4-Cl-IAA levels and (B) *PsTAR1*, *PsTAR2* and *PsTAR3* transcript levels over the course of seed development. Shown are mean ± se (n = 3 for auxin and 4 for transcript levels). Mean seed fresh weights for each time point, in order of increasing age, were 3.8 ± 0.4 mg, 54 ± 4 mg, 199 ± 10 mg, 293 ± 8 mg, 432 ± 27 mg and 459 ± 12 mg.

To complement the *in vitro* analyses of PsTAR1 and PsTAR2, Dr Marion Dalmais, Dr Abdelhafid Bendahmane (both of the Unité de Recherche en Génomique Végétale, Evry, France) and some of our own group members (A/Prof John Ross, Mr Raj Bala and Dr Laura Quittenden) investigated the role of aminotransferases in 4-Cl-IAA biosynthesis *in vivo*; a mutant population, created through TILLING, was used to identify mutants affected in the *PsTAR2* gene and a *tar2* knockout mutant was isolated, on the genetic background Cameor. Full characterisation of this mutant, including detailed analysis of the visual mutant phenotype and the levels of auxin over the course of seed development, can be found in Tivendale et al. (2012). The seeds of the mutant

contained much less 4-Cl-IAA than the WT at the later stages of development ($P<0.001$); by 20 DPA, the reduction was approximately 90 %. However, effects of the *tar2* mutation on IAA content were relatively small.

The large drop in 4-Cl-IAA content in mutant seeds would be expected to be physiologically significant, since markedly smaller reductions in auxin levels are thought to be responsible for large phenotypic effects in *Arabidopsis* (Stepanova et al., 2011) and maize shoots (Phillips et al., 2011). Accordingly, the *tar2* genotype was associated with a seed deformity, which is best described as 'dimpled'; *tar2* mutant seeds are also smaller and have lower dry weights than WT seeds. This is an important discovery, given much of the world's pea crop is harvested as the dry seed. The *tar2* mutation did not affect pod elongation, consistent with the finding that 4-Cl-IAA levels are normal in seeds soon after anthesis, when it is postulated that this hormone moves from seeds to pods to stimulate elongation (Reinecke, 1999; Ozga et al., 2009).

Discussion

There has recently been renewed focus on IPyA-dependent IAA biosynthesis, due to isolation of Trp aminotransferases from two species (Stepanova et al., 2008; Tao et al., 2008; Chourey et al., 2010; Phillips et al., 2011) and reports that the YUC family acts in this pathway (Kriechbaumer et al., 2011; Mashiguchi et al., 2011; Stepanova et al., 2011; Won et al., 2011). The experiments described here focus on the biosynthesis of the auxins IAA and 4-Cl-IAA *via* IPyA and 4-Cl-IPyA respectively. First IPyA was characterised; IPyA, like all compounds containing a carbonyl adjacent to a carbon bonded to a hydrogen, exists as a mixture of two tautomers (Schwartz, 1961; Bruice, 2004): keto and enol (Figure 6.3). Normally, the equilibrium between these forms is rapid and favours the keto tautomer, as it is more stable (Bruice, 2004). However, in some cases, the enol tautomer is stabilised by intramolecular interactions (Floris, 1990; Bruice, 2004; Zhou and Hill, 2007). In this study it was shown that IPyA and its chlorinated derivative both exist as mixtures of their respective keto and enol tautomers, these tautomers may be readily separated by UPLC and, under most conditions tested, the enol tautomer dominates the equilibrium. This is probably due to the extended conjugation in this form (Figure 6.3). The LC separation of keto and enol tautomers has been previously reported by Zhou and Hill (2007), who separated the two forms of ethyl butyryl acetate and separation of IPyA tautomers by paper chromatography has been also been reported (Schwartz, 1961); it is therefore surprising that separation of IPyA

tautomers by LC has not previously been reported, especially since IPyA is a reasonably well characterised intermediate in various microbial species (Koga et al., 1991a; Koga et al., 1991b; Koga et al., 1992; Koga et al., 1994; Koga, 1995; Patten and Glick, 1996; Vandeputte et al., 2005; Tsavkelova et al., 2007; Malhotra and Srivastava, 2008).

Trp aminotransferases have been shown to catalyse the first step in IPyA-dependent auxin biosynthesis from Trp (Stepanova et al., 2008; Tao et al., 2008; He et al., 2011). In this study, it was shown, by *in vitro* assay analyses, that the products of two newly-isolated genes from pea, *PsTAR1* and *PsTAR2* (Tivendale et al., 2012), which are homologous to the *TAA* family (Stepanova et al., 2008; Tao et al., 2008) and *vt2* and *ZmTAR* from corn (Chourey et al., 2010; Phillips et al., 2011), can act as aminotransferases using Trp or its 4-chlorinated derivative. This is the first demonstration that Trp aminotransferases can also use 4-Cl-Trp, the first isolation of a 4-Cl-IAA biosynthesis gene and the first identification of the 4-Cl-IAA biosynthesis intermediate, 4-Cl-IPyA. In *in vitro* assays of PsTAR1 and PsTAR2 with Trp or 4-Cl-Trp as the substrate, both keto and enol tautomers of IPyA and 4-Cl-IPyA were detected as products but the keto form predominated (Figure 6.15). Previously, aminotransferases appear to have yielded mainly the enol form of IPyA (on the basis of LC RTs relative to that of IAA; He et al., 2011). Tao et al. (2008), Stepanova et al. (2008) and He et al. (2011) all report the production of IPyA from *in vitro* Trp aminotransferase assays, but not the phenomenon of tautomerisation. However, an unidentified broad peak is visible on the UV chromatogram presented by Tao et al. (2008), which could be due to the keto tautomer of IPyA. Similarly, in the chromatograms presented by He et al. (2011) there was small unidentified peak eluting early than Trp and the peak designated 'IPyA' that may have been keto IPyA. The issue of which form is predominantly produced by aminotransferases remains to be resolved. Interestingly, however, direct monitoring of endogenous 4-Cl-IPyA and IPyA extracted from pea seeds yielded evidence for the keto tautomers only (at low levels; see Chapter 7).

In summary, the results reported here provide evidence that in pea seeds IAA and 4-Cl-IAA are synthesized in parallel *via* the IPyA pathway and its chlorinated version (Figure 6.20), with PsTAR1 acting as the key enzyme at earlier stages of seed development and PsTAR2 playing a more important role at later stages. In this study, the IAM pathway (thought by some to be widespread; see Lehmann et al., 2010) is not excluded as a possible auxin biosynthesis route in pea seeds (see Chapter 7), but it has been shown definitively that the majority of 4-Cl-IAA is

produced *via* the chlorinated version of the IPyA pathway through characterization of the *tar2* mutant (Tivendale et al., 2012), the seeds of which contain dramatically reduced 4-Cl-IAA levels, as they mature, compared to WT plants, which contain high levels of 4-Cl-IAA in the later stages of seed development, when *PsTAR2* is strongly expressed. However, since IAA levels were not substantially affected in the *tar2* mutant (Tivendale et al., 2012), it may be that the function of PsTAR2 may be compensated by PsTAR1 and/or PsTAR3 to maintain relatively normal levels of this hormone. Alternatively, inactivation of PsTAR2 may result in increased conversion of IAA conjugates to free IAA. Nevertheless, it appears that PsTAR1 and PsTAR2 are essential for normal biosynthesis of 4-Cl-IAA and IAA in these organs and the effects of the *tar2* mutation on the dry seed phenotype indicate that 4-Cl-IAA is a key hormone in seed development.

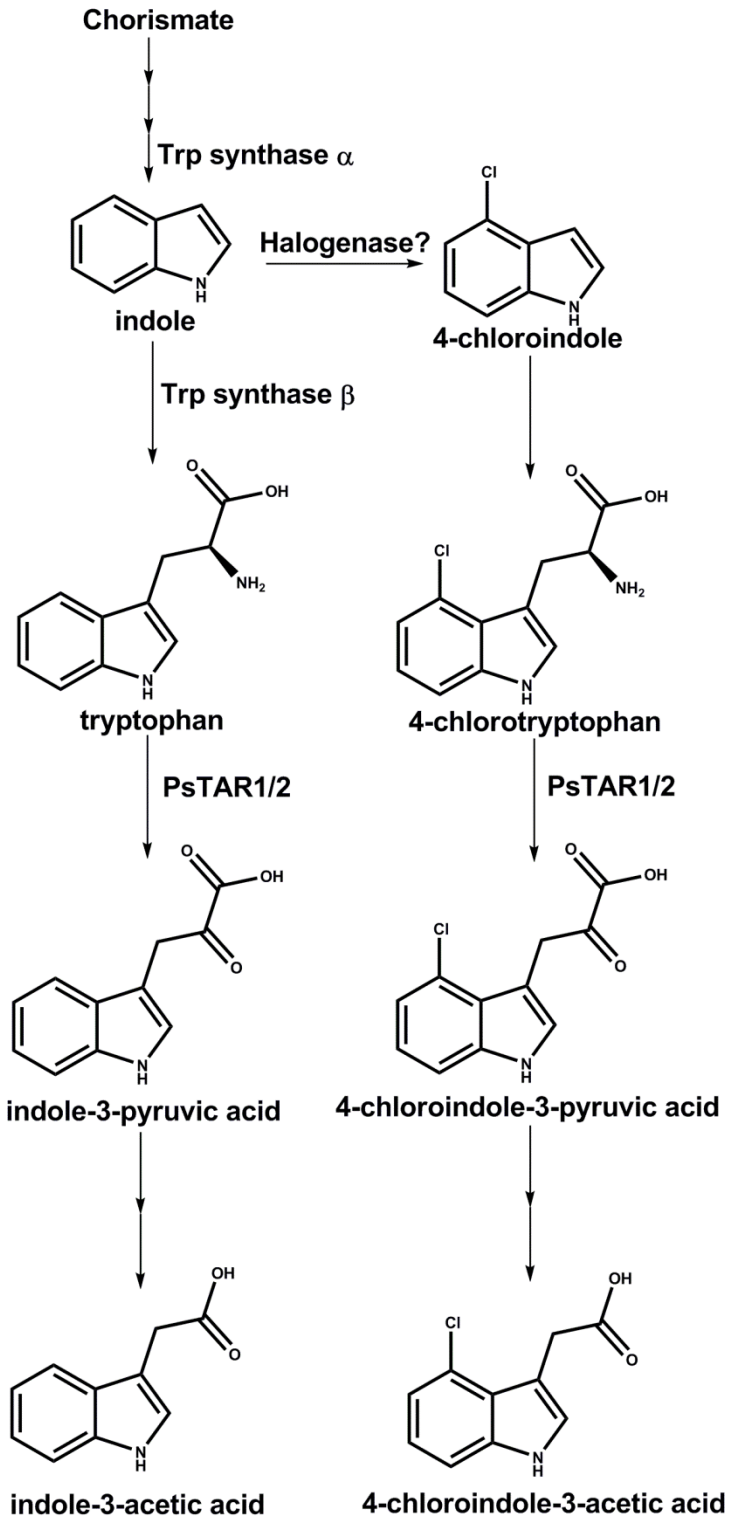

Figure 6.20 - Proposed parallel IAA and 4-Cl-IAA biosynthetic pathways in pea seeds, based on the current study and previous evidence (Manabe et al., 1999; Reinecke, 1999; Quittenden et al., 2009; Tivendale et al., 2010; Zhao, 2010; He et al., 2011; Kriechbaumer et al., 2011; Mashiguchi et al., 2011; Stepanova et al., 2011; Won et al., 2011). The point of halogenation is not known but it appears to precede Trp.

Chapter 7 Auxin biosynthesis in developing pea seeds: a compound-based approach[5]

Introduction

As noted in previous chapters, although the primary auxin (IAA) was identified over 80 years ago, the discovery of a primary biosynthetic route has been problematic (for reviews of the current state of knowledge, see Bartel et al., 2001; Ljung et al., 2005; Woodward and Bartel, 2005; Normanly, 2010; Ross and Reid, 2010; Zhao, 2010). One reason for is that IAA biosynthetic schemes that incorporate data from all species are intensely complicated (e.g. Normanly, 2010 Figure 2; Zhao, 2010 Figure 1). However, in a single species, the reality may be much simpler. Indeed this was recently shown in *Arabidopsis*, where the TAA/YUC pathway is reported to be the primary auxin biosynthetic route (Mashiguchi et al., 2011). Even so, *Arabidopsis* is known to utilize Brassicaceae-specific biosynthetic pathways (Sugawara et al., 2009), so the TAA/YUC pathway may not predominate in all species, although this thesis previously presented *in vitro* evidence in favour of this pathway in pea (see Chapter 6). Nevertheless, even within a single species there is variation between organs, which further complicates the study of auxin biosynthesis. In pea it has previously been shown that TAM is an IAA precursor in the roots (Quittenden et al., 2009) but this does not necessarily imply TAM is a precursor in pea seeds. Based on these observations and others (discussed previously in this thesis), it is proposed that either the IPyA, TAM and/or IAM pathways (Figure 7.1) predominate in pea seeds. Alternatively, IAA could be synthesised *via* the Trp-independent pathway, which may originate from Trp precursors, such as indole-3-glycerol phosphate (see Figure 7.1) or indole (Normanly et al., 1993; Normanly et al., 1995; Ouyang et al., 2000). The Trp-independent pathway was proposed after *Arabidopsis* Trp auxotroph mutants, *trp3-1* and *trp2-1*, were reported to accumulate amide- and ester-linked IAA conjugates, despite having low Trp levels (Normanly et al., 1993). Normanly et al. (1993) also grew WT and *trp2-1 Arabidopsis* seedlings on media containing [^{15}N]anthranilate (an indole precursor); they found the proportion of ^{15}N-

[5] Part of the study reported here was published in the research article Tivendale ND, Davies NW, Molesworth PP, Davidson SE, Smith JA, Lowe EK, Reid JB, Ross JJ (2010) Reassessing the role of *N*-hydroxytryptamine in auxin biosynthesis. Plant Physiology **154:** 1957-1965 and the addendum Ross JJ, Tivendale ND, Reid JB, Davies NW, Molesworth PP, Lowe EK, Smith JA, Davidson SE (2011) Reassessing the role of YUCCAs in auxin biosynthesis. Plant Signaling and Behavior **6:** 437-439.

label incorporation into IAA was greater than the proportion of labelling in Trp, which indicates a Trp-independent pathway. The Trp-independent pathway may operate in pea seeds because, although Trp has long been considered a precursor for IAA in a variety of species (Sembdner et al., 1981), including pea, it was previously demonstrated that the proportion of label incorporation into IAA after applying deuterated Trp to pea seeds was relatively low (Tivendale, 2008). Therefore, it is formally possible that a Trp-independent IAA biosynthetic pathway is operating in pea.

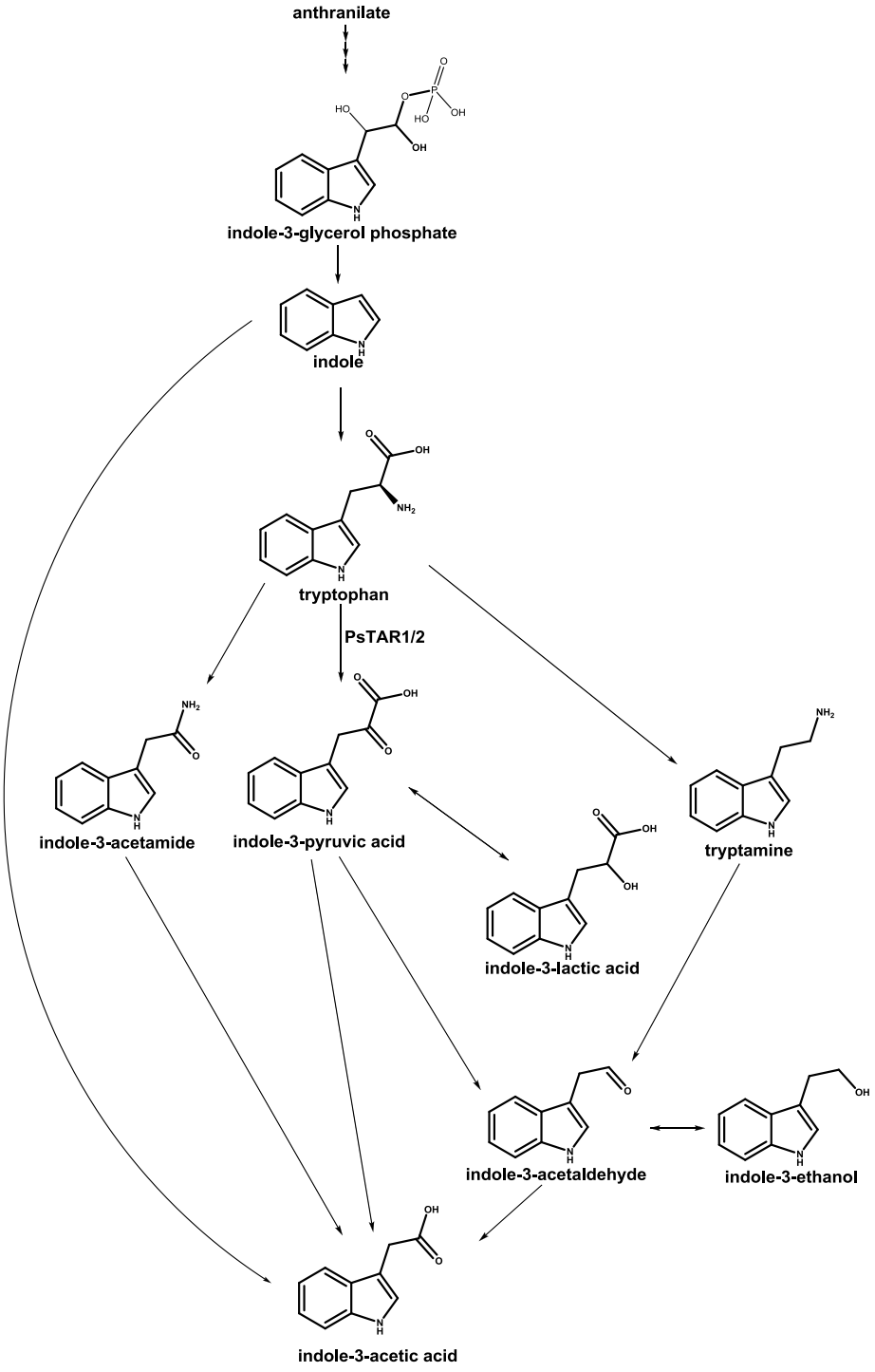

Figure 7.1 - Proposed IAA biosynthetic pathways in pea seeds, based on evidence from previous studies in pea and other species (Brown and Purves, 1980; Ludwig-Müller and Hilgenberg, 1989; Sprunck et al., 1995; Brandl and Lindow, 1996; Pollmann et al., 2002; Stepanova et al., 2008; Tao et al., 2008; Quittenden et al., 2009; Chourey et al., 2010; reviewed in Lehmann et al., 2010; Mano et al., 2010; Tivendale et al., 2010; reviewed in Zhao, 2010; Kriechbaumer et al., 2011; Mashiguchi et al., 2011; Phillips et al., 2011; Stepanova et al., 2011; Won et al., 2011) and discussed earlier in this thesis.

The IPyA pathway is important in a number of IAA-synthesising microorganisms (Koga et al., 1992; Koga, 1995) and has long been thought to operate in some plant species as well (Cooney and Nonhebel, 1989; Tam and Normanly, 1998). As discussed previously, Trp aminotransferases have been isolated from pea (Tivendale et al., 2012; see also Chapter 6), *Arabidopsis* (Stepanova et al., 2008; Tao et al., 2008) and maize (Chourey et al., 2010; Phillips et al., 2011) and catalyse the formation of IPyA (see Chapter 6 for more on this pathway). The IPyA decarboxylase that would be required to convert IPyA to IAAld has not been identified in plants, although this enzyme has been identified in various auxin-synthesising microbes, such as *Enterobacter cloacae* (Koga et al., 1992), *Azospirillum brasilense* (Vande Broek et al., 1999; Vande Broek et al., 2005) and *Paenibacillus polymyxa* (Quyet-Tien et al., 2008). IAAld may be converted to IEt, a putative storage product possibly involved in homeostatic regulation of IAA (Brown and Purves, 1980; Ludwig-Müller and Hilgenberg, 1989). Enzymes reported to catalyse the formation of IAA from IAAld, aldehyde oxidases, have been identified in a number of species, including *Arabidopsis* (Seo et al., 1998) and pea (Zdunek-Zastocka, 2007). However, this does not confirm the operation of the IPyA pathway in these species, as IAAld may be an intermediate for other pathways (see Woodward and Bartel, 2005; Normanly, 2010; Zhao, 2010) and the aldehyde oxidases may function in other pathways, such as abscisic acid biosynthesis (Harrison et al., 2011). Furthermore, several groups have recently reported the direct conversion of IPyA to IAA by the YUC enzyme family (Kriechbaumer et al., 2011; Mashiguchi et al., 2011; Stepanova et al., 2011; Won et al., 2011), thus casting further doubt over the role of IAAld and the aldehyde oxidases in IAA biosynthesis.

ICA, a breakdown product of IPyA (see Chapter 6), has been reported as an endogenous compound in various microbial species (see Discussion), and also pea root nodules (Badenoch-Jones et al., 1984), but is yet to be investigated in pea seeds. Another compound associated with IPyA is ILA. This compound is also present in pea root nodules (Badenoch-Jones et al., 1984), tomato shoots (Gibson et al., 1972), as well as some species of fungi (Glombitza and Hartmann, 1966; Perley and Stowe, 1966) and microbes (Kaper and Veldstra, 1958; Rigaud, 1970; Rovenská et al., 1988; Berry et al., 1989) and is a weak auxin analogue (Sprunck et al., 1995). This compound may be a storage product of IPyA (Brandl and Lindow, 1996), in much the same way IEt is thought to be a storage product of IAAld (Brown and Purves, 1980; Ludwig-Müller and Hilgenberg, 1989).

It has been shown in previous chapters of this thesis that the 4-chlorinated version of the IPyA pathway accounts for a large portion of the biosynthesis of one of the main auxins in maturing pea seeds, 4-Cl-IAA. Nevertheless, the previous analyses do not preclude the operation of another auxin biosynthetic pathway earlier in seed development (prior to ca. 11 DPA). Moreover, the mutation described in Chapter 6 (see also Tivendale et al., 2012) did not substantially affect IAA levels at any stage of seed development measured, raising the possibility of the operation of another pathway for the synthesis of this auxin.

Furthermore, the analyses in pea reported in this thesis thus far do not preclude operation of TAM- or IAM-dependent auxin biosynthetic pathways. IAM has been identified as an endogenous compound in *Arabidopsis* (Pollmann et al., 2002; Sugawara et al., 2009), rice, maize and tobacco (Sugawara et al., 2009), and may be an IAA biosynthetic intermediate in pea seeds, although it has been shown that this is not the case in pea roots (Quittenden, 2011). The IAM pathway is thought, by some, to be widespread in the plant kingdom (reviewed in Lehmann et al., 2010), but the role of IAM in auxin biosynthesis in pea seeds is yet to be investigated.

In this thesis so far, it has been shown that the YUCs do not use TAM as a substrate and NHT is unlikely to be involved in IAA biosynthesis (Chapter 4). It has also been shown, using various molecular biology techniques, that PsTAR-catalysed IPyA/4-Cl-IPyA-dependent auxin biosynthesis is important in pea seeds (Chapter 6). In this chapter, the molecular analysis of auxin biosynthesis is complemented through a series of *in vivo* experiments using developing pea seeds, with particular focus on indole, Trp, 4-Cl-Trp, TAM, IAM, IPyA and IAAld (also ILA and IEt) as putative intermediates. Two broad groups of experiments were performed: (1) Endogenous compounds from pea seeds were identified; if a putative intermediate cannot be detected as an endogenous compound, then it is less likely that it is involved in auxin biosynthesis. (2) Labelled forms of putative precursors were injected into pea seeds to determine if they were metabolised to IAA in these organs.

Materials and Methods

Identification of endogenous compounds

Endogenous compounds in whole seeds

For detection of endogenous IPyA by GC-MS, whole seeds were harvested into liquid N_2 as described in Chapter 2. The extract (2 mL) was methylated (4.0 mL of diazomethane in diethyl ether). The solvent was evaporated under N_2 and the residue resuspended in 2.0 mL of ACN in water (5 % v/v). The resulting suspension was centrifuged at 4 °C and 2 x 10^4 g for 25 min. The supernatant was separated on HPLC (Program 2, without acetic acid). The solvent was removed from fractions 19-27 under reduced pressure and the residues transferred in diethyl ether (3 x 200 μL) to separate scintillation vials. The solvents were then evaporated under N_2, the residues trimethylsilylated as described in Chapter 2 to produce TMS-IPyA methyl ester (Figure 7.2) and the samples were analysed by GC-MS.

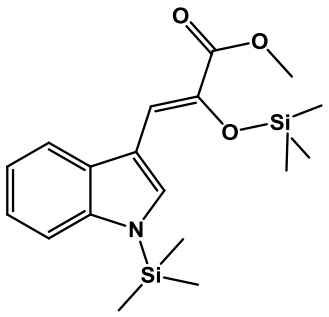

Figure 7.2 – Structural formula for the *bis*-trimethylsilyl methyl ester derivative of IPyA.

Using the liquid N_2 extraction method extracts were prepared and analysed by UPLC-MS for IPyA, 4-Cl-IPyA, ILA, IAAld, IEt, IAA, 4-Cl-IAA and ICA.

An extract was prepared from three ‘table-ready’ pea seeds (post contact point), using the MeOH/BHT method. [D_6]IAM (150 ng) was added to the extract, which was purified using a Sep-Pak and then analysed by UPLC-MS

Endogenous compounds in pea liquid endosperm

To determine whether IAM was endogenous in pea liquid endosperm, the endosperm of seven L107 pea seeds was combined (V = 100 µL) and 10 ng of [D_6]IAM in MeOH was added to it. This mixture was prepared for analysis by UPLC-MS as described in Chapter 2.

The endosperm from eight pea seeds (total FW: 0.42 g) was combined (V_T = 95 µL) and prepared for UPLC-MS analysis. ILA, IPyA, IEt (*m/z* 162.1 to 144.05), IAAld (*m/z* 160.1 to 132.05, *m/z* 160.1 to 118.05), IAA, ICA were monitored by MRM.

Feeding putative intermediates

[^{14}C]Trp

To determine if there was any substantial substrate transfer from the site of injection (the endosperm) to the rest of the seed, six pea seeds were excised (FW_T: 339 mg; average FW per seed: 56 mg) and placed on moist filter paper in a Petri dish. Each seed was injected with [^{14}C]Trp (1 µL; 1000 DPM.µL^{-1}). The seeds were left at room temperature under a mixed white light source (fluorescent/natural daylight) for 3 h before harvesting. The tops of the seeds were removed with a razor blade and the endosperm pipetted into a scintillation vial. The embryos were then removed and placed into a separate vial. The testas were placed into a third vial. MeOH/H_2O (4:1) with BHT (250 mg.L^{-1}; 1.00 mL) was added to the latter two vials and all three vials were left overnight at 4°C, after which they were analysed for radioactivity by scintillation counting.

[D_6]Indole, [D_4/D_5]Trp and [D_5]TAM

To determine the metabolism of Trp and indole in pea seeds, three series of feeding experiments were conducted. In the first experiment, [D_5]Trp was injected into seven *in situ* pea seeds, which were then harvested after ca. 17 h, using the MeOH/BHT extraction method, but replacing the normal solvent with H_2O. A 4-ml aliquot of the extract was treated with pentafluoropropanol (400 µL), pyridine (100 µL) and ethylchloroformate (100 µL) to obtain the *N*-ethoxycarboxyltrimethylsilylpentafluoro propyl ester derivative of Trp (Figure 7.3), as described by Quittenden et al. (2009). This sample was then analysed by GC-MS (SIM; Varian). The SIM

channels used was *m/z* 202 (unlabelled) and *m/z* 207 (labelled), which represent the predominant daughter ion for this derivative.

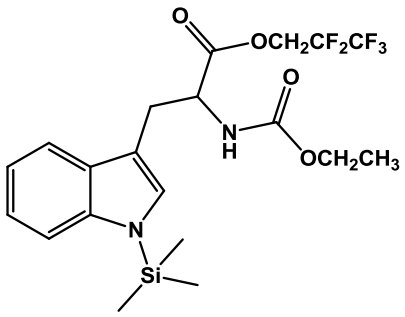

Figure 7.3 – Structural formula for the *N*-ethoxycarboxyltrimethylsilylpentafluoro propyl ester derivative of Trp.

In the second experiment, a solution containing a mixture of [D_4]Trp (400 ng.μL^{-1}) and [^{14}C]Trp (100 ng.μL^{-1}) was prepared in H_2O, along with a solution containing a mixture of [D_6]indole (400 ng.μL^{-1}) and [^{14}C]indole (70 ng.μL^{-1}) in H_2O. The Trp solution was injected into each of eight pea seeds and the indole solution was injected into each of another eight pea seeds (1 μL into each). After 15 h the seeds were harvested using the MeOH/BHT method to give two extracts. Aliquots of each extract were subject to HPLC-radiocounting (Program 2), and separate aliquots of each were dried *in vacuo* and purified using a Sep-Pak (187.5:124:1 MeOH/H_2O/acetic acid). The liquid was removed under reduced pressure, and the residue transferred in MeOH, methylated and trimethylsilylated as described in Chapter 2 and analysed for label incorporation into IAA by GC-MS on the Varian. IAA was analysed as the trimethylsilyl methyl ester derivative.

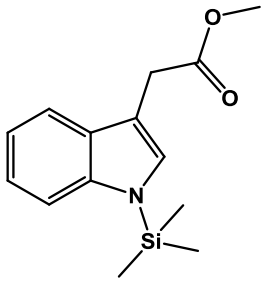

Figure 7.4 – Structural formula for the trimethylsilyl methyl ester derivative of IAA.

To determine if the label incorporation into IAA after deuterated Trp feeding was statistically significant, a further feeding experiment was conducted, using [D_4]Trp (1000 ng.μL^{-1}) and [D_5]TAM (100 ng.μL^{-1}). 72 seeds were excised from the pods and split into 24 equal groups

(three seeds per group), each of which was placed on moist filter paper in separate Petri dishes. Excised seeds were left for 3, 6 or 12 h after substrate administration (four replicates (three seeds each) of each treatment at each time point), before being harvested using the MeOH/BHT method. There were four replicates of each treatment. Each extract was purified using a Sep-Pak, eluting with 125:124:1 MeOH/H_2O/acetic acid, the solvent was removed under reduced pressure, and the residue was transferred to an Eppendorf tube, which was centrifuged at 1.3 x 10^4 rpm, and supernatant was analysed by UPLC-MS.

Upon analysis the amount of TAM fed in the previous experiment was found to be excessive. Therefore, the TAM feeding was repeated, performing four replicates of 3 and 6 h incubations, injecting 1 µL of [D_5]TAM (5 ng.µL^{-1}) into each seed.

To determine if it was possible analyse the endosperm only, rather than the whole seed, pea seeds at the liquid endosperm stage (total FW: 0.59 g) were excised and injected with 1 µL of [D_4]Trp (2 µg.µL^{-1}) and left at room temperature on moist filter paper in a closed Petri dish, under a mixed white light source (fluorescent and natural daylight) for 2 h. After this, the endosperm was removed and diluted with acetic acid in MeOH (5% v/v) to make the final mixture 80:19:1 endosperm/MeOH/acetic acid. This was treated and analysed by UPLC-MS as described in Chapter 2.

To determine if Trp was metabolised by the liquid endosperm only, endosperm from seven pea seeds was combined in an Eppendorf tube (V_T = 100 µL) To this was added 100 µL of [D_4]Trp (50 ng.µL^{-1}). The mixture was left at room temperature for 3 h, after which 55.5 µL of acetic acid in methanol (5% v/v) was added. The final mixture was 80:19:1 endosperm/methanol/acetic acid.

[D_6]IAM

To determine the possible involvement of IAM in IAA biosynthesis, nine seeds (average FW per seed = 120 mg) were excised and divided into three equal groups, each of which was placed on moist filter paper in a Petri dish. Each seed was injected with 1 µL of [D_6]IAM (20 ng.µL^{-1}). The seeds were left at room temperature under a mixed white light source (natural and fluorescent light) for several hours before harvesting. To ensure that the seeds under these conditions were synthesising IAA from Trp, [D_5]Trp was fed to a second group of nine seeds (three equal groups

of three) under the same conditions. A control group of nine seeds (average FW per see = 103 mg; three equal groups of three) was injected with 1 µL of H_2O. After harvesting, all extracts were analysed by UPLC-MS for label incorporation into IAM and IAA.

[D_5]IAAld

To determine the possible involvement of IAAld in IAA biosynthesis, six pea seeds (average FW = 45 mg) were excised and split into two equal groups (test and control) and 2 µL of free [D_5]IAAld in K_2HPO_4/KH_2PO_4 buffer (pH 6.5; 250 ng.µL) was injected into the three test seeds. All seeds were left for 4 h on moist filter paper under a mixed white light source (fluorescent/natural daylight), after which each group was harvested using the liquid N_2 method.

Investigating 4-Cl-IAA biosynthesis

The possibility that 4-Cl-IAA is synthesised directly from IAA was tested, by injecting a mixture of [$^{13}C_6$]IAA (20 ng in 1 µL) and [D_5]Trp (5 µg in 1 µL) into developing pea seeds (ca. 70 mg). The amount of [$^{13}C_6$]IAA injected was low to avoid a physiologically unrealistic situation. Three replicates, of three seeds each, were prepared and the seeds were left for 3 h under a mixed white light source (fluorescent/natural daylight) before harvesting using the MeOH/BHT method. In a separate experiment, to determine the involvement of 4-Cl-Trp in 4-Cl-IAA synthesis, [D_3,D_4]4-Cl-Trp (2 µg in 1 µL) was injected into comparable seeds. Three replicates of three seeds were also prepared in this experiment and all other conditions were the same as described above. Controls were prepared by injecting H_2O into seeds, instead of substrate.

Summary of extracts

A summary of the extracts prepared in this series of experiments is shown in Table 7.1.

Table 7.1 – Extracts prepared from pea seeds and analysed using various methods. FW: fresh weight; GW: ground weight; NR: not recorded. *For these experiments, four replicates of each treatment were performed; each replicate consisted of three seeds, giving a total of 36 seeds. $^{+}$For this experiment, three replicates, each consisting of three seeds, were performed, giving a total of 9 seeds.

Extract	Substrate	No. seeds	Weight (mg)/endosperm volume (µL)	Extraction method	Analysis method	Analyte(s)
23	-	10	1106.9 (FW)	Liquid N_2	GC-MS	IPyA
85	-	NR	316.1 (GW)	Liquid N_2	UPLC-MS	IPyA, ILA, IAAld, IEt, IAA, ICA
92	-	3	NR (table-ready seeds)	MeOH/BHT	UPLC-MS	IAM
49	-	7	NR/100	Endosperm	UPLC-MS	IAM
58	-	8	420 (FW)/95	Endosperm	UPLC-MS	Trp, IPyA, ILA, IAA
86	-	12	NR/90	Endosperm	UPLC-MS	ILA, IPyA, IEt, IAAld, IAA, ICA
108	-	9	780 (FW)	Liquid N_2	UPLC-MS	IPyA, 4-Cl-IPyA, IAA, 4-Cl-IAA
14	[D_5]Trp	7	580 (FW)	MeOH/BHT	GC-MS	Trp, IAA
24.1	[D_4]Trp/[^{14}C]Trp	8	1117 (FW)	MeOH/BHT	HPLC-radiocounting; GC-MS	IAA, 4-Cl-IAA, IAM
24.2	[D_6]indole/[^{14}C]indole	8	890 (FW)	MeOH/BHT	HPLC-radiocounting; GC-MS	IAA and 4-Cl-IAA
45A1,2,3*	[D_4]Trp	36	2818.4 (FW)	MeOH/BHT	UPLC-MS	IAA
45B1,2,3*	[D_5]TAM	36	3376.2	MeOH/BHT	UPLC-MS	IAA
47	[D_5]TAM	24	1264.9	MeOH/BHT	UPLC-MS	IAA
57	[D_4]Trp	NR	590.2	Endosperm	UPLC-MS	IAA, ILA, IEt, 4-Cl-IAA
53	[D_4]Trp (fed to isolated endosperm)	7	100	Endosperm	UPLC-MS	IAA
88	[^{14}C]Trp	6	339.3 (FW)	Each part harvested separately into MeOH/BHT	HPLC-radiocounting	-
82	[D_5]IAAld	3	158.3	Liquid N_2	UPLC-MS	IAA, IEt
113.1, 2, 3^{+}	[D_3/D_4]4-Cl-Trp	9	1008 (FW)	MeOH/BHT	UPLC-MS	4-Cl-IAA
114.1, 2, 3^{+}	[D_5]Trp + [$^{13}C_6$]IAA	9	789 (FW)	MeOH/BHT	UPLC-MS	4-Cl-Trp, IAA, 4-Cl-IAA
115A1, 2, 3^{+}	[D_5]Trp	9	1081	MeOH/BHT	UPLC-MS	Trp, IAM, IAA
115B1,2,3^{+}	[D_6]IAM	9	929	MeOH/BHT	UPLC-MS	IAM, IAA

Results

Identification of endogenous compounds

Endogenous compounds in whole seeds

HPLC (Program 2 without acetic acid) followed by GC-MS analysis of extract 23 revealed that IPyA is present as an endogenous compound in whole pea seeds (eluted in fraction 24; Figure 7.5). Keto IPyA was also detected by UPLC-MS as an endogenous compound (extract 108; although the signal was weak; Figure 7.6), as was keto 4-Cl-IPyA (Figure 7.6). ILA and ICA were also detected as endogenous compounds by UPLC-MS, but IEt and IAAld were not (extract 85; Figure 7.7). IAM was also below the limit of detection in table-ready seeds (extract 92; Figure 7.8), although a compound with a fragmentation pattern very similar to IAM was detected at appreciable levels.

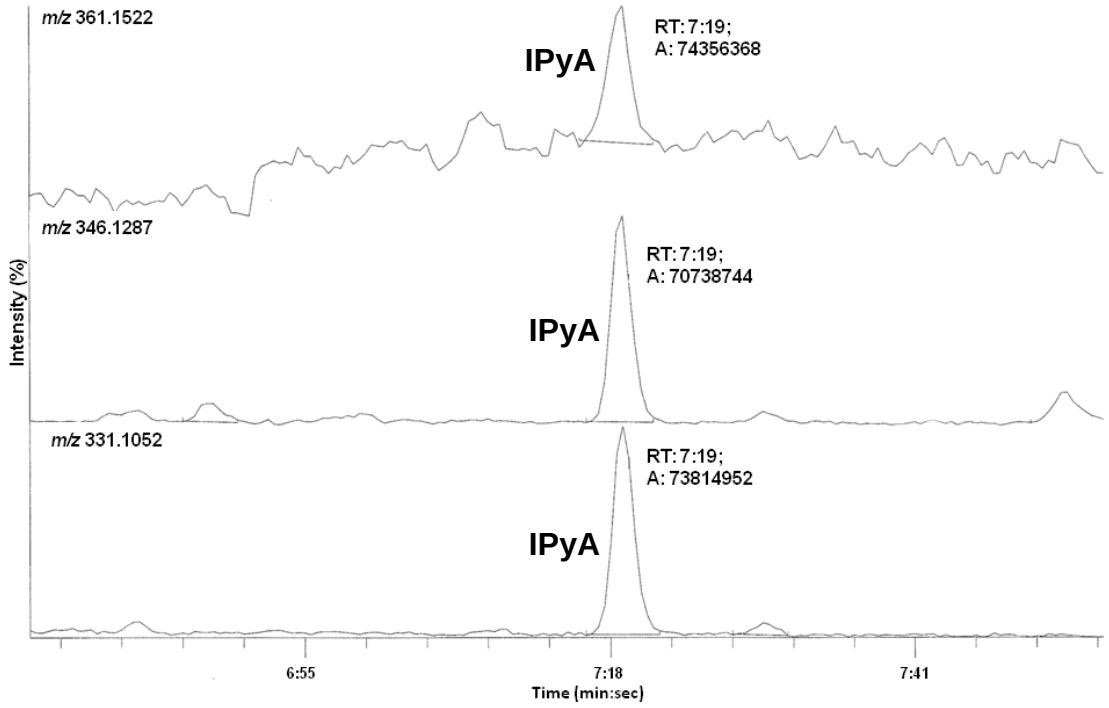

Figure 7.5 - GC-MS separation (SIM mode for the *bis*-trimethylsilyl methyl ester derivative of IPyA) of an extract prepared from pea seeds (extract 23).

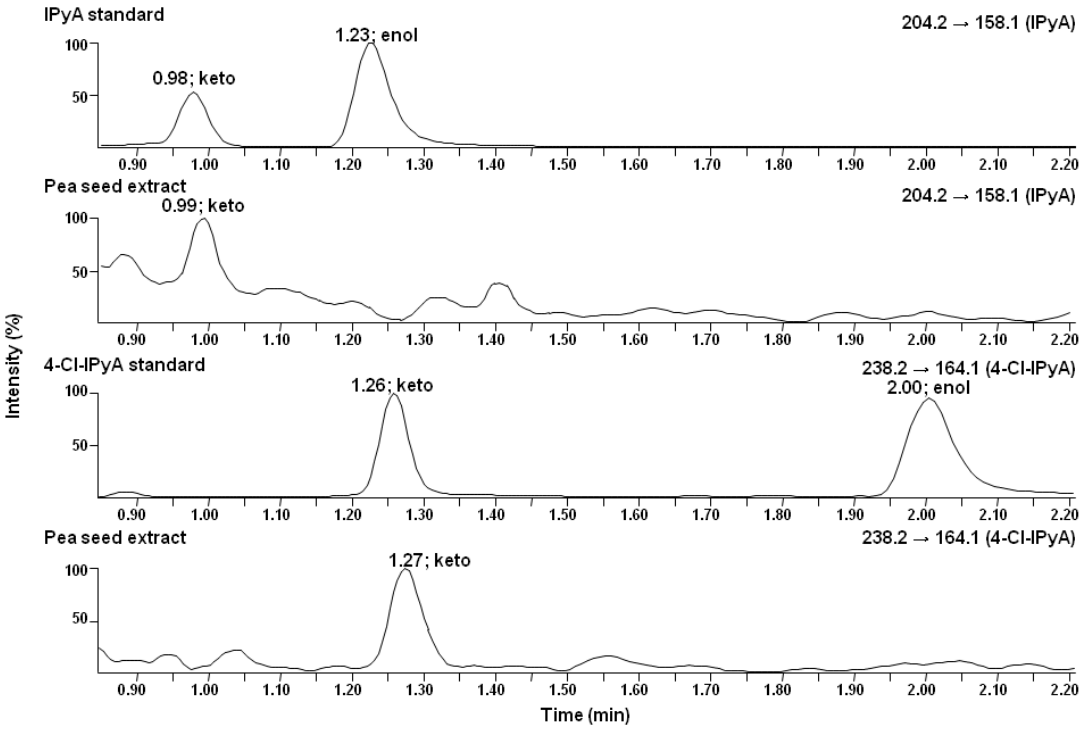

Figure 7.6 - UPLC-MS chromatograms (MRM mode; pH 5.4 program) showing endogenous keto IPyA (0.99 min; two lower channels) and keto 4-Cl-IPyA (1.27 min; two upper channels) in an extract prepared from immature pea seeds (extract 108). The enol tautomers (1.23 min and 2.00 min for IPyA and 4-Cl-IPyA, respectively, in the standard channels) were not observed in the extract.

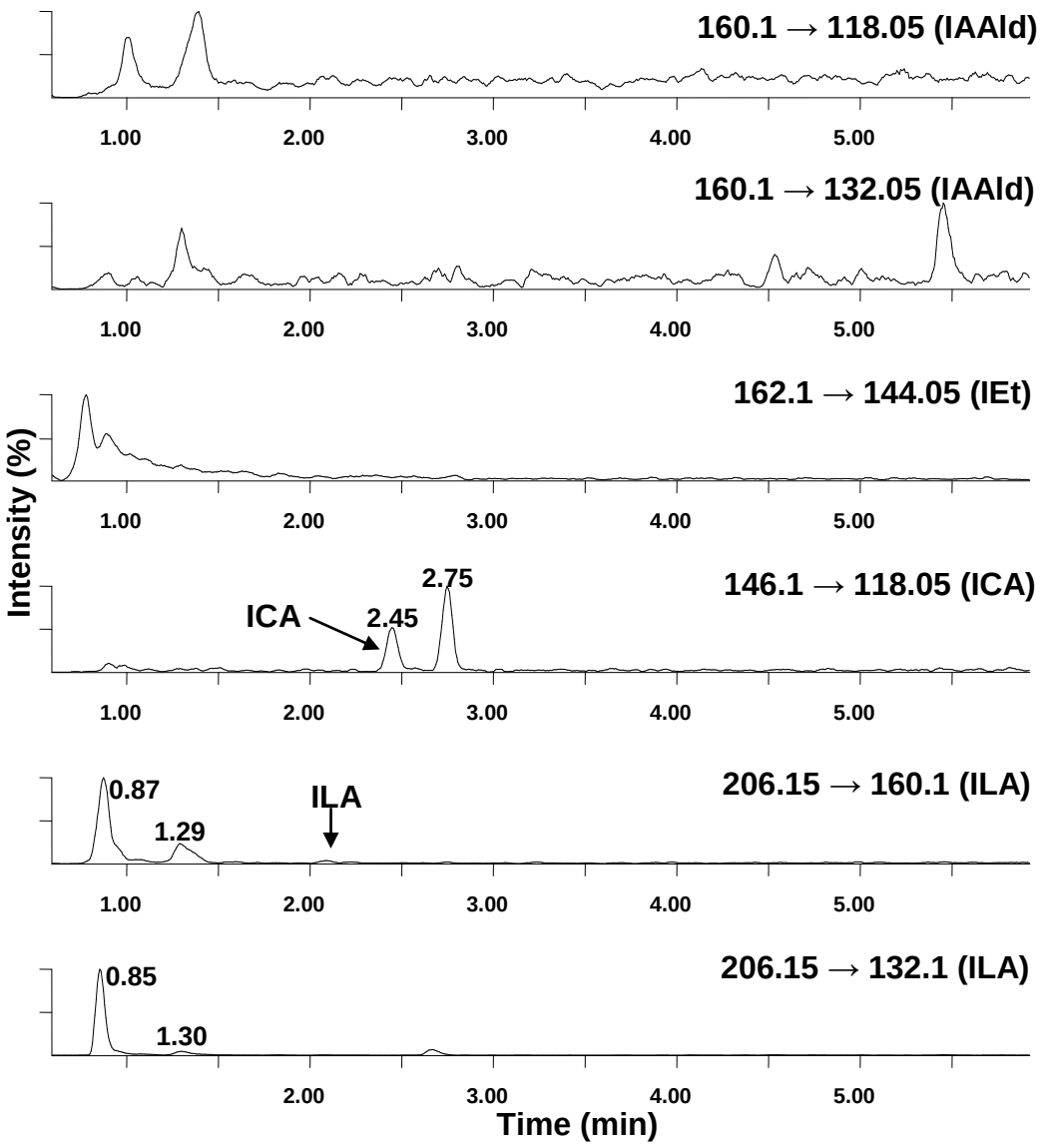

Figure 7.7 - UPLC-MS chromatograms (MRM mode; pH 5.4 program) of a pea seed extract (85), showing endogenous ICA and ILA, but not IEt or IAAld. Compounds were identified by comparing RTs and MRM transitions with those of relevant standards (data not shown).

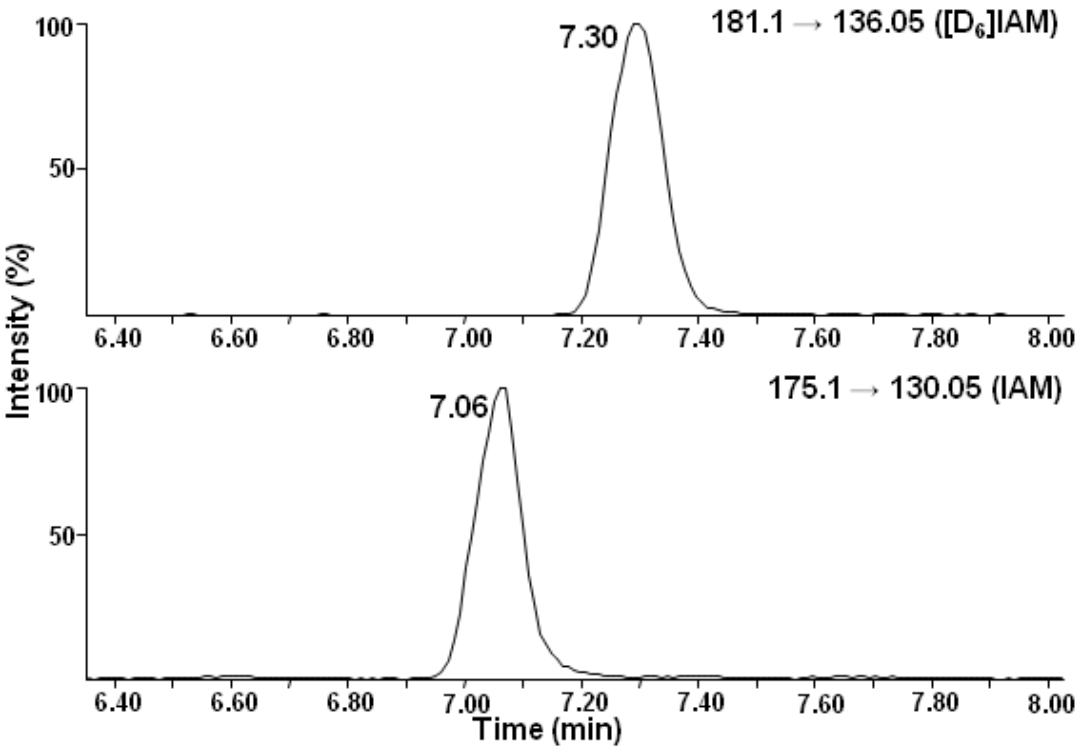

Figure 7.8 - UPLC-MS (MRM mode; 'slow' program) chromatograms of a pea seed extract (92) with internal standard [D_6]IAM (top channel). Endogenous IAM was not detected (bottom channel). The peak observed in the IAM channel has the wrong RT for IAM, although its fragmentation pattern is remarkably similar.

Endogenous compounds in liquid endosperm

Endogenous IAM (extract 49) from pea liquid endosperm were undetectable by UPLC-MS (Figure 7.9).

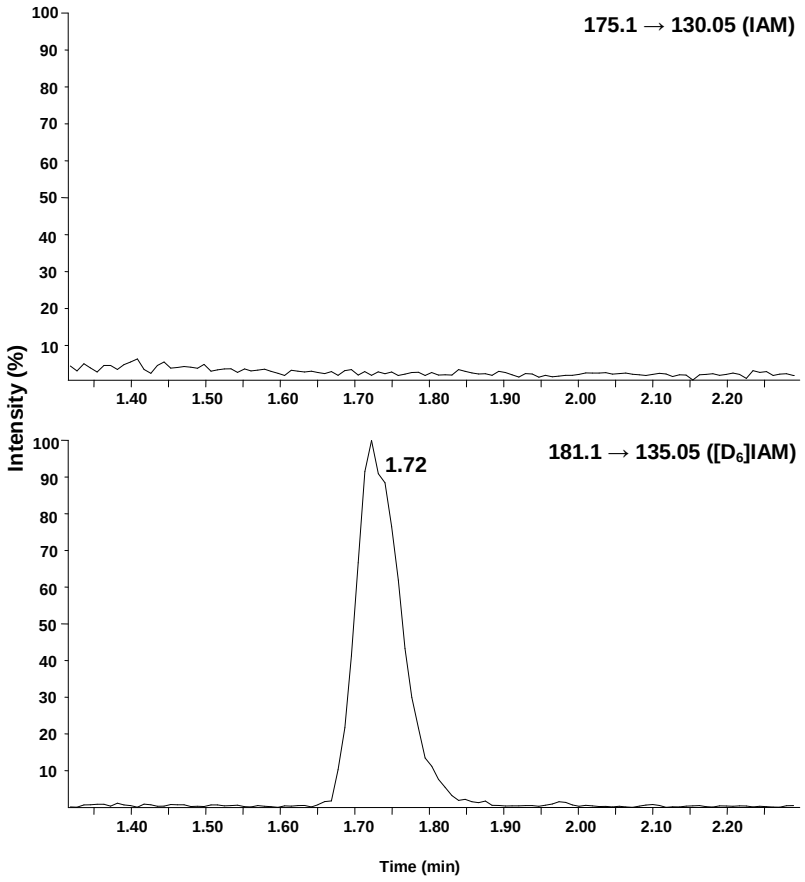

Figure 7.9 - UPLC-MS chromatogram (MRM mode for IAM; acetic acid program) of pea liquid endosperm (extract 49) with [D_6]IAM internal standard added.

ILA, IAA and ICA were all identified in the liquid endosperm (extract 86; Figure 7.10); however, IPyA, IEt and IAAld were below the limit of detection (Figure 7.10). The concentration of IAA in the liquid endosperm at this stage was calculated to be 3.0 ng.μl^{-1}.

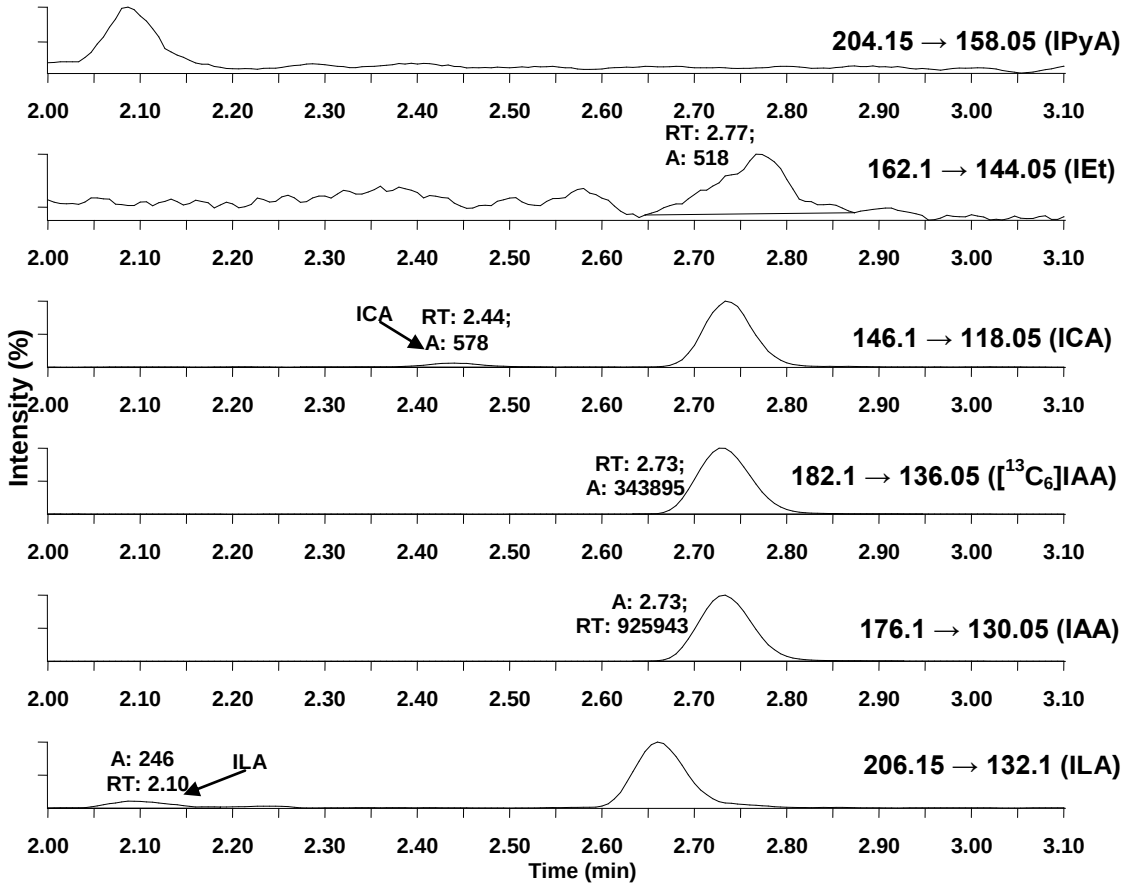

Figure 7.10 – UPLC-MS chromatograms (MRM mode; pH 5.4) of pea liquid endosperm (extract 86) showing the presence of ILA (2.09 min), IAA (2.73 min) and ICA (2.44 min). There was some evidence of endogenous IEt (2.77 min), but IPyA, and IAAld were below the limit of detection. Compounds were identified by comparing RTs and MRM transitions with those of relevant standards (data not shown).

Feeding studies

Movement of Trp throughout the system

Administration of [^{14}C]Trp followed by separate harvesting of each seed component (extract 88) revealed that approximately half the administered radioactivity had moved into the testa, and a small portion had moved into the embryo (although this may have been due to residual endosperm on the surface of the embryo), over the 3-h incubation (see Table 7.2). This means that substrates which are injected into the liquid endosperm are distributed fairly evenly between the endosperm and testa during the incubation time. Hence the observed chemical transformations in the feeding experiments described in this study occur mainly in the endosperm and/or the testa.

Table 7.2 – Radioactivity of three pea seed components after injection of [^{14}C]Trp into the endosperm (extract 88).

Organ	Radioactivity (DPM)
Endosperm	429.44
Testa	579.23
Embryo	32.21

Examining the Trp-independent and Trp-dependent pathways in whole seeds

Two feeding experiments, using deuterated Trp and deuterated indole, were conducted. In the first experiment, application of [D_5]Trp to *in situ* seeds (extract 14.1) led to only minimal label incorporation into IAA (Figure 7.11), which means that either a Trp-dependent pathway does not predominant in pea seeds or the applied labelled Trp was overshadowed by large a large endogenous Trp pool. Consistent with the latter hypothesis, after the initial application of [D_5]Trp, only 0.5 % of the Trp pool was labelled (Figure 7.12). In the second experiment, twice the amount of [D_5]Trp was fed (extract 24.1), which gave increased label incorporation into IAA (Figure 7.13), demonstrating that a Trp-dependent pathway occurs in pea seeds. If a Trp-independent pathway (originating from indole) was important, the extent of labelling should be greater or equal when indole is fed, compared to when Trp is fed. However when the same amount of [D_6]indole (extract 24.2) as [D_5]Trp was fed, the extent of labelling was still minimal (Figure 7.14), The label incorporation observed when indole was fed may be explained by Trp dependent biosynthesis, given that indole is a Trp precursor. Hence, these data provide no evidence in support for the Trp-independent pathway from indole in these organs.

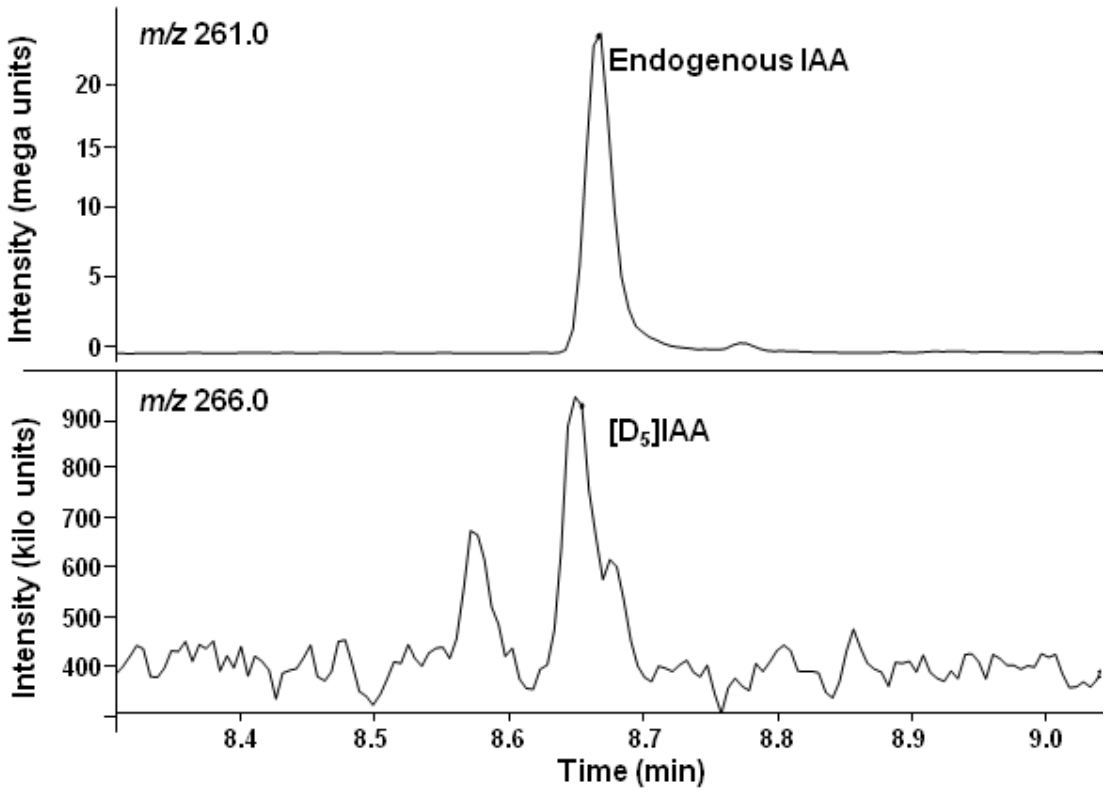

Figure 7.11 - GC-MS separation (SIM mode for the trimethylsilyl methyl ester derivative of IAA) of an extract (14) prepared from pea seeds after application of [D_5]Trp.

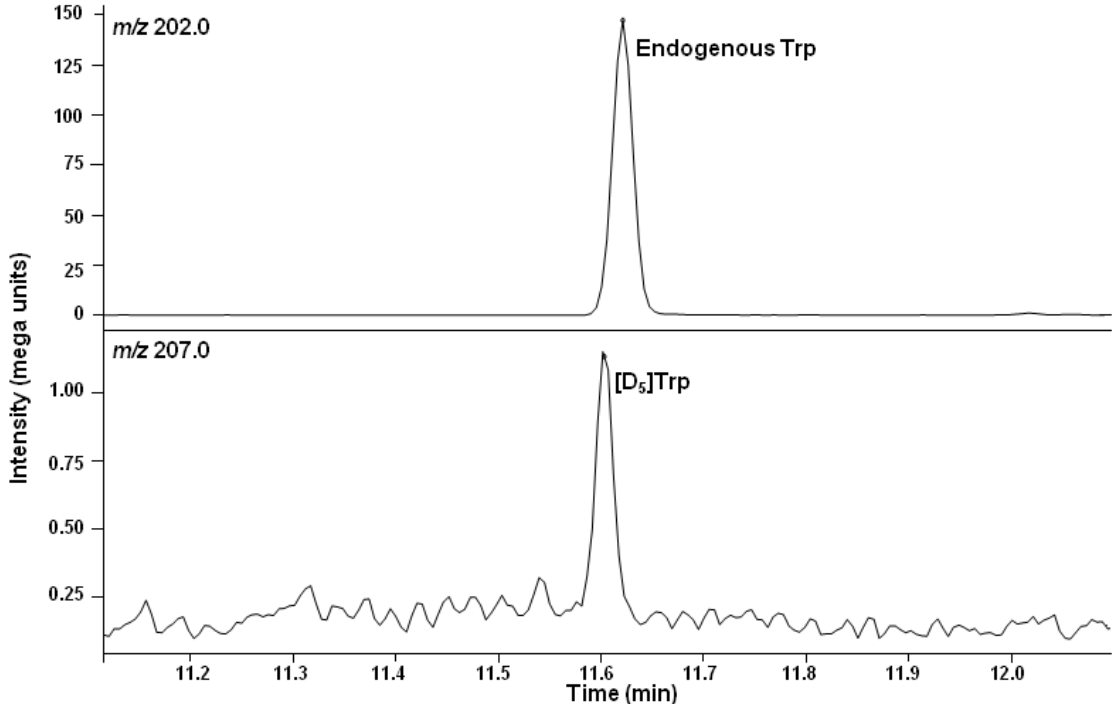

Figure 7.12 - GC-MS separation (SIM mode for the *N*-ethoxycarboxyltrimethylsilylpentafluoro propyl ester derivative of Trp) of an extract (14) prepared from pea seeds after application of [D_5]Trp.

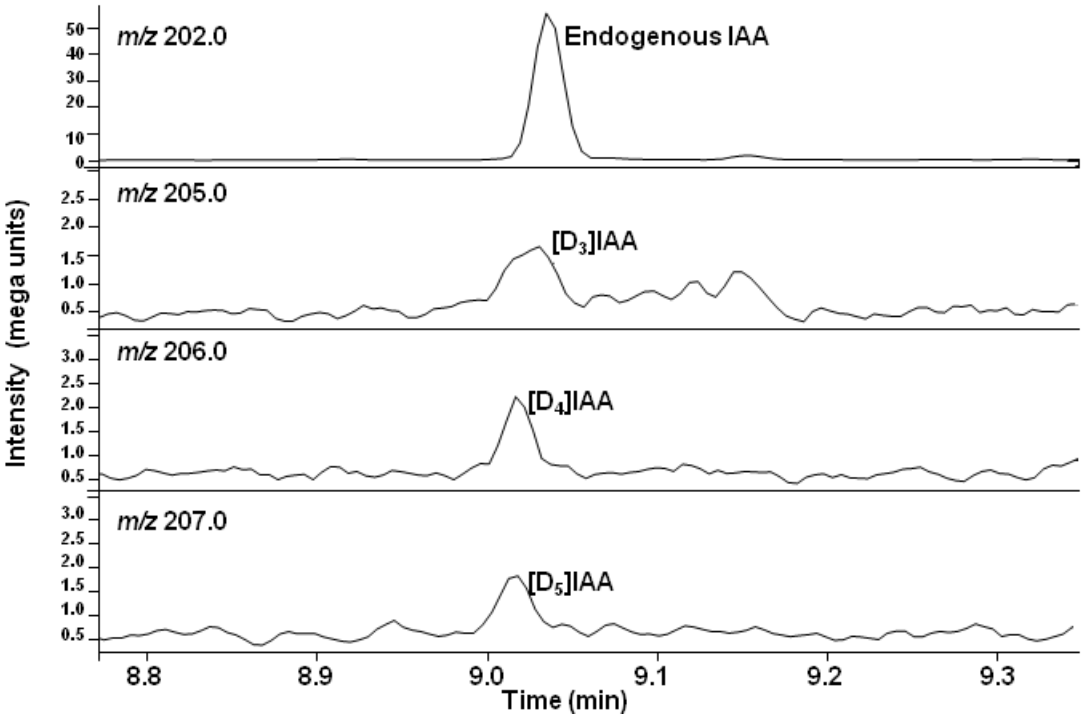

Figure 7.13 - GC-MS separation (SIM mode for the trimethylsilyl methyl ester derivative of IAA) of an extract (24.1) prepared from pea seeds after application of [D_5]Trp.

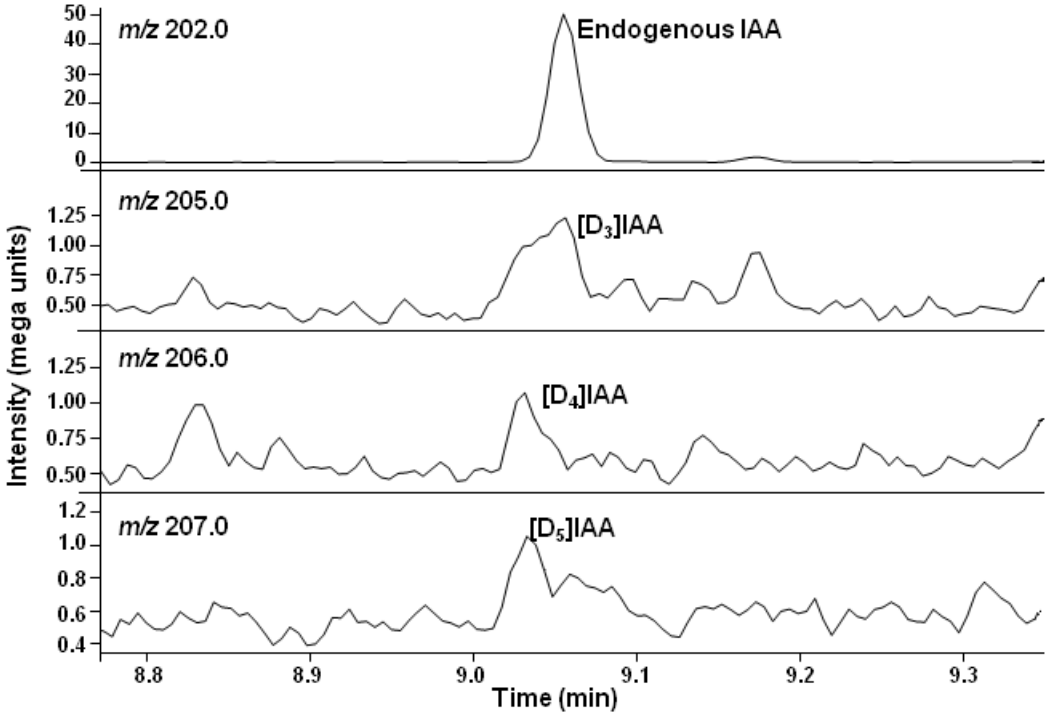

Figure 7.14 - GC-MS separation (SIM mode for the trimethylsilyl methyl ester derivative of IAA) of an extract (24.2) prepared from pea seeds after application of [D_6]indole.

Examining the TAM pathway in whole seeds

A series of feeding experiments was conducted to determine if TAM was an IAA precursor in pea seeds. IAA became labelled after labelled Trp feeding (extracts 45A1, 2, and 3) but did not become labelled after TAM feeding (extracts 45B1, 2, and 3; Figure 7.15; Table 7.3), indicating TAM is not an IAA precursor in these organs. This experiment also reinforced the importance of the Trp-dependent pathway, as IAA labelling after three hours was 29 %.

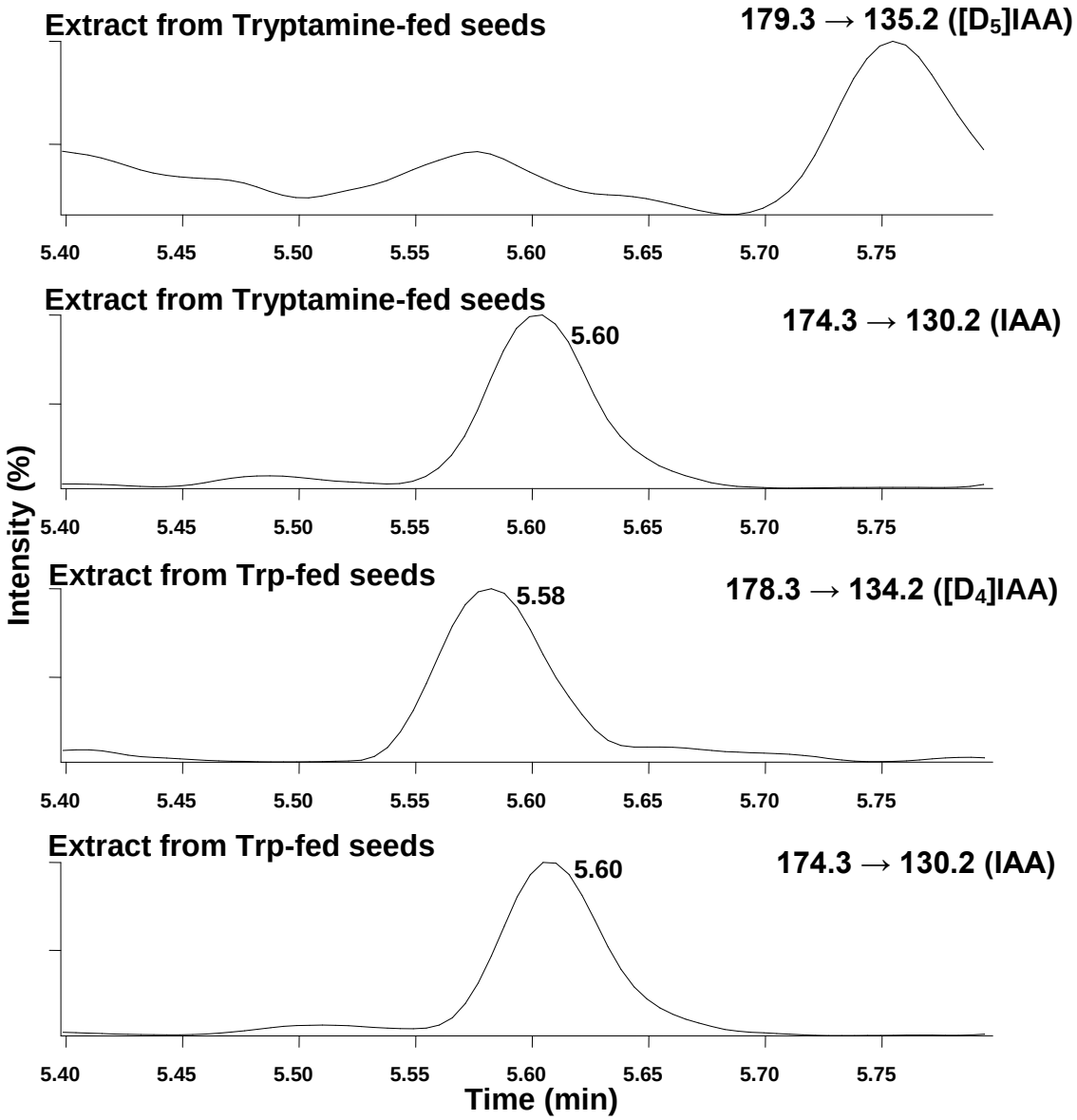

Figure 7.15 – UPLC-MS chromatogram (MRM mode; acetic acid program) of an extract prepared from pea seeds that had been previously injected with [D_5]TAM (extract 45B; top two channels) or [D_4]Trp (extract 45A; bottom two channels), showing label incorporation into IAA after [D_4]Trp feeding but not after [D_5]TAM feeding.

Table 7.3 - Percent label incorporation into Trp, tryptamine and IAA after feeding [D_4]Trp and [D_5]TAM (extracts 45A and 45B) to excised pea seeds, as determined by UPLC-MS. For [D_4]Trp treatments, 1 µL of a 1000-ng.µL^{-1} solution was injected. For [D_5]TAM treatments, 1 µL of a 100-ng.µL^{-1} solution was injected. The % deuterium labelling was calculated by dividing the area of the labelled peak by the sum of the areas of the labelled and unlabelled peaks. Shown are means ± se (n = 4). '0 % labelling' means that any labelling was below the limit of detection.

Substrate injected	Period of incubation (h)	Compound analysed	Average %deuterium labelling
[D_4]Trp	3	Trp	18 ± 5
		IAA	29 ± 6
[D_4]Trp	6	Trp	8 ± 4
		IAA	13 ± 4
[D_4]Trp	12	Trp	6 ± 4
		IAA	0.0
[D_5]TAM	3	TAM	99.7 ± 0.4
		IAA	0.0
[D_5]TAM	6	TAM	99.8 ± 0.1
		IAA	0.0
[D_5]TAM	12	TAM	99.9 ± 0.1
		IAA	0.0

Upon feeding 20-fold less [D_5]TAM (extract 47), there was still no detectable conversion to IAA after 3 (Figure 7.16) or 6 h.

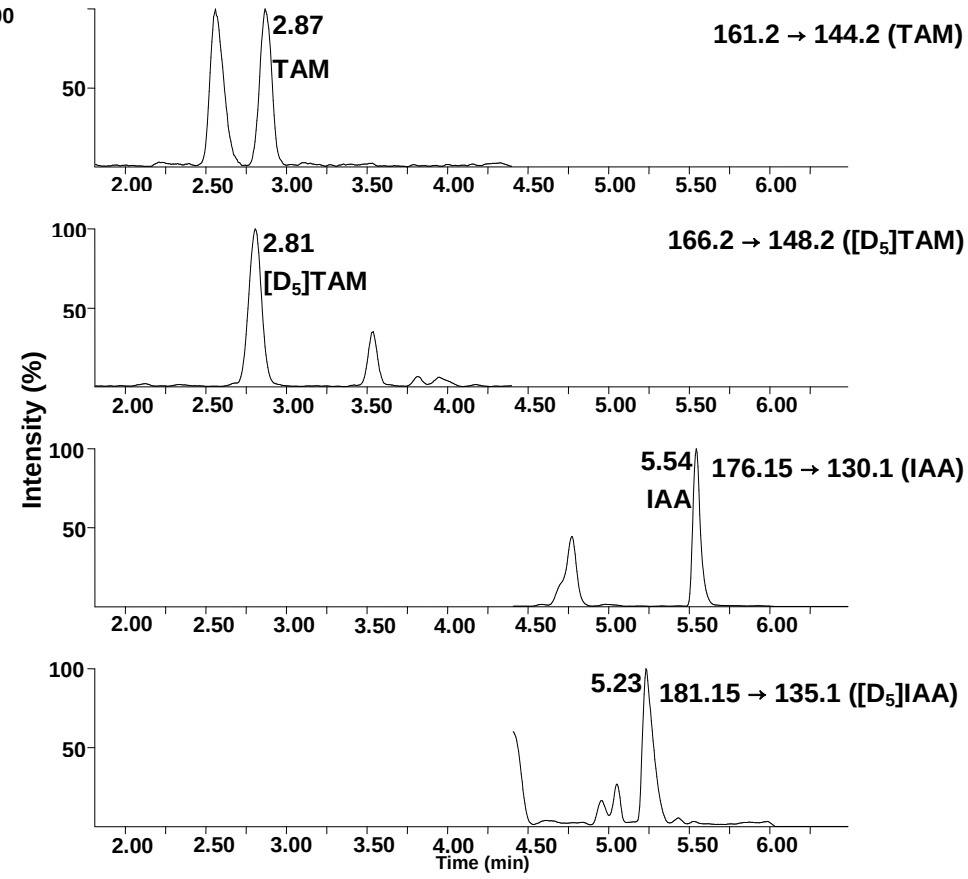

Figure 7.16 – UPLC-MS chromatogram (MRM mode; acetic acid program) of a pea seed extract (47) prepared after feeding [D_5]TAM and harvesting after 3 h. No D_5-labelled IAA was detected.

Trp metabolism in liquid endosperm

[D_4]Trp was also fed to excised pea seeds and harvested the endosperm only (extract 57). This showed label incorporation into ILA and IEt (Figure 7.17), but not IAM. In addition [D_4]Trp was fed to isolated pea liquid endosperm (extract 53). This resulted in label incorporation into IAA but not into IPyA or ILA (Figure 7.18). Endogenous ILA was detected but IPyA was not.

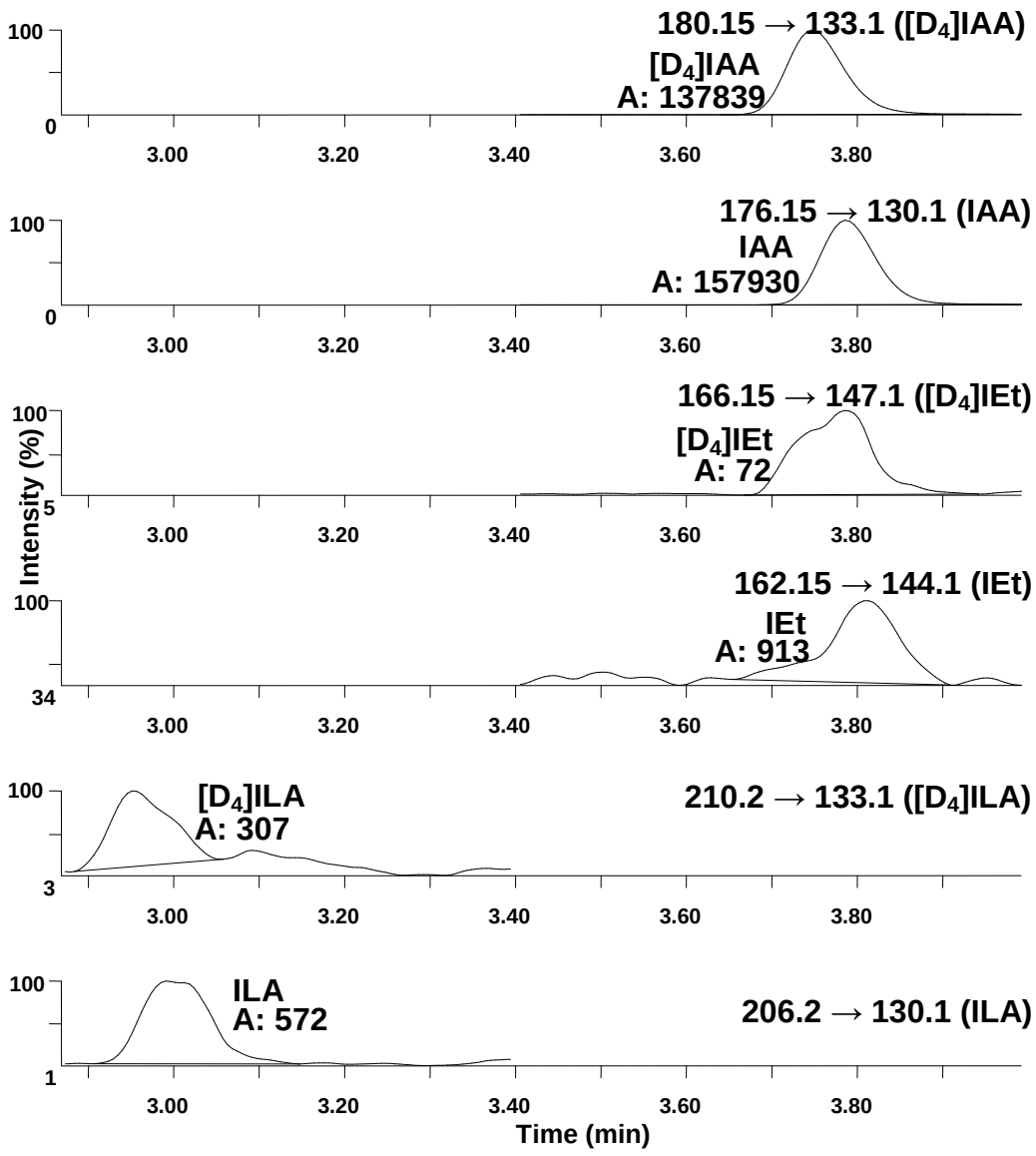

Figure 7.17 - UPLC-MS (MRM mode; acetic acid program) chromatogram of pea liquid endosperm (extract 57) prepared after application of [D_4]Trp. Label incorporation into IAA, IEt and ILA may be observed; incorporation into IAM was not observed.

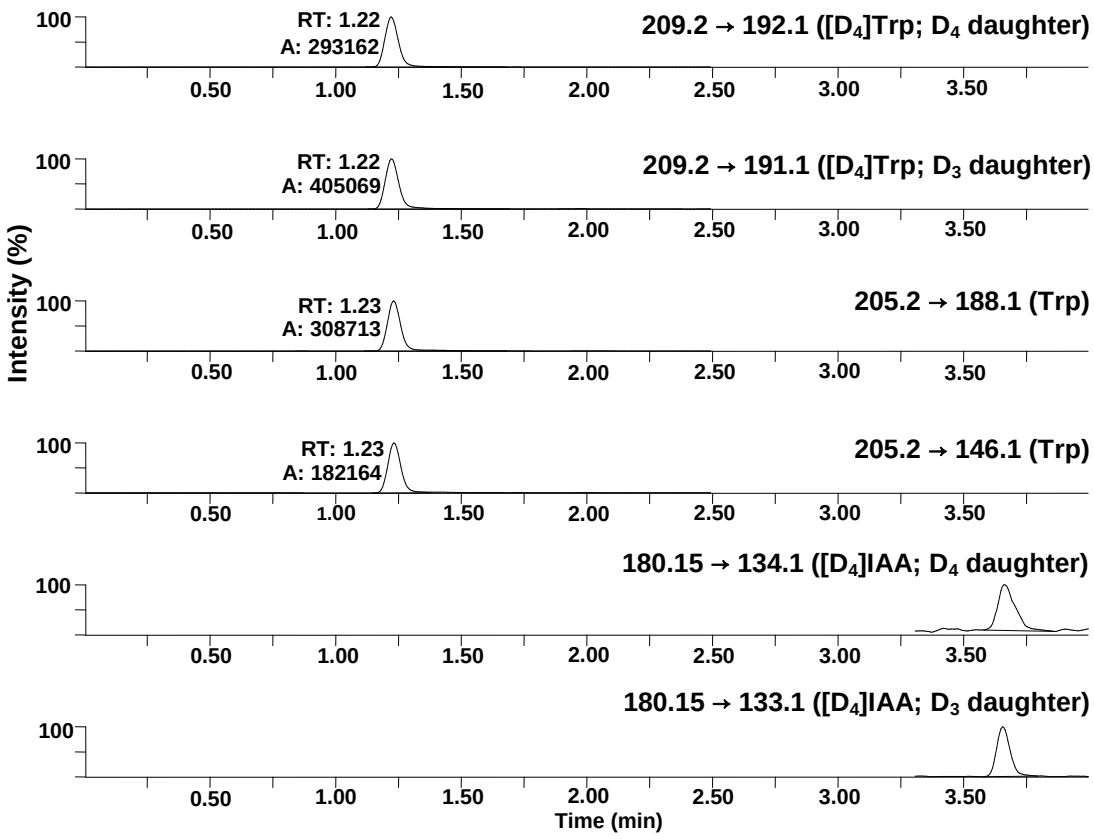

Figure 7.18 - UPLC-MS (MRM mode; acetic acid program) chromatogram of a pea liquid endosperm, (extract 53) after incubation with [D_4]Trp.

Examining the IAM pathway in whole seeds

When [D_6]IAM was fed to excised pea seeds (extract 115B), no label incorporation into IAA was observed (Figure 7.19), indicating that IAM is not a precursor for IAA in pea seeds. In this experiment when [D_5]Trp was fed to a separate group of seeds and up to 51 % label incorporation into IAA was observed, but no label incorporation into IAM was observed; endogenous IAM was similarly below the limit of detection. These results indicate that Trp-dependent IAA biosynthesis was occurring during the feeding period, but IAM was not involved as an intermediate.

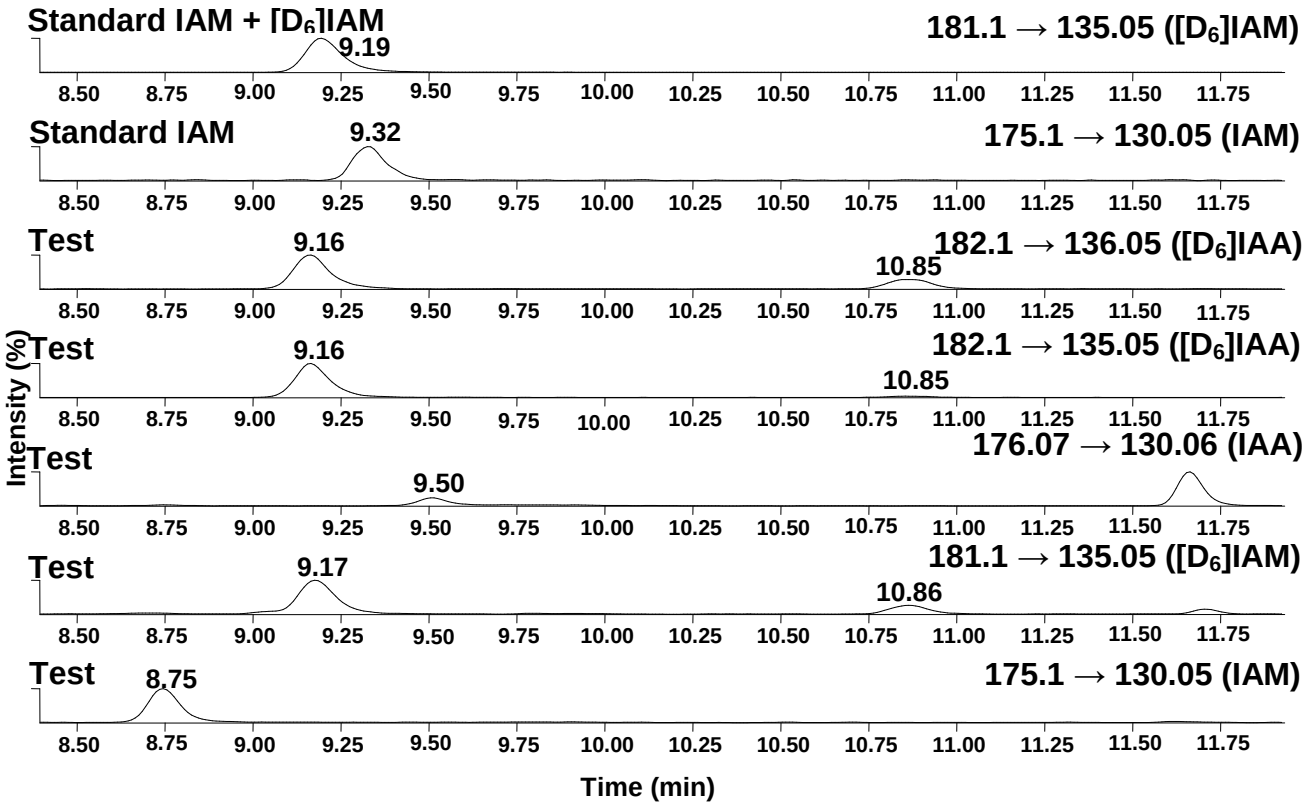

Figure 7.19 – UPLC-MS (MRM mode; 'slow' program) chromatogram of a pea seed extract (115B) prepared after application of [D_6]IAM. No label incorporation into IAA was evident.

Determining the involvement of IAAld in IAA biosynthesis in whole seeds

Feeding [D_5]IAAld to pea seeds (extract 82) resulted in label incorporation into IEt, but a minute amount of labelling of IAA was detected (Figure 7.20). Therefore, although the seeds may have the ability to metabolise IAAld, IAA does not appear to be a major product.

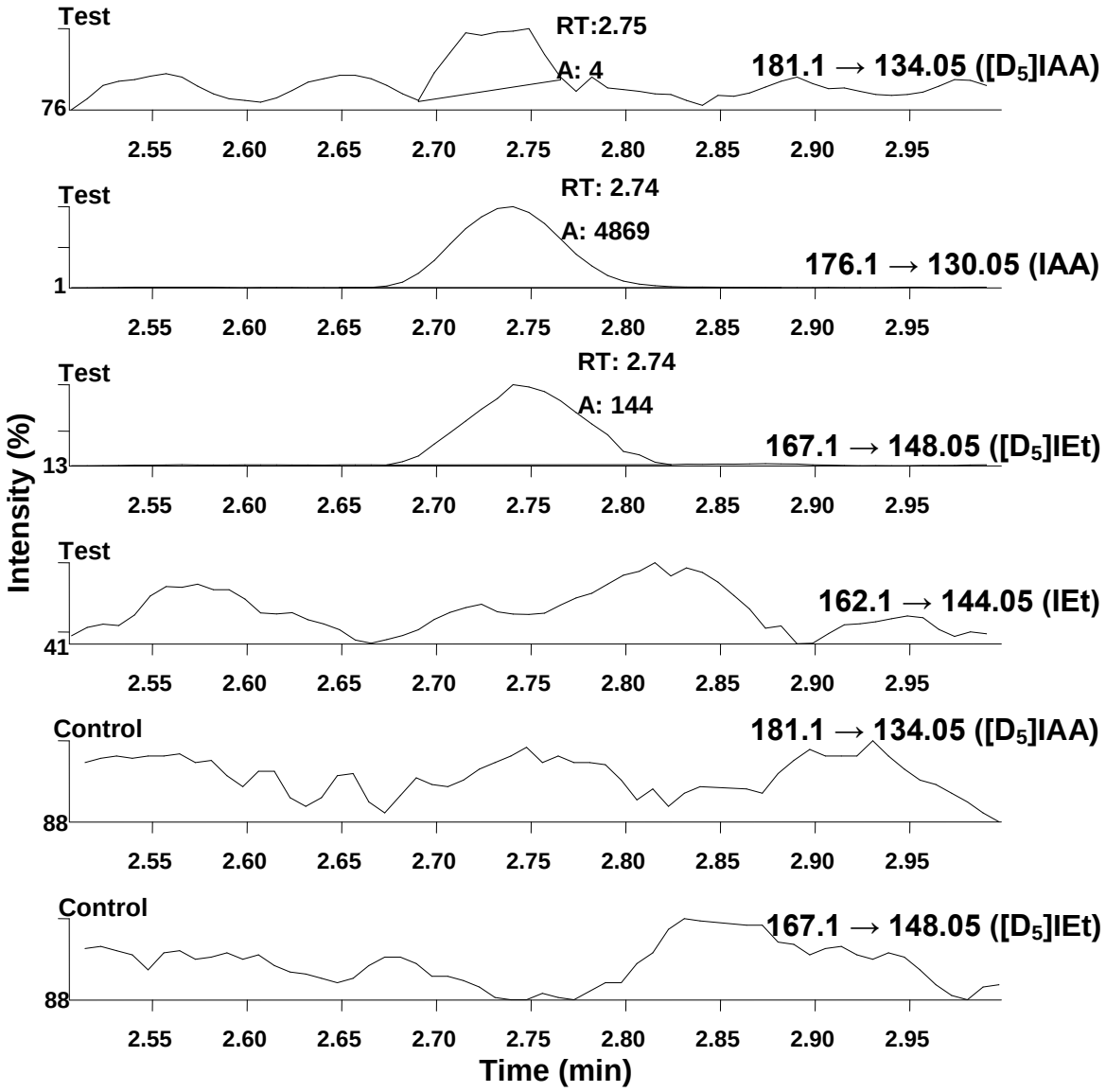

Figure 7.20 – UPLC-MS (MRM mode; acetic acid program) chromatogram of a pea seed extract (82) prepared after application of [D_5]IAAld.

Investigating 4-Cl-IAA biosynthesis

When [D_5]Trp and [$^{13}C_6$]IAA were fed to excised seeds (extract 114), incorporation of the D_5-label from Trp into IAA was observed (Figure 7.21A) and the IAA conjugate, indole-3-acetylaspartate (IAAsp), contained ^{13}C-label (Figure 7.22), indicating that IAA metabolism was occurring during the feeding period, but 4-Cl-IAA was not diluted with ^{13}C-label (Figure 7.21B), indicating that it is not IAA itself which becomes chlorinated. In the same experiment, D_4-label (from the [D_5]Trp) was detected in both 4-Cl-Trp and 4-Cl-IAA (Figure 7.21B, C), indicating

that Trp is a point of chlorination, and that the biosynthesis of 4-Cl-IAA continues parallel to that of IAA (see Chapter 6). Consistent with the theory that Trp is a point of chlorination, when deuterated 4-Cl-Trp was injected (extract 113), label incorporation into 4-Cl-IAA was observed (Figure 7.21D). It cannot be excluded, however, that chlorination also occurs at a stage prior to tryptophan.

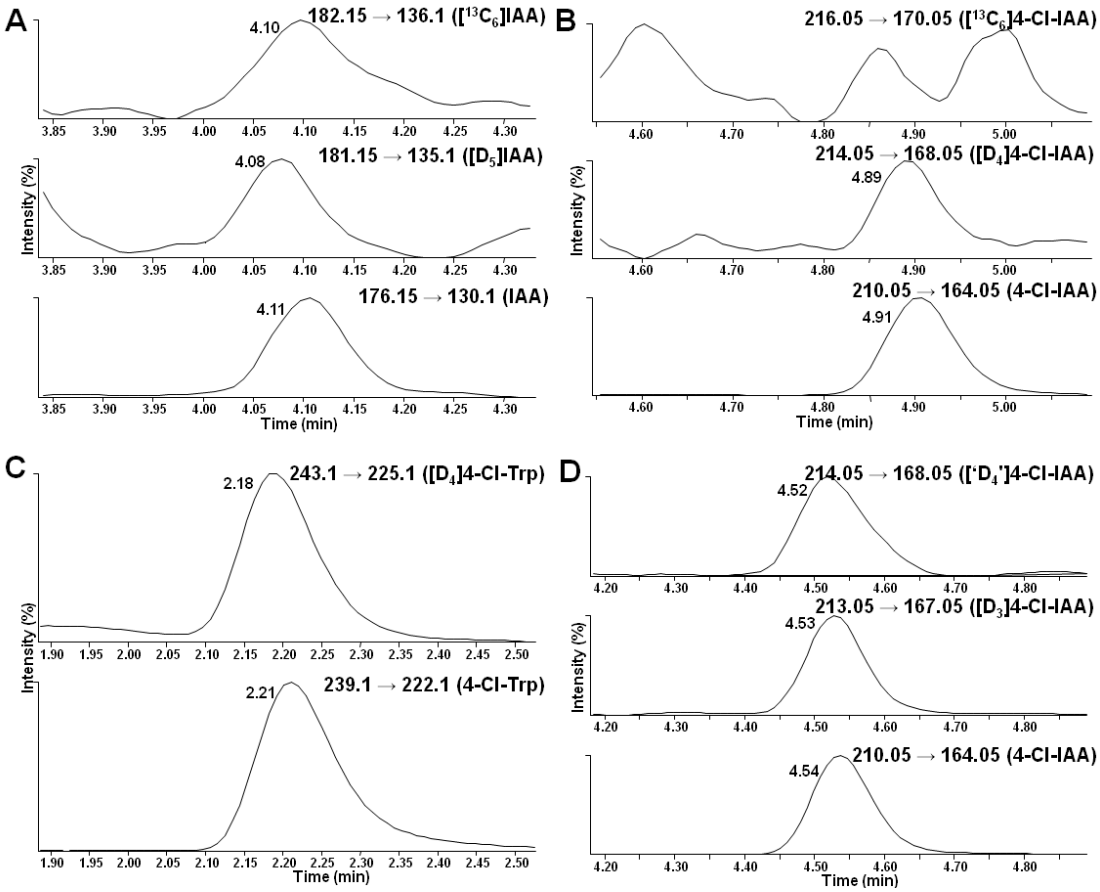

Figure 7.21 - UPLC-MS chromatograms (MRM mode; acetic acid program) obtained from extracts of pea seeds, which had been previously injected with a mixture of [D_5]Trp and [$^{13}C_6$]IAA (A-C; extract 114) or [D_4]4-Cl-Trp (D; extract 113). On UPLC, the RT of a deuterated species is earlier than the RT for the endogenous species; ^{13}C-labeled species have the same RT as their endogenous counterparts (on the UPLC-MS system used, within 0.01 min). (A) IAA became enriched with D_5-label (middle channel; RT 4.08) after injections of [D_5]Trp; the endogenous IAA (bottom channel; RT 4.11) and the injected [$^{13}C_6$]IAA (top channel; RT 4.10) were also detected. (B) 4-Cl-IAA also became enriched with D_4-label (middle channel; RT 4.89) from the injected [D_5]Trp (one deuterium is replaced with a chlorine atom), but the $^{13}C_6$-label from the injected [$^{13}C_6$]IAA was not incorporated into 4-Cl-IAA (top channel; the peaks observed in this channel did not have the correct RT for [$^{13}C_6$]4-Cl-IAA). (C) 4-Cl-Trp became enriched with D_4-label (top channel; RT 2.18) from the injected [D_5]Trp. (D) In a separate experiment, 4-Cl-IAA became enriched with deuterium label (top two channels) after deuterated 4-Cl-Trp was injected; endogenous 4-Cl-IAA was also detected (bottom channel). The ['D_4']4-Cl-IAA signal detected in this experiment contained a small contribution from [^{37}Cl, D_2]4-Cl-IAA.

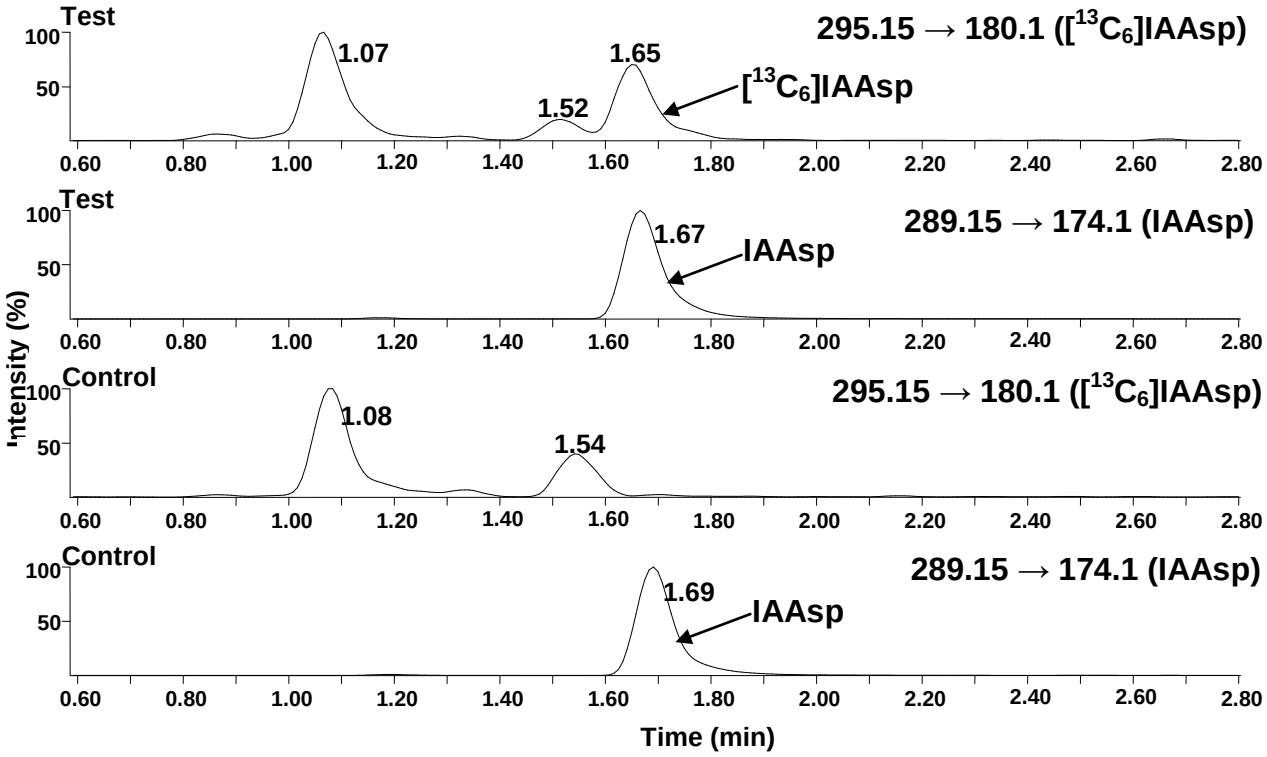

Figure 7.22 - UPLC-MS chromatograms (MRM mode; acetic acid program) obtained from an extract (114) of pea seeds, which had been previously injected with a mixture of [D_5]Trp and [$^{13}C_6$]IAA. [$^{13}C_6$]-label incorporation into IAAsp was observed.

Results Summary

The table below summarises the results reported in this chapter

Table 7.4 – Summary of chemical analysis of developing pea seeds. Labelled forms were enriched with deuterium or ^{13}C. NT: not tested.

Compound	Endogenous in whole seeds?	Endogenous in endosperm?	Label incorporated into compound from Trp in seeds?	Label incorporated from intermediate into IAA?	Label incorporated from intermediate into 4-Cl-IAA?
Trp	Yes	Yes		Yes	Yes
4-Cl-Trp	Yes	NT	Yes	No	Yes
TAM	Yes	NT	No	No	NT
IAM	No	No	No	No	NT
IPyA	Yes	No	NT	NT	NT
ILA	Yes	Yes	Yes	NT	NT
ICA	Yes	Yes	No	NT	NT
IAAld	No	No	NT	No	NT
IEt	No	Yes	Yes	NT	NT
IAA	Yes	Yes	Yes		No

The evidence reported here indicates that Trp (and by implication 4-Cl-Trp) is not converted to auxin in pea seeds *via*, IAM or TAM (or their 4-chlorinated derivatives). The incorporation of deuterium into 4-Cl-Trp and 4-Cl-IAA, from labelled Trp, indicates that Trp is a biosynthetic point of origin of 4-Cl-IAA; furthermore, $[D_3/D_4]$4-Cl-Trp feeding to excised pea seeds (extract 113) resulted in label incorporation into 4-Cl-IAA (Figure 7.21), which is consistent with the previously proposed model (see Chapter 6).

Discussion

There are four major pathways proposed for Trp-dependent IAA biosynthesis: the IAOx, TAM, IAM and IPyA pathways (for reviews on these pathways, see Bartel et al., 2001; Davies, 2004; Woodward and Bartel, 2005; Normanly, 2010; Zhao, 2010). As mentioned earlier the IAOx

pathway probably does not operate in pea (Tivendale, 2008; Quittenden et al., 2009); consequently, the focus of this study was upon the TAM, IAM, Trp-independent and IPyA pathways. IAA biosynthesis was examined in young developing pea seeds through quantification of endogenous compounds and administration of various labelled compounds.

TAM was identified as an endogenous compound in pea seeds and the TAM pathway was investigated *via* a series of feeding experiments using excised seeds. Labelled Trp and labelled TAM were injected into separate groups of seeds, but only label from Trp was incorporated into IAA, indicating that TAM is not an IAA precursor in these organs. While this is consistent with reports from other species (e.g. tomato; Cooney and Nonhebel, 1991), the TAM pathway was, until recently, thought to be relatively widespread throughout the plant kingdom (Winter, 1966; Gibson et al., 1972; Zhao et al., 2001; Expósito-Rodríguez et al., 2007; Yamamoto et al., 2007; Quittenden et al., 2009; LeClere et al., 2010), based largely on the presence of *YUC* genes in a number of species. TAM is reportedly a substrate for YUCs, but strong evidence against this hypothesis has been produced (Chapter 4; see also Tivendale et al., 2010). Since evidence has been obtained for at least two *PsYUC*-like genes that are strongly expressed in pea seeds (Tivendale et al., 2010), the lack of tryptamine metabolism in these organs provides further support for the hypothesis that the YUCs may catalyse other reactions, as previously suggested (Tobeña-Santamaria et al., 2002; Tivendale et al., 2010). The TAM pathway may operate in some systems (e.g pea roots; Quittenden et al., 2009), but it does not operate in pea seeds and may not as widespread as previously thought.

The possible role of IAM in auxin biosynthesis in pea seeds was also examined. IAM, which was once thought to be restricted to bacteria, has previously been identified in *Arabidopsis* (Pollmann et al., 2002), rice, corn and tobacco (Sugawara et al., 2009). Here it was demonstrated that IAM is below the limit of detection in pea seeds and no evidence of label incorporation into IAM, when either [D_5]Trp or [D_6]indole were injected into seeds, was obtained. Moreover, when [D_6]IAM was injected into seeds, no label incorporation into IAA was detected. Taken together, these results demonstrate that, despite claims that the IAM pathway is widespread among plants (Lehmann et al., 2010), IAM is not an IAA precursor in pea seeds.

It has previously been shown that Trp is an IAA precursor in pea seeds (Tivendale, 2008; see also Chapter 4; Tivendale et al., 2010) but the extent of labelling was relatively low, which gave

rise to the notion that a Trp-independent pathway originating from indole-3-glycerol phosphate or indole, previously proposed as a major pathway in *Arabidopsis* (Normanly et al., 1993; Normanly et al., 1995; Ouyang et al., 2000), was also operating in pea seeds. If this were the case, then application of labelled indole should lead to a greater or equal extent of label incorporation into IAA, compared to application of labelled Trp. However, in the current study, when indole was fed, the amount of label incorporation into IAA was even less than the amount observed after Trp feeding. The isotopic composition of the Trp pool after [D_5]Trp feeding was found to contain only a relatively small proportion of label, and when the amount of labelled Trp applied was increased, the extent of labelling of IAA increased proportionately, indicating that the small percentage of labelling was due not to the operation of a Trp-independent pathway but rather to a large endogenous Trp pool. Thus the observations in the current study do not support the occurrence of a Trp-independent pathway originating from indole in pea seeds; although on the basis of the evidence presented here a Trp-independent pathway originating from indole-3-glyerol phosphate (Figure 7.1), as has been previously suggested (Normanly et al., 1993), cannot be excluded. Nonetheless, it has been suggested that the apparent Trp-independent auxin biosynthesis in *Arabidopsis* may be an artefact (Müller and Weiler, 2000). Trp auxotroph mutants accumulate indole-3-glycerol phosphate, which, when extracted from the plant, degrades spontaneously to IAA; Müller and Weiler (2000) claim that this accounts for the observed increase in IAA conjugates in these mutants.

Previously this thesis reported evidence for the IPyA pathway in pea seeds (see Chapter 6). The evidence obtained here is also consistent with this hypothesis. Prior to this study, in which IPyA was identified in pea seeds, IPyA had been found only in *Arabidopsis* (Tam and Normanly, 1998), tomato shoots (Cooney and Nonhebel, 1989, 1991) and pea root nodules (Badenoch-Jones et al., 1984). The suggested IPyA storage product, ILA, was also detected in whole pea seeds and isolated liquid endosperm. This compound became labelled after applications of [D_5]Trp, which is consistent with synthesis of IPyA from Trp in seeds.

The IPyA breakdown product, ICA was also detected in whole seeds and at low levels in isolated liquid endosperm. ICA has been identified in various species of fungal plant pathogens (as a detoxification product of brassinin; Pedras and Jha, 2006; Lin et al., 2010; Pedras et al., 2011) and *Picea schrenkiana* (Li et al., 2011). The possible biological roles of this compound in pea

are yet to be investigated. However, it may simply be a physicochemical breakdown product of IPyA (see Chapter 6).

Two variants of the IPyA pathway have been proposed (see Figure 7.1). The pathway originally proposed included IAAld as an intermediate between IPyA and IAA (Cooney and Nonhebel, 1989; Koga et al., 1991b; Koga et al., 1992; Koga, 1995; Tam and Normanly, 1998). As noted in Chapter 6, the recently reported TAA/YUC variant did not include this intermediate, and it was reported that IPyA was converted directly to IAA (Kriechbaumer et al., 2011; Mashiguchi et al., 2011; Stepanova et al., 2011). Consistent with the latter variant, when labelled Trp was fed to pea seeds, label was incorporated into IEt, but labelled and unlabelled IAAld were below the limit of detection. Moreover when labelled IAAld was fed to these organs, label was incorporated into IEt but not IAA. Hence, the evidence reported here shows that while pea seeds have the necessary cellular machinery to metabolise IAAld, IAA does not appear to be a major product.

This study also shed more light on the biosynthesis of 4-Cl-IAA. Previously, there have been few reports of the biosynthetic origin of this compound, and the evidence presented was far from convincing (Manabe et al., 1999). In the present study it was shown definitively that IAA does not become chlorinated to produce 4-Cl-IAA (consistent with preliminary results published in Tivendale, 2008), and the majority of 4-Cl-IAA in maturing seeds is synthesised *via* the 4-Cl-IPyA pathway. Also in the current study, endogenous 4-Cl-IPyA was detected in developing pea seeds; this is the first report of this compound in any plant species. Furthermore, when deuterated Trp was injected, label incorporation into 4-Cl-Trp and 4-Cl-IAA was observed and 4-Cl-IAA became labelled after injection of deuterated 4-Cl-Trp. This indicates that Trp is a point of chlorination, but it cannot be excluded that there are other points of chlorination, prior to Trp.

In conclusion, the *in vivo* evidence presented here supports parallel biosynthesis of IAA and 4-Cl-IAA *via* IPyA and 4-Cl-IPyA in the early stages of seed development. The findings presented are entirely consistent with evidence reported in previous chapters (see especially Chapter 6). Taken together, evidence obtained here and previously indicates that Trp (and by implication 4-Cl-Trp) is not converted to auxin in pea seeds *via* TAM or IAM, and previous studies have excluded the IAOx pathways in pea seeds (Tivendale, 2008; Quittenden et al., 2009). While a Trp-independent pathway cannot be completely ruled out, the results reported here do not

provide support for a pathway from indole and others have suggested that apparent Trp-independent auxin biosynthesis may be an artefact, even in *Arabidopsis* (Müller and Weiler, 2000). The results of this study support the occurrence of the IPyA/4-Cl-IPyA pathway (Figure 6.20), but none of the other proposed pathways, in developing pea seeds.

Chapter 8 Conclusions[6]

This thesis reports a series of experiments that have examined auxin biosynthesis in pea, using a combination of molecular biology and chemistry-based approaches. Auxin biosynthesis has been reported to occur by five proposed pathways (see Figure 1.1). The IAOx pathway was not considered in this study as previous evidence indicates this pathway is probably restricted to the Brassicaceae (Quittenden et al., 2009; Sugawara et al., 2009). As a result of the current study, all but one of the remaining four pathways may be discounted in pea seeds, and strong evidence that the remaining pathway is responsible for the vast majority of auxin biosynthesis in these organs is provided.

In the present study, it was shown that TAM is metabolised by pea roots (Chapter 3) and the major metabolite detected was NAcTAM, the *in vivo* function of which is yet to be determined. Even though IAA is not the major TAM metabolite in roots, it has been shown previously that the TAM pathway can operate in these organs (Quittenden et al., 2009). However, through injection of labelled TAM it was shown that TAM is not an IAA precursor in pea seeds (Chapter 7). Analysis of the TAM pathway (Chapter 4) also cast serious doubts over the proposed role of the YUCs and NHT in this pathway in other species (Tivendale et al., 2010). Previous reports of NHT as a product of YUC enzymes supplied with TAM *in vitro* were based on mass spectral analyses with no authentic NHT for comparison (Zhao et al., 2001; LeClere et al., 2010). The analysis of authentic NHT synthesised in our laboratory showed that the spectra presented by LeClere et al. (2010) did not represent NHT (Tivendale et al., 2010). The spectra and TLC properties reported by this group were consistent with 2-OT (an auto-oxidation product of TAM), which was synthesised and analysed in our laboratory (Chapter 5). The spectrum presented by Zhao et al. (2001) was too 'noisy' to allow any firm conclusions to be drawn, but it probably does not represent NHT either (Tivendale et al., 2010). After the publication of our analysis of NHT, several groups reported that the YUCs function in the IPyA pathway

[6] Some of the conclusions presented here have been published in the research articles Tivendale ND, Davies NW, Molesworth PP, Davidson SE, Smith JA, Lowe EK, Reid JB, Ross JJ (2010) Reassessing the role of *N*-hydroxytryptamine in auxin biosynthesis. Plant Physiology **154:** 1957-1965 and Tivendale ND, Davidson SE, Davies NW, Smith JA, Dalmais M, Bendahmane A, Quittenden LJ, Sutton L, Bala RK, Le Signor C, Thompson R, Horne J, Reid JB, Ross JJ (2012) Biosynthesis of the halogenated auxin, 4-chloroindole-3-acetic acid. Plant Physiology **159:** 1055-1063, and the addendum Ross JJ, Tivendale ND, Reid JB, Davies NW, Molesworth PP, Lowe EK, Smith JA, Davidson SE (2011) Reassessing the role of YUCCAs in auxin biosynthesis. Plant Signaling and Behavior **6:** 437-439.

(Kriechbaumer et al., 2011; Mashiguchi et al., 2011; Stepanova et al., 2011; Won et al., 2011), although these reports are not without their own incongruities (see Chapter 6).

Through administration of labelled precursors, evidence that the IAM pathway (Pollmann et al., 2002; Lehmann et al., 2010; Mano and Nemoto, 2012) does not operate in pea seeds was also produced (Chapter 7; see also Tivendale et al., 2012). Endogenous IAM was below the limit of detection in pea seeds. Moreover, these organs utilise Trp as an IAA precursor, but IAM did not become labelled when labelled Trp was injected, and label from IAM injected into these seeds was not incorporated into IAA. These results indicate that the IAM pathway does not operate in these organs.

Evidence for a Trp-independent pathway (Normanly et al., 1993) in pea seeds was not forthcoming (Chapter 7). If the Trp-independent pathway was in operation, one would expect to observe equal or greater percentage label in IAA when labelled indole is fed compared to when labelled Trp is fed. However, this was not observed. In fact, the percentage of label incorporation was lower when indole was fed compared to when Trp was fed. This indicates the Trp-independent pathway is not a major source of IAA in pea seeds. The evidence reported in this thesis does not allow the possibility of a Trp-independent pathway originating from a Trp precursor earlier than indole, such as indole-3-glycerol phosphate—as previously suggested (Normanly et al., 1993), to be discounted. Yet, others have suggested that Trp-independent auxin biosynthesis may be an artefact, even in *Arabidopsis* (Müller and Weiler, 2000), which is consistent with the findings reported in Chapter 7.

The evidence reported in this thesis supports the operation of the IPyA pathway, and its chlorinated version, in pea seeds. Two newly isolated Trp aminotransferases from pea were shown to convert Trp and its 4-chlorinated analogue to IPyA and 4-Cl-IPyA, respectively; the latter two compounds were also found as endogenous compounds in seeds. Mutating the *PsTAR2* gene so that it was non-functional caused a significant decrease in 4-Cl-IAA levels in these organs (Tivendale et al., 2012). Furthermore, when deuterated Trp was fed to pea seeds, label incorporation into ILA and IEt (two compounds associated with IPyA-dependent auxin biosynthesis; Brown and Purves, 1980; Brandl and Lindow, 1996) was observed. Label incorporation into IPyA and IAAld was not detected, probably due to the instability of these compounds. However, when labelled IAAld was injected, label was incorporated into IEt but not

IAA. This suggests that IAAld is not involved in IAA biosynthesis in pea seeds, as previously suggested for *Arabidopsis* (Kriechbaumer et al., 2011; Mashiguchi et al., 2011; Stepanova et al., 2011; Won et al., 2011).

Taken together, the evidence presented in this thesis indicates that the TAM, IAM and Trp-independent auxin biosynthetic pathways do not operate in developing pea seeds. Moreover, the evidence supports the operation of the IPyA pathway as the dominant pathway to auxin in these organs. The evidence presented here also illuminated the biosynthesis of the only halogenated plant hormone, 4-Cl-IAA, *via* a chlorinated version of the IPyA pathway that operates in parallel to the IPyA pathway (see Chapter 6).

There is currently a renewed focus on auxin biosynthesis due to reports that, rather than acting in the tryptamine pathway (Tivendale et al., 2010), the YUC proteins operate in the IPyA pathway (Kriechbaumer et al., 2011; Mashiguchi et al., 2011; Stepanova et al., 2011; Won et al., 2011), as previously suggested by Strader and Bartel (2008). Still, Mano and Nemoto (2012) recently noted that, since functional activity for Trp aminotransferases from the IPyA pathway has been demonstrated only for *Arabidopsis* genes, the IPyA pathway might be restricted to the Brassicaceae. However the evidence presented here indicates that the IPyA pathway does operate, and indeed can predominate, in some tissues of other species.

References

Adelstein SJ, Manning FJ, eds (1995) Isotopes for Medicine and the Life Sciences. National Academy Press, Washington

Ali B, Hayat S, Aiman Hasan S, Ahmad A (2008) A comparative effect of IAA and 4-Cl-IAA on growth, nodulation and nitrogen fixation in *Vigna radiata* (L.) Wilczek. Acta Physiologiae Plantarum **30:** 35-41

Alonso JM, Ecker JR (2006) Moving forward in reverse: Genetic technologies to enable genome-wide phenomic screens in Arabidopsis. Nature Reviews Genetics **7:** 524-536

Ames D, Bowman R, Evans D, Jones W (1956) The synthesis of some indolylalkylamines. Journal of the Chemical Society (Resumed)**:** 1963-1969

Aubry C, Wilson AJ, Emmerson D, Murphy E, Chan YY, Dickens MP, García MD, Jenkins PR, Mahale S, Chaudhuri B (2009) Fascaplysin-inspired diindolyls as selective inhibitors of CDK4/cyclin D1. Bioorg Med Chem **17:** 6073-6084

Badenoch-Jones J, Summons RE, Rolfe BG, Letham DS (1984) Phytohormones, Rhizobium mutants, and nodulation in legumes IV. Auxin metabolites in pea root nodules. J Plant Growth Regul **3:** 23-39

Bak S, Tax FE, Feldmann KA, Galbraith DW, Feyereisen R (2001) CYP83B1, a cytochrome P450 at the metabolic branch point in auxin and indole glucosinolate biosynthesis in Arabidopsis. Plant Cell **13:** 101-111

Barlier I, Kowalczyk M, Marchant A, Ljung K, Bhalerao R, Bennett M, Sandberg G, Bellini C (2000) The *SUR2* gene of *Arabidopsis thaliana* encodes the cytochrome P450 CYP83B1, a modulator of auxin homeostasis. Proc Natl Acad Sci USA **97:** 14819-14824

Bartel B (1997) Auxin Biosynthesis. Annu Rev Plant Physiol Plant Mol Biol **48:** 51-66

Bartel B, LeClere S, Magidin M, Zolman BK (2001) Inputs to the active indole-3-acetic acid pool: *de novo* synthesis, conjugate hydrolysis, and indole-3-butyric cid β-oxidation. J Plant Growth Regul **20:** 198-216

Benková E, Michniewicz M, Sauer M, Teichmann T, Seifertová D, Jürgens G, Friml J (2003) Local, efflux-dependent auxin gradients as a common module for plant organ formation. Cell **115:** 591-602

Berry AM, Kahn R, Booth MC (1989) Identification of indole compounds secreted by *Frankia* HFPArI3 in defined culture medium. Plant Soil **118:** 205-209

Brandl M, Lindow S (1996) Cloning and characterization of a locus encoding an indolepyruvate carboxylase involved in indole-3-acetic acid synthesis in *Erwinia herbicola*. Appl Environ Microbiol **62:** 4121-4128

Bretschneider H, Hörmann H (1953) ω-Azidoacetophenone und ihre katalytische Reduktion - Über Azidoverbindungen, l. Mitteilung. Monatshefte für Chemie **84:** 1021-1032

Brown H, Purves W (1980) Indoleacetaldehyde reductase of *Cucumis sativus*. Plant Physiol **65:** 107-113

Bruice PY (2004) Organic Chemistry, 4th Ed. Pearson Education Inc, Upper Saddle River

Camilleri C, Jouanin L (1991) The TR-DNA region carrying the auxin synthesis genes of the *Agrobacterium rhizogenes* agropine-type plasmid pRiA4: nucleotide sequence analysis and introduction into tobacco plants. Mol Plant-Microbe Interact **4:** 155-162

Chandler JW (2009) Local auxin production: A small contribution to a big field. Bioessays **31:** 60-70

Cheng Y, Dai X, Zhao Y (2006) Auxin biosynthesis by the YUCCA flavin monooxygenases controls the formation of floral organs and vascular tissues in *Arabidopsis*. Genes Dev **20:** 1790-1799

Cheng Y, Dai X, Zhao Y (2007) Auxin synthesized by the YUCCA flavin monooxygenases is essential for embryogenesis and leaf formation in *Arabidopsis*. Plant Cell **19:** 2430-2439

Chourey PS, Li QB, Kumar D (2010) Sugar-hormone cross-talk in seed development: two redundant pathways of IAA biosynthesis are regulated differentially in the invertase-deficient *miniature1* (*mn1*) seed mutant in maize. Molecular Plant **3:** 1026-1036

Ciesielski T (1872) Untersuchungen über die Abwärtskrümmung der Wurzel. Beitrage zur Biologie der Pflanzen **1:** 1-30

Cohen JD, Slovin JP, Hendrickson AM (2003) Two genetically discrete pathways convert tryptophan to auxin: More redundancy in auxin biosynthesis. Trends Plant Sci **8:** 197-199

Comai L, Kosuge T (1982) Cloning and characterization of iaaM, a virulence determinant of *Pseudomonas savastanoi*. J Bacteriol **149:** 40-46

Cooney TP, Nonhebel HM (1989) The Measurement and mass spectral identification of indole-3-pyruvate from tomato shoots. Biochem Biophys Res Commun **162:** 761-766

Cooney TP, Nonhebel HM (1991) Biosynthesis of indole-3-acetic acid in tomato shoots: measurement, mass-spectral identification and incorporation of ^{2}H from $^{2}H_2O$ into indole-3-acetic acid, D- and L-tryptophan, indole-3-pyruvate and tryptamine. Planta **184:** 368-376

Costacurta A, Vanderleyden J (1995) Synthesis of phytohormones by plant-associated bacteria. Crit Rev Microbiol **21:** 1-18

Darwin C (1880) The power of movement in plants, 1st Ed. John Murray, London

Davies PJ, ed (2004) Plant Hormones: Biosynthesis, Signal Transduction, Action! Kluwer Academic Publishers, London

Driscoll JP, Aliagas I, Harris JJ, Halladay JS, Khatib-Shahidi S, Deese A, Segraves N, Khojasteh-Bakht SC (2010) Formation of a quinoneimine intermediate of 4-fluoro-*N*-methylaniline by FMO1: carbon oxidation plus defluorination. Chem Res Toxicol **23:** 861–863

Engin S, Nurhan K, Latif K, Ebru M, Hasan S, Ramazan A, Yunus K (2007) An efficient synthesis of (R)-gabob and of (+)-gabob. Organic Preparations and Procedures International **39:** 509-522

Engvild KC, Egsgaard H, Larsen E (1980) Determination of 4-chloroindole-3-acetic acid methyl-esters in *Lathyrus, Vicia* and *Pisum* by gas chromatography-mass spectrometry. Physiol Plant **48:** 499-503

Engvild KC, Egsgaard H, Larsen E (1981) Determination of 4-chloroindoleacetic acid methyl-ester in Vicieae species by gas chromatography-mass spectrometry. Physiol Plant **53:** 79-81

Erdmann N, Schiewer U (1971) Tryptophan-dependent indoleacetic acid biosynthesis from indole demonstrated by double labelling experiments. Planta **97:** 135-141

Ernstsen A, Sandberg G (1986) Identification of 4-chloroindole-3-acetic acid and indole-3-aldehyde in seeds of *Pinus sylverstris*. Physiol Plant **68:** 511-518

Ernstsen A, Sandberg G, Crozier A, Wheeler CT (1987) Endogenous indoles and the biosynthesis and metabolism of indole-3-acetic acid in cultures of *Rhizobium phaseoli*. Planta **171:** 422-428

Expósito-Rodríguez M, Borges AA, Borges-Pérez A, Hernández M, Pérez JA (2007) Cloning and biochemical characterisation of *ToFZY*, a tomato gene encoding a flavin monooxygenase involved in a tryptophan-dependent auxin biosynthesis pathway. J Plant Growth Regul **26:** 329-340

Floris B (1990) NMR, IR conformation of hydrogen bonding. *In* Z Rappoport (ed) The Chemistry of Enols. Wiley, Chichester, p 147

Gallavotti A, Barazesh S, Malcomber S, Hall D, Jackson D, Schmidt RJ, McSteen P (2008) *sparse inflorescence1* encodes a monocot-specific YUCCA-like gene required for vegetative and reproductive development in maize. Proc Natl Acad Sci USA **105:** 15196-15201

Garcia-Tabares F, Herraiz-Tomico T, Amat-Guerri F, Bilbao JLG (1987) Production of 3-indoleacetic acid and 3-indolelactic acid in Azotobacter vinelandii cultures supplemented with tryptophan. Appl Microbiol Biotechnol **25:** 502-506

Gibson R, Schneider E, Whightman F (1972) Biosynthesis and metabolism of indol-3yl-acetic acid: III. Partial purification and properties of a tryptamine-forming l-tryptophan dbcarboxylase from tomato shoots. J Exp Bot **23:** 381-389

Glawischnig E, Tomas A, Eisenreich W, Spiteller P, Bacher A, Gierl A (2000) Auxin biosynthesis in maize kernels. Plant Physiol **123:** 1109-1119

Glombitza K, Hartmann T (1966) Der Tryptophanabbau bei *Rhizobium leguminosarurn*. Planta **69:** 135-145

Gomez-Roldan V, Fermas S, Brewer PB, Puech-Pagès V, Dun EA, Pillot JP, Letisse F, Matusova R, Danoun S, Portais JC, Bouwmeester H, Bécard G, Beveridge CA, Rameau C, Rochange SF (2008) Strigolactone inhibition of shoot branching. Nature **455:** 189-194

Goodwin T, Mercer E (1983) Introduction to Plant Biochemistry, 1st Ed. Pergamon Press Australia, Potts Point

Gribble GW (1998) Naturally occurring organohalogen compounds. Accounts of Chemical Research **31:** 141-152

Harrison E, Burbidge A, Okyere JP, Thompson AJ, Taylor IB (2011) Identification of the tomato ABA-deficient mutant sitiens as a member of the ABA-aldehyde oxidase gene family using genetic and genomic analysis. Plant Growth Regul **64:** 301-309

He W, Brumos J, Li H, Ji Y, Ke M, Gong X, Zeng Q, Li W, Zhang X, An F, Wen X, Li P, Chu J, Sun X, Yan C, Yan N, Xie D, Raikhel N, Yang Z, Stepanova AN, Alonso JM, Guo H (2011) A small molecule screen identifies L-Kynurenine as a competitive inhibitor of TAA1/TAR activity in ethylene-directed auxin biosynthesis and root growth in *Arabidopsis*. Plant Cell **23:** 3944-3960

Helmlinger J, Rausch T, Hilgenberg W (1987) A soluble protein factor from chinese cabbage converts indole-3-acetaldoxime to IAA. Phytochemistry **26:** 615-618

Hendrickson Culler A, Cohen JD (2007) Novel pathway for IAA biosynthesis in maize endosperm. *In* International Plant Growth Substance Association 19th Annual Meeting, Puerto Vallarta Mexico

Hendrickson JB (1965) The Molecules of Nature, Ed. W. A. Benjamin Inc, New York

Herbert RB (1989) The Biosynthesis of Secondary Metabolites, Ed. Chapman and Hall, New York

Hino T, Hasegawa A, Liu J-J, Nakagawa M (1990) 2-Hydroxy-1-substituted-1,2,3,4-tetrahydro-β–carbolines. The Pictet-Spengler reaction of *N*-hydroxytryptamine with aldehydes. Chemical and Pharmaceutical Bulletin **38:** 59-64

Hull AK, Vij R, Celenza JL (2000) Arabidopsis cytochrome P450s that catalyze the first step of tryptophan-dependent indole-3-acetic acid biosynthesis. Proc Natl Acad Sci USA **97:** 2379-2384

Igoshi M, Yamaguchi I, Takahashi N, Hirose K (1971) Plant growth substances in the young fruit of *Citrus unshiu*. Agric Biol Chem **35:** 629-361

Ikeda Y, Men S, Fischer U, Stepanova AN, Alonso JM, Ljung K, Grebe M (2009) Local auxin biosynthesis modulates gradient-directed planar polarity in Arabidopsis. Nat Cell Biol **11:** 731-738

Ishihara A, Hashimoto Y, Tanaka C, Dubouzet J, Nakao T, Matsuda F, Nishioka T, Miyagawa H, Wakasa K (2008) The tryptophan pathway is involved in the defence responses of rice against pathogenic infection *via* serotonin production. Plant J **54:** 481-495

Jackson RG, Kowalczyk M, Li Y, Higgins G, Ross J, Sandberg G, Bowles DJ (2002) Over-expression of an Arabidopsis gene encoding a glucosyltransferase of indole-3-acetic acid: phenotypic characterisation of. The Plant Journal, 32 (4) pp 573-583 ISSN 0960-7412

Jager C, Symons G, Ross JJ, Smith JA, Reid JB (2005) The brassinosteroid growth response in pea is not mediated by changes in gibberellin content. Planta **221:** 141-148

Jager CE, Symons GM, Nomura T, Yamada Y, Smith JJ, Yamaguchi S, Kamiya Y, Weller JL, Yokota T, Reid JB (2007) Characterization of two brassinosteroid C-6 oxidase genes in pea. Plant Physiol **143:** 1894-1904

Jeong IK, Sharkhuu A, Jing BJ, Li P, Jae CJ, Baek D, Sang YL, Blakeslee JJ, Murphy AS, Bohnert HJ, Hasegawa PM, Yun DJ, Bressan RA (2007) *yucca6*, a dominant mutation in arabidopsis, affects auxin accumulation and auxin-related phenotypes. Plant Physiol **145:** 722-735

Johnstone MMG, Reinecke DM, Ozga JA (2005) The auxins IAA and 4-Cl-IAA differentially modify gibberellin action via ethylene response in developing pea fruit. J Plant Growth Regul **24:** 214-225

Kaper J, Veldstra H (1958) On the metabolism of tryptophan by *Agrobacterium tumefaciens*. Biochimica et Biophysica Acta **30:** 401-420

Karni M, Mandelbaum A (1980) The even-electron rule. Organic Mass Spectrometry **15:** 53-64

Katayama M, Thiruvikraman S, Marumo S (1988) Localization of 4-Chloroindole-3-acetic acid in seeds of *Pisum sativum* and its absence from all other organs. Plant Cell Physiology **29:** 889-891

Kim J, Murphy A, Baek D, Lee S, Yun D-J, Bressan RA, Narasimhan M (2011) *YUCCA6* over-expression demonstrates auxin function in delaying leaf senescence in *Arabidopsis thaliana*. J Exp Bot **62:** 3981-3992

Kim J, Sharkhuu A, Jin J, Li P, Jeong J, Baek D, Lee S, Blakeslee J, Murphy A, Bohnert H, Hasegawa PM, Yun D-J, Bressan RA (2007) *yucca6*, a dominant mutation in Arabidopsis, affects auxin accumulation and auxin-related phenotypes. Plant Physiol **145:** 722-732

Koga J (1995) Structure and function of indolepyruvate decarboxylase, a key enzyme in indole-3-acetic acid biosynthesis. Biochimica et Biophysica Acta - Protein Structure and Molecular Enzymology **1249:** 1-13

Koga J, Adachi T, Hidaka H (1991a) Molecular cloning of the gene for indolepyruvate decarboxylase from *Enterobacter cloacae*. Mol Genet Genomics **226:** 10-16

Koga J, Adachi T, Hidaka H (1992) Purification and characterization of indolepyruvate decarboxylase: A novel enzyme for indole-3-acetic acid biosynthesis in *Enterobacter cloacae*. J Biol Chem **267:** 15823-15828

Koga J, Adachi T, Hidemasa H (1991b) IAA biosynthetic pathway from tryptophan *via* indole-3-pyruvic acid in *Enterobacter cloacae*. Agricultural Biology and Chemistry **55:** 701-706

Koga J, Syono K, Ichikawa T, Takashi A (1994) Involvement of L-tryptophan aminotransferase in indole-acetic acid biosynthesis in *Enterobacter cloacae*. Biochemica et Biophysica Acta **1209:** 241-247

Kriechbaumer V, Park WJ, Gierl A, Glawischnig E (2006) Auxin biosynthesis in maize. Plant Biol **8:** 334-339

Kriechbaumer V, Wang P, Hawes C, Abell BM (2011) Alternative splicing of the auxin biosynthesis gene *YUCCA4* determines its subcellular compartmentation. Plant J **70:** 292–302

LeClere S, Schmelz EA, Chourey PS (2010) Sugar levels regulate tryptophan-dependent auxin biosynthesis in developing maize kernels. Plant Physiol **153:** 306-318

Lehmann T, Hoffmann M, Hentrich M, Pollmann S (2010) Indole-3-acetamide-dependent auxin biosynthesis: A widely distributed way of indole-3-acetic acid production? Eur J Cell Biol **89:** 895-905

Li ZH, Wang Q, Ruan X, Pan CD, Zhang JC, Jiang DA, Wang GG (2011) Biological activity and quantification of potential autotoxins from *Picea schrenkiana* leaves. Allelopathy Journal **27:** 245-262

Lin AS, Engel S, Smith BA, Fairchild CR, Aalbersberg W, Hay ME, Kubanek J (2010) Structure and biological evaluation of novel cytotoxic sterol glycosides from the marine red alga *Peyssonnelia sp*. Bioorg Med Chem **18:** 8264-8269

Ljung K, Hull AK, Celenza J, Yamada M, Estelle M, Normanly J, Sandberg G (2005) Sites and regulation of auxin biosynthesis in Arabidopsis roots. Plant Cell **17:** 1090-1104

Ljung K, Hull AK, Kowalczyk M, Marchant A, Celenza J, Cohen JD, Sandberg G (2002) Biosynthesis, conjugation, catabolism and homeostasis of indole-3-acetic acid in *Arabidopsis thaliana*. Plant Mol Biol **49:** 249-272

Ludwig-Müller J, Hilgenberg W (1989) Purification of NADPH-specific indole-3-acetaldehyde reductase from *Cucumis sativus* by two-dimensional native polyacrylamide gel electrophoresis. Physiol Plant **77:** 613-619

Malhotra M, Srivastava S (2008) Organization of the ipdC region regulates IAA levels in different *Azospirillum brasilense* strains: Molecular and functional analysis of *ipdC* in strain SM. Environ Microbiol **10:** 1365-1373

Manabe K, Higashi M, Hatori M, Sakagami Y (1999) Biosynthetic studies on chlorinated indoles in *Vicia faba*. Plant Growth Regul **27:** 15-19

Mann J (2004) Chemical Aspects of Biosynthesis, 4 Ed. Oxford University Press, New York

Mano Y, Nemoto K (2012) The pathway of auxin biosynthesis in plants. J Exp Bot **63:** 2853-2872

Mano Y, Nemoto K, Suzuki M, Seki H, Fujii I, Muranaka T (2010) The *AMI1* gene family: Indole-3-acetamide hydrolase functions in auxin biosynthesis in plants. J Exp Bot **61:** 25-32

Mashiguchi K, Tanaka K, Sakai T, Sugawara S, Kawaide H, Natsume M, Hanada A, Yaeno T, Shirasu K, Yao H, McSteen P, Zhao Y, Hayashi K, Kamiya Y, Kasahara H (2011) The main auxin biosynthesis pathway in *Arabidopsis*. Proc Natl Acad Sci USA **108:** 18512-18517

McClean S, Robinson RC, Shaw C, Smyth WF (2002) Characterisation and determination of indole alkaloids in frog-skin secreation by electrospray ionisation ion trap mass spectromemtry. Rapid Communications in Mass Spectrometry **16:** 346-354

Mikkelsen MD, Hansen CH, Wittstock U, Halkier BA (2000) Cytochrome P450 CYP79B2 from *Arabidopsis* catalyzes the conversion of tryptophan to indole-3-acetaldoxime, a precursor of indole glucosinolates and indole-3-acetic acid. The Journal of Biological Chemistry **275:** 33712-33717

Mikkelsen MD, Naur P, Halkier BA (2004) Arabidopsis mutants in the C-S lyase of glucosinolate biosynthesis establish a critical role for indole-3-acetaldoxime in auxin homeostasis. Plant J **37:** 770-777

Miyake F, Yakushijin K, Horne D (2000a) A concise synthesis of topsentin A and nortopsentins B and D. Organic Letters **2:** 2121-2123

Miyake F, Yakushijin K, Horne D (2000b) A Facile Synthesis of Dragmacidin B and 2,5-Bis(6'-bromo-3'-indolyl)piperazine. Organic Letters **2:** 3185-3187

Monteiro AM, Sandberg G, Crozier A (1987) Detection of abscisic acid, indole-3-acetic acid and indole-3-ethanol in seeds of *Dalbergia dolichopetala*. Phytochemistry **26:** 327-328

Moore TC (1969) Comparative net biosynthesis of indoleacetic acid from tryptophan in cell-free extracts of different parts of *Pisum sativum* plants. Phytochemistry **8:** 1109-1120

Moore TC, Shaner CA (1968) Synthesis of indoleacetic acid from tryptophan via indolepyruvic acid in cell-free extracts of pea seedlings. Arch Biochem Biophys **127:** 613-621

Müller A, Weiler EW (2000) Indolic constituents and indole-3-acetic acid biosynthesis in the wild-type and tryptophan auxotroph mutant of *Arabidopsis thaliana*. Planta **211:** 855-863

Normanly J (2010) Approaching cellular and molecular resolution of auxin biosynthesis and metabolism. Cold Spring Harbor Perspectives in Biology 2:a001594

Normanly J, Cohen JD, Fink GR (1993) *Arabidopsis thaliana* auxotrophs reveal a tryptophan-independent biosynthetic pathway for indole-3-acetic acid. Proc Natl Acad Sci USA **90:** 10355-10359

Normanly J, Slovin JP, Cohen JD (1995) Rethinking auxin biosynthesis and metabolism. Plant Physiol **107:** 323-329

Novagen (2007) GST•Bind Kits, 1st Ed, Darmstadt

Ouyang J, Xiang S, Jiayang L (2000) Indole-3-glycerol phosphate, a branchpoint of indole-3-acetic acid biosynthesis from the tryptophan biosynthetic pathway in *Arabidopsis thaliana*. The Plant Journal **24:** 327-333

Ozga J, Reinecke D, Ayele B, Ngo P, Nadeau C, Wickramarathna A (2009) Developmental and hormonal regulation of gibberellin biosynthesis and catabolism in pea fruit. Plant Physiol **150:** 448-462

Pagnussat G, Alandete-Saez M, Bowman J, Sundaresan V (2009) Auxin-dependent patterning and gemete specification in the Arabidopsis femal gametophyte. Science **324:** 1684-1689

Patten CL, Glick BR (1996) Bacterial biosynthesis of indole-3-acetic acid. Canadian Journal of Microbiology **42:** 207-220

Pedras MSC, Jha M (2006) Toward the control of *Leptosphaeria maculans*: Design, syntheses, biological activity, and metabolism of potential detoxification inhibitors of the crucifer phytoalexin brassinin. Bioorg Med Chem **14:** 4958-4979

Pedras MSC, Minic Z, Sarma-Mamillapalle VK (2011) Brassinin oxidase mediated transformation of the phytoalexin brassinin: Structure of the elusive co-product, deuterium isotope effect and stereoselectivity. Bioorg Med Chem **19:** 1390-1399

Pedraza RO, Ramarez-Mata A, Xiqui ML, Baca BE (2004) Aromatic amino acid aminotransferase activity and indole-3-acetic acid production by associative nitrogen-fixing bacteria. FEMS Microbiol Lett **233:** 15-21

Perley J, Stowe B (1966) On the ability of *Taphrina deforroans* to produce indoleacetic acid from tryptophan by tryptamine. Plant Physiol **41:** 243-237

Pham V, Ma J, Thomas S, Xu Z, Hecht S (2005) Alkaloids from *Alangium javanicum* and *Alangium grisolleoides* that mediate Cu-dependent DNA strand scission. J Nat Prod **68:** 1147-1152

Phillips K, Skirpan A, Christensen A, Slewinski T, Hudson C, Barazesh S, Cohen JD, Malcomber S, McSteen P (2011) *vanishing tassel2* endcodes a grass-specific tryptophan aminotransferase required for vegetative and reproductive development in maize. Plant Cell **53:** 550-566

Politi V, De Luca G, Di Stazio G, Materazzi M inventors. 20th November, 1996. 3-Indolepyruvic acid derivatives their method of production and therapeutic use. European Patent EP0421946

Pollmann S, Müller A, Piotrowski M, Weiler EW (2002) Occurrence and formation of indole-3-acetamide in *Arabidopsis thaliana*. Planta **216:** 155-161

Poole C (2003) The Essence of Chromatography, Ed. Elsevier, Sydney

Promega Corporation (2000) *E. coli* Competent Cells, 1st Ed, Madison

Promega Corporation (2010) Wizard® Plus SV Minipreps DNA Purification System, 1st Ed, Madison

Quittenden LJ (2011) Auxin Biosynthesis in *Pisum sativum*: A Physicochemical Perspective. University of Tasmania, Hobart

Quittenden LJ, Davies NW, Smith JA, Molesworth PP, Tivendale ND, Ross JJ (2009) Auxin biosynthesis in pea: characterization of the tryptamine pathway. Plant Physiol **151:** 1130-1138

Quyet-Tien P, Park Y, Ryu C, Park S, Ghim S (2008) Functional identification and expression of indole-3-pyruvate decarboxylase from *Paenibacillus polymyxa* E681. Journal of microbiology and biotechnology **18:** 1235-1244

Rajagopal R, Tsurusaki K, Kannangara G, Kuraishi S, Sakurai N (1994) Natural occurrence of indoleacetamide and amidohydrolase activity in etiolated aseptically-grown squash seedlings. Plant Cell and Physiology **35:** 329-339

Reinecke D, Ozga J, Ilic N, Magnus V, Kojic-Prodic B (1999) Molecular properties of 4-substituted indole-3-acetic acids affecting pea pericarp elongation. Plant Growth Regul **27:** 39-48

Reinecke DM (1999) 4-Chloroindole-3-acetic acid and plant growth. Plant Growth Regul **27:** 3-13

Rigaud J (1970) L'acide indolyl-3-1actique chez Rhizobium. Archiv fur Mikrobiologie **72:** 297-307

Roberts J, Rosenfeld HJ (1977) Isolation, crystallization, and properties of indolyl 3 alkane α-hydroxylase. A novel tryptophan metabolizing enzyme. J Biol Chem **252:** 2640-2647

Ross JJ, Reid JB (2010) Evolution of growth-promoting plant hormones. Funct Plant Biol **37:** 795-805

Ross JJ, Reid JB, Swain SM (1993) Control of stem elongation by gibberellin A_1: evidence from genetic studies including the slender mutant *sln*. Aust J Plant Physiol **20:** 585-599

Rovenská J, Kutácek M, Opatrny Z, Eder J (1988) *Agrobacterium* T-DNA encoded IAA biosynthesis. *In* M Kutacek, R Bandurski, J Krekule (eds) Physiology and biochemistry of auxins in plants. SPB Academic Publishing, The Hague

Roy S, Haque S, Gribble GW (2006) Synthesis of novel oxazolyl-indoles. Synthesis**:** 3948–3954

Saotome M, Shirahata K, Nishimura R, Yahaba M, Kawaguchi M, Syõno K, Kitsuwa T, Ishii Y, Nakamura T (1993) The identification of indole-3-acetic acid and indole-3-acetamide in the hypocotyls of japanese cherry. Plant Cell and Physiology **34:** 157-159

Satoh T, Suzuki S, Susuki Y, Miyaji Y, Imai Z (1969) Reduction of organic compounds with sodium borohydride-transition metal salt systems 1: Reduction of organic nitrile, nitro and amide compounds to primary amines. Tetrahedron Lett **52:** 4555-4558

Schneider E, Gibson R, Wightman F (1972) Biosynthesis and metabolism of indol-3yl-acetic acid I: the native indoles of barley and tomato shoots. J Exp Bot **23:** 152-170

Schwartz K (1961) Separation of enol and keto tautomers of aromatic pyruvic acids. Arch Biochem Biophys **92:** 168-175

Sembdner G, Gross D, Liebisch H, Schneider G (1981). *In* J MacMillan (ed) Hormonal Regulation of Plant Development I Molecular Aspects of Plant Hormones. Springer-Verlag, Berlin, pp 281-289

Seo M, Akaba S, Oritani T, Delarue M, Bellini C, Caboche M, Koshiba T (1998) Higher activity of an aldehyde oxidase in the auxin-overproducing *superroot1* mutant of *Arabidopsis thaliana*. Plant Physiol **116:** 687-693

Smith RD, Loo JA, Edmonds CG, Barinaga CJ, Udseth HR (1990) New developments in biochemical mass spectrometry: electrospray ionisation. Analytical Chemistry **62:** 882-899

Songstad DD, De Luca V, Brisson N, Kurz WGW, Nessler CL (1990) High Levels of Tryptamine Accumulation in Transgenic Tobacco Expressing Tryptophan Decarboxylase. Plant Physiol **94:** 1410-1413

Spaepen S, Versées W, Gocke D, Pohl M, Steyaert J, Vanderleyden J (2007) Characterization of phenylpyruvate decarboxylase, involved in auxin production of *Azospirillum brasilense*. J Bacteriol **189:** 7626-7633

Sprunck S, Jacobsen HJ, Reinard T (1995) Indole-3-lactic acid is a weak auxin analogue but not an anti-auxin. J Plant Growth Regul **14:** 191-197

Stepanova AN, Robertson-Hoyt J, Yun J, Benavente LM, Xie D, Doležal K, Schlereth A, Jürgens G, Alonso JM (2008) TAA1-mediated auxin biosynthesis is essential for hormone crosstalk and plant development. Cell **133:** 177-191

Stepanova AN, Yun J, Robles L, Novak O, He W, Guo H, Ljung K, Alonso J (2011) The *Arabidopsis* YUCCA1 flavin monooxygenase functions in the indole-3-pyruvic acid branch of auxin biosynthesis. Plant Cell **23:** 3961-3973

Strader L, Bartel B (2008) A new path to auxin. Nat Chem Biol **4:** 337-339

Sugawara S, Hishiyama S, Jikumaru Y, Hanada A, Nishimura T, Koshiba T, Zhao Y, Kamiya Y, Kasahara H (2009) Biochemical analyses of indole-3-acetaldoxime-dependent auxin biosynthesis in *Arabidopsis*. Proc Natl Acad Sci USA **106:** 5430-5435

Sutton L (2009) IAA biosynthesis - *Pisum sativum*. Honours. University of Tasmania, Hobart

Takahashi N, I Y, Kõno T, Igoshi M, Hirose K, Suzuki K (1975) Characterization of plant growth substances in *Citrus unshiu* and their change in fruit development. Plant Cell and Physiology **16:** 1101-1111

Tam YY, Normanly J (1998) Determination of indole-3-pyruvic acid levels in *Arabidopsis thaliana* by gas chromatography selected ion monitoring-mass spectrometry. J Chromatogr **800:** 101-108

Tao Y, Ferrer JL, Ljung K, Pojer F, Hong F, Long JA, Li L, Moreno JE, Bowman ME, Ivans LJ, Cheng Y, Lim J, Zhao Y, Ballaré CL, Sandberg G, Noel JP, Chory J (2008) Rapid synthesis of auxin *via* a new tryptophan-dependent pathway is required for shade avoidance in plants. Cell **133:** 164-176

Thain M, Hickman M (2001) The Penguin Dictionalry of Biology, 10th Ed. Penguin, Ringwood

Thurman EM, Ferrer I, Pozo OJ, Sancho JV, Hernandez F (2007) The even-electron rule in electrospray mass spectra of pesticides. Rapid Communications in Mass Spectrometry **21:** 3855-3868

Tivendale ND (2008) Investigating auxin biosynthesis in the garden pea. Honours. University of Tasmania, Hobart

Tivendale ND, Davidson SE, Davies NW, Smith JA, Dalmais M, Bendahmane A, Quittenden LJ, Sutton L, Bala RK, Le Signor C, Thompson R, Horne J, Reid JB, Ross JJ (2012) Biosynthesis of the halogenated auxin, 4-chloroindole-3-acetic acid. Plant Physiol **159:** 1055-1063

Tivendale ND, Davies NW, Molesworth PP, Davidson SE, Smith JA, Lowe EK, Reid JB, Ross JJ (2010) Reassessing the role of *N*-hydroxytryptamine in auxin biosynthesis. Plant Physiol **154:** 1957-1965

Tobeña-Santamaria R, Bliek M, Ljung K, Sandberg G, Mol JNM, Souer E, Koes R (2002) FLOOZY of petunia is a flavin mono-oxygenase-like protein required for the specification of leaf and flower architecture. Genes and Development **16:** 753-763

Tsavkelova EA, Cherdyntseva TA, Klimova SY, Shestakov AI, Botina SG, Netrusov AI (2007) Orchid-associated bacteria produce indole-3-acetic acid, promote seed germination, and increase their microbial yield in response to exogenous auxin. Arch Microbiol **188:** 655-664

Umehara M, Hanada A, Yoshida S, Akiyama K, Arite T, Takeda-Kamiya N, Magome H, Kamiya Y, Shirasu K, Yoneyama K, Kyozuka J, Yamaguchi S (2008) Inhibition of shoot branching by new terpenoid plant hormones. Nature **455:** 195-200

Van Puyvelde S, Cloots L, Engelen K, Das F, Marchal K, Vanderleyden J, Spaepen S (2011) Transcriptome analysis of the rhizosphere bacterium *Azospirillum brasilense* reveals an extensive auxin response. Microb Ecol**:** 1-6

Vande Broek A, Gysegom P, Ona O, Hendrickx N, Prinsen E, Van Impe J, Vanderleyden J (2005) Transcriptional analysis of the *Azospirillum brasilense* indole-3-pyruvate decarboxylase gene and identification of a cis-acting sequence involved in auxin responsive expression. Mol Plant-Microbe Interact **18:** 311-323

Vande Broek A, Lambrecht M, Eggermont K, Vanderleyden J (1999) Auxins upregulate expression of the indole-3-pyruvate decarboxylase gene in *Azospirillum brasilense*. J Bacteriol **181:** 1338-1342

Vandeputte O, Oden S, Mol A, Vereecke D, Goethals K, Jaziri ME, Prinsen E (2005) Biosynthesis of auxin by the gram-positive phytopathogen *Rhodococcus fascians* is controlled by compounds specific to infected plant tissues. Appl Environ Microbiol **71:** 1169-1177

Vanneste S, Friml J (2009) Auxin: A Trigger for Change in Plant Development. Cell **136:** 1005-1016

Walton N, Brown D, eds (1999) Chemicals from Plants: Perspectives on Plant Secondary Metabolites. Imperial College Press, London

Wang Y-Y, Chen C (2007) Synthesis of deuterium labeled tryptamine derivatives. Journal of the Chinese Chemical Society **54:** 1363-1368

Went F, Thimann K (1937) Phytohormones, 1st Ed, New York

Winter A (1966) A hypothetical route for the biogenesis of IAA. Planta **71:** 229-239

Won C, Shen X, Mashiguchi K, Zheng Z, Dai X, Cheng Y, Kasahara H, Kamiya Y, Chory J, Zhao Y (2011) Conversion of tryptophan to indole-3-acetic acid by TRYPTOPHAN AMINOTRANSFERASES OF *ARABIDOPSIS* and YUCCAs in *Arabidopsis*. Proc Natl Acad Sci USA **108:** 18518-18523

Woodward AW, Bartel B (2005) Auxin: regulation, action, and interaction. Ann Bot **95:** 707-735

Yamada M, Greenham K, Prigge M, Jensen P, Estelle M (2009) The *TRANSPORT INHIBITOR RESPONSE2* gene is require for auxin synthesis and diverse aspects of plant development. Plant Physiol **151:** 168-179

Yamada T, Palm C, Brooks B, Kosuge T (1985) Nucleotide sequence of the *Pseudomonas savastanoi* indoleacetic acid genes show homology with *Agrobacterium tumerfaciens* T-DNA. Proc Natl Acad Sci USA **82:** 6522-6526

Yamamoto Y, Kamiya N, Morinaka Y, Matsuoka M, Sazuka T (2007) Auxin biosynthesis by the YUCCA genes in rice. Plant Physiol **143:** 1362-1371

Zazimalova E, Napier RM (2003) Points of regulation for auxin action. Plant Cell Rep **21:** 625-634

Zdunek-Zastocka E (2007) Molecular cloning, characterization and expression analysis of three aldehyde oxidase genes from *Pisum sativum*. Plant Physiol Biochem **46:** 19-28

Zhao Y (2010) Auxin biosynthesis and its role in plant development. Annu Rev Plant Biol **61:** 49-64

Zhao Y, Christensen SK, Fankhauser C, Cashman JR, Cohen JD, Weigel D, Chory J (2001) A role for flavin monooxygenase-like enzymes in auxin biosynthesis. Science **291:** 306-309

Zhou C, Hill D (2007) The keto-enol tautomerization of ethyl butyryl acetate studies by LC-NMR. Magnetic Resonance Chemistry **45:** 128-132